THESIS FOR THE DEGREE OF DOCTOR OF PHILOSOPHY (PHD)

HIV-2: insight into viral replication dynamics, evolutionary rate and role in dual HIV infection

Szojka Zsófia Ilona

UNIVERSITY OF DEBRECEN
DOCTORAL SCHOOL OF MOLECULAR, CELL AND IMMUNE BIOLOGY
Debrecen, 2020.

THESIS FOR THE DEGREE OF DOCTOR OF PHILOSOPHY (PHD)

HIV-2: insight into viral replication dynamics, evolutionary rate and role in dual HIV infection

Szojka Zsófia Ilona

Supervisor: Prof. Dr. *József Tőzsér*

UNIVERSITY OF DEBRECEN
DOCTORAL SCHOOL OF MOLECULAR, CELL AND IMMUNE BIOLOGY
Debrecen, 2020

Table of Contents

LIST OF ABBREVIATIONS

AIDS	Acquired Immunodeficiency Syndrome
AFF4	FMR2 family member 4
APOBEC3G	Apolipoprotein B mRNA editing enzyme, catalytic polypeptide-like 3G
ART	Antiretroviral therapy
CA	Capsid protein
CCR1	C-C chemokine receptor type 1
CCR2	C-C chemokine receptor type 2
CCR3	C-C chemokine receptor type 3
CCR5	C-C chemonike receptor type 5
CXCR6	C-X-C chemokine receptor type 6 (Bonzo)
CD4 + T-cells	Cluster of differentiation 4 positive T cells
CD8 + T-cells	Cluster of differentiation 8 positive T cells
CD38	Cluster of differentiation 38 (cyclic ADP ribose hydrolase)
%CD4+	Percentage of cluster of differentiation 4 positive T cells
CMV	Cytomegalovirus
CXCR4	C-X-C chemokine receptor type 4
DNA	Deoxyribonucleic acid
DMEM	Dulbecco's modified eagle medium
ELISA	Enzyme-linked immunosorbent assay
ENV	Envelope
FBS	Fetal Bovine Serum
GFP	Green Fluorescent Protein
GPR15 G	Protein-coupled receptor 15 (BOB, Brother of Bonzo)
HAART	Highly Active Anti-retroviral Therapy
HIV-D	Dual infection with HIV-1 and HIV-2
HIV-1	Human Immunodeficiency Virus type 1
HIV-2	Human Immunodeficiency Virus type 2
HIVAN	HIV-associated nephropathy
HLA-DR	Human Leucocyte Antigen DR-isotype
HUSH	Human Silencing Hub
IN	Integrase
LOD	Limit of detection
LOQ	Limit of quantification
LTR	Long Terminal Repeat
MA	Matrix protein
MHCI	Major Histocompatibility Complex class I
mRNA	messenger Ribonucleic acid
NC	Nucleocapsid
NEF	Negative Regulatory Factor
NNRTI	Non-nucleoside Reverse Transcriptase Inhibitor
NRTI	Nucleoside Reverse Transcriptase Inhibitor
PBDG	Porphobilinogen deaminase
PBS	Phosphate-buffered saline
PCR	Polymerase Chain Reaction
PEI	Polyethyleneimine
PI	Protease Inhibitor
PIC	Pre-integration complex
PR	Protease

P-TEFb	Positive transcriptional elongation factor b
RNA	Ribonucleic acid
REV	RNA-splicing regulator protein
RNAP II	RNA Polymerase II
RRE	Rev response element
RT	Reverse Transcriptase
SAMHD1	Sterile α motif (SAM) domain and HD domain-containing protein 1
SDS	Sodium Dodecyl Sulfate
SEC	Super elongation complex
SIV	Simian immunodeficiency virus
SU	Surface Protein
TAR	Tat-responsive region
TAT	Transcriptional trans-activator
TCR-CD3	T cell receptor (TCR), in association with the CD3 (Cluster of differentiation 3)
TM	Transmembrane
TRIM5α	Tripartate motif protein 5 α
VL	Viral Load
VPR	Viral protein R
VPU	Viral protein U
VPX	Viral protein X
WHO	World Health Organization

INTRODUCTION

Human immunodeficency viruses type 1 and 2 (HIV-1 and HIV-2) are causative agents of the acquired immunodeficiency syndrome (AIDS). HIV-1 was first descibed in 1983, and 3 years later, HIV-2 was identified from a patient in West Africa, where the virus remains endemic (Clavel et al., 1986), The two RNA viruses share roughly a 55-48 % similarity in their nucleotide sequence (Motomura et al., 2008) (Li et al., 2015), while markedly differing in epidemiologic distribution and their manifestation of infection. While HIV-1 is responsible for infections worldwide; with more than 37 million registered patients, HIV-2 infection, and dual-infection with both viruses (HIV-D), are mostly prevalent in West Africa, and in regions sharing socio-ecomomic relations to that region; such as Portugal, France, India, and Brazil (Gomes et al., 2003) (Faria et al., 2012) (Kanki and DeCock, 1994).

Phylogenetic analyses have shown that HIV viruses came into existance as a result of inter-viral recombination events from their ancestors; the simmian immunodeficency viruses (SIV) (Sharp et al., 2000). While HIV-1 is closely related to SIV chimpanzee and gorilla (SIV cpz / gor) (Gao et al., 1999), HIV-2 is related to SIV of sooty mangabey (smm) (Cavaco-Silva et al., 1998) (Santiago et al., 2005). Even though both viruses share a common ancestor, variability in their genomic sequences accounts for the presence of unique accessory proteins. For example, HIV-2 codes for the viral protein X (vpx) accessory protein, while HIV-1 codes for the viral protein U (vpu). Additionally, a difference can also be observed in the regulatory proteins; such as the transcriptional trans-activator protein (Tat). Tat plays an important role in the initiation of viral transcription, through binding to RNAP II elongation factor, P-TEFb and interacting with the super elongation complex (Karn and Stoltzfus, 2012) (Zhu et al., 1999) (Rice, 2017). Although Tat protein of both HIV viruses induces transcription, several differences can be observed. HIV-2 Tat is much longer compared to that of HIV-1 (Jeang et al., 1999) (Kurnaeva et al., 2019), and the estimated homology in the amino acid sequence is less than 30 %. While the first three domains:

the Pro-rich, Cys-rich and core region of Tat are involved in the function of transactivation, the N-terminal region of HIV-2 Tat shows only a 10 % homology with the Pro-rich domain of HIV-1 Tat (Pagtakhan and Tong-Starksen, 1997). Whereas many of the HIV proteins; such as Tat, are polymorphic, mutations in the acidic domain of HIV-1 Tat have no effect on the function of the protein (Ruben et al., 1989) (Rossenkhan et al., 2012). It is well described that tyrosine to alanine substitution in the Cys-rich domain of HIV-1 and SIV results in aberrant folding, leading to the inactivation of Tat (Verhoef and Berkhout, 1999) (Verhoef et al., 1997) (Das et al., 2007), but no effect of tyrosine to alanine subsitution in the Pro-rich region of HIV-2 has been described.

Compared to HIV-1, infection with HIV-2 is less pathogenic, patients usually have undetectable or low plasma viral load (Avettand-Fenoel et al., 2014) (Damond et al., 2002) (MacNeil et al., 2007), slower CD4+ decline (Van der Loeff et al., 2002) and a slower rate of progression to AIDS, even in antiretroviral-therapy (ART) naive patients. CD4+ T-cell decline is strongly associated with disease progression, and its rapid decrease delineates the rate of progession (Esbjörnsson et al., 2018) (Audige et al., 2010).

Plasma viral load is a prognostic marker of HIV infection, and has been found to be significantly lower in HIV-2 infection, compared to that of HIV-1 (Andersson et al., 2000). Thus, monitoring of ART efficacy in HIV-2 infected individuals is challenging, since 25-40 % of HIV-2 infected individuals have undetectable viral load (Gottlieb et al., 2018). In this case, detection of HIV-2 DNA load provides a more sensitive approach for monitoring of HIV-2 infected patients.

Another important determinant of disease progression is the evolutionary rate of the viruses, which is dependent on their high replication and mutation rates (Mikhail et al., 2005) (Lemey et al., 2005). Although association between evolutionary rates and disease progression shows correlation in HIV-1 infection, such information is lacking in the case of HIV-2. Despite abundance of phenotypic assays on the virus, intra-patient evolution of HIV-2 is understudied (Lemey et al., 2005) (Salemi, 2013) (Borrego et al., 2008) (Skar et al., 2010).

Patients can be dually infected with both HIV viruses, especially in areas where these two lentiviruses are prevalent; such as West Africa, where an estimated prevalence of HIV-D was found to be 0-3,2 % (Hamel et al., 2007). Dually infected patients were shown to have a significantly higher percentage of CD4+ and CD8+ T-cells, slower decline of T-helper cells, and higher immunactivation of CD8+ T-cells, compared to patients with HIV-1 mono-infection (Esbjörnsson et al., 2012) (Esbjörnsson et al., 2014) (Koblavi-Dème et al., 2004). Similarly to HIV-2 mono-infection, HIV-D patients have undetectable viral load (Landman et al., 2009) and slower progression to AIDS, than those with HIV-1 mono-infection (Esbjörnsson et al., 2012). Even though dual infection had been described in the literature more than two decades ago, its pathomechanism remains poorly understood. Some studies suggest a protective role of HIV-2 against HIV-1 infection (Travers et al., 1995), while other studies were not able to verify this finding (Norrgren et al., 1999) (Greenberg, 2001).

Given the relative lack of studies on HIV-2 infection, and the low plasma viral RNA load in HIV-2 infected patients, our aim was to develope a highly sensititve qPCR method which can be used to detect HIV-2's DNA in patients with undetectable viral RNA level, and to define the relation between disease progression and viral evolutionary rate of HIV-2. We also focused on studying HIV-D in cell culture, in order to explore possible mechanisms by which HIV-2 may protect against HIV-1 superinfection, identifying accessory / regulatory proteins that may be responsible for the attenuated pathogenicity of HIV-1, dectribed in HIV-D infected patients. Additionally, we explored the function of HIV-2 Tat, and identified a new mutation in the barely studied Pro-rich region, using a structure-based design, and studying the effect of Y44A mutation in HIV-2 Tat on capsid production, reverse transcription, and the efficiency of proviral transcription.

THEORETICAL BACKGROUND

Origin and classification of Human Immunodeficiency Viruses

HIV-1 can be subdivided into 4 groups: M (major), N (non-M, non-O), P (pending identification) and O (outliner). While group M; which can be classified into nine more subtypes (Huet et al., 1990), is responsible for most of HIV-1 infections worldwide, other groups remain more or less confined to certain countries (Peeters et al., 2014). Both groups P; identified in 2009 (Plantier et al., 2009), and group N; discovered in 1998, have been isolated from Cameroonian patients (Simon et al., 1998) (Vallari et al., 2011). Based on phylogenetic analysis, M and O groups of HIV-1 originated from SIV in chimpanzees (Vanden Haesevelde et al., 1996) (Simon et al., 1998) (Sharp and Hahn, 2011), while groups P and O were found to be closely related to SIV in gorillas (Plantier et al., 2009) (Vallari et al., 2011). Molecular clock analysis indicates that HIV-1 M and O lineages appeared between 1900-1920, HIV-1 P appeared between 1845-1989, while group N was transmissed around 1963 (1948-1977) (Wertheim and Worobey, 2009) (Figure 1).

Nine HIV-2 groups have been described to date (A-I). Whereas group A is the most prevalent worldwide, group B is the most frequently encountered in Ivory Coast, Mali, Burkina Faso and Equatorial Guinea, (Cavaco-Silva et al., 1998) (Soriano et al., 2000) (Machuca et al., 1998) (Soriano et al., 1996) (Heredia et al., 1997) (Ayouba et al., 2013) (Visseaux et al., 2016). Groups A and B are the only epidemiologically successful HIV-2 strains (de Mendoza et al., 2014) (Gottlieb et al., 2003) (Damond et al., 2001). Lemey and his coworkers described that the estimated date of transmission of HIV-2 groups A and B to humans was around the 1930's (Lemey et al., 2003). While circulating groups A and B have been identified in symptomatic HIV-2 infected patients, the other groups (C-H) were only identified in local / unique infections (Damond et al., 2004) (Chen et al., 1997) (Ayouba et al, 2013). Groups C and D were isolated from Liberian patients, groups E and F were identified in Sierra Leoneans (Gao et al., 1994) (Chen et al., 1997), group G was identified from blood sample of an asyomptomic patient from Ivory Coast

(Yamaguchi et al., 2000) (Brennan et al., 1997), and group H, was identified in 2004 from a male patient originating from Ivory Coast, and seems to be pathogenic (Damond et al., 2004). The ninth lineage, group I, was identified from an eight year-old boy from Ivory Coast (Ayouba et al., 2013). Most of the non-epidemic variants cannot, or hardly replicate *in vitro* (Gao et al., 1994), and do not appear to cause symptomatic infections (Damond et al., 2004) (see Figure 1).

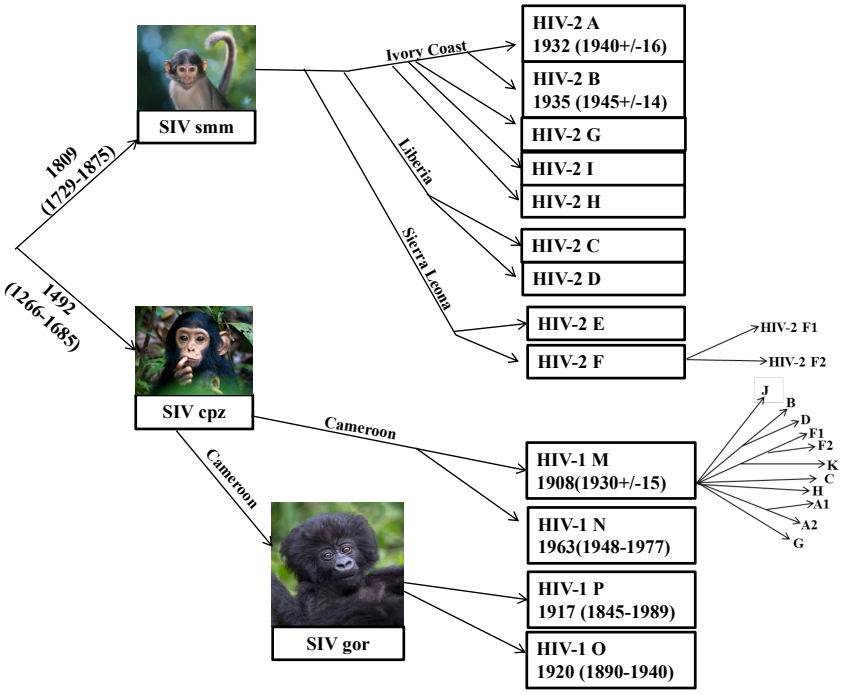

Figure 1. Phylogenetic tree of HIV and its SIV predecessor. HIV had evolved from SIVs of chimpanzees and gorillas (HIV-1); and sooty mangabeys (HIV-2) (Figure was modified and generated based on: Lemey et al., 2003; Damond et al., 2004; deMendoza et al., 2017; Wertheim and Worobey, 2009)).

Epidemiology of Human Immunodeficiency Virus type 2

According to WHO, it is estimated that approximately 37.9 million persons are infected with HIV worldwide, 62 % of which are receiving antiretroviral treatment (ART) (WHO, 2019). Most of the infections are caused by HIV-1, and while recent statistical data about HIV-2 infection is lacking, early estimates put the total number of HIV-2 infected patients at around 1-2 million, which also included patients dually infected with HIV-1 and HIV-2 (Gottlieb et al., 2018) (Gottlieb et al., 2008) (Figure 2 A).

HIV-2 is restricted primarily to West Africa and countries that share past socio-economic relation with this region; such as Portugal and France (Sallman-Raynar and Cliff, 1991) (Gomes et al., 2003) (Faria et al., 2012). Furthermore, HIV-2 infections have been reported from countries with Portuguese socio-economic ties; such as Brazil, Mozambique and Angola (Kanki and DeCock., 1994). The prevalence of HIV-2 was reported in several West African countries; such as Sierra Leone, Gambia, Senegal, Cape Verde, Ivory Coast, Guinea and Guinea-Bissau, where the highest prevalence was reported (De Cock et al., 1991) (Gottlieb et al., 2008) (Horsburgh and Holmberg, 1988) (Poulsen et al., 1989) (Nicolás et al., 2015) (Gilbert et al., 2003) (see Figure 2 B). A study in Senegal had shown that 20 % of HIV seropositive women are HIV-2 infected, however, the percentage of HIV-2 infection decreased from 54 % to 20 % between 1990 and 2009, while the percentage of HIV-1 positivity increased during that period (Heitzinger et al., 2012). A similar pattern was observed in Guinea-Bissau, wherein 1990-1992, about 11.3 % of HIV patients were HIV-2 positive, and in 1997, the number had dropped down to 6.5 %. During the same period, registered HIV-1 cases significantly increased from 0.4 % to 2.0 % (Norrgren et al., 1999). Another Senegalese study showed that the number of registered HIV-2 infections declined from 11 % to 5.5 %, between 1985 and 2003 (Hamel et al., 2007).

While HIV-2 is mostly endemic in West Africa, a global pattern has emerged (Dougan et al., 2005) (Grez et al., 1994) (Barin et al., 2007) (Torian et al., 2010). The highest number of European HIV-2 cases has been reported in Portugal, where 5 % of HIV registered infection is HIV-2 related, of which around 50 % of HIV-2 infected patients have ties to Guinea-Bissau (Soriano et al., 2000). In France, the prevalence of HIV-2 infections was 2 % (Barin et al., 2007), mostly in patients with Sub-Saharan African origin (Damond et al., 2001). HIV-2 infections have also been reported in other European countries; such as the United Kingdom, where 52 out of 1324 patients; who probably contracted the infection in West Africa, were registered with HIV-2 and/or HIV-D (Dougan et al., 2005). In 2013, 297 patients were registered with HIV-2 infection in Spain, 71 %

of which have Sub-Saharan African origin (de Mendoza et al., 2014). In Switzerland, the prevalence of HIV-2 was 0.7 % of total HIV infections, and 25 % of the cases were dually infected patients (Zbinden et al., 2016). HIV-2 infection had also been reported in Belgium, Italy, and India as well (Ruelle et al., 2008) (D'Ettorre et al., 2013) (Grez et al., 1994) (Babu et al., 1993).

Based on the findings of previous studies, where an African origin of HIV-2 cases have been reported (Soriano et al., 2000) (de Mendoza et al., 2014) (Barin et al., 2007), and the geographical origin of the reservoirs of SIV (Apetrei et al., 2005) (Ayouba et al., 2013), it is safe to assume that Guinea-Bissau and Cote d'Ivory may be regarded as the epicenters for HIV-2 infection (see Figure 2 B).

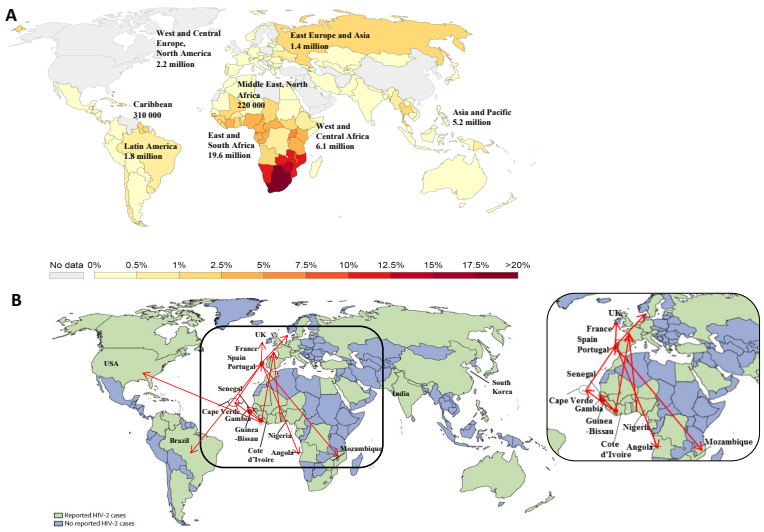

Figure 2. Epidemiology of HIV infection and the global spread of HIV-2. A: Estimation of HIV prevalence worldwide **B:** Reported cases of HIV-2 infections worldwide; green colours indicates reported HIV-2 cases worldwide, while red arrows show the possible circulation and epicentres of HIV-2 infection from West Africa and Europe. (Figure was modified and generated based on: de Menoza et al., 2017; WHO database, 2019; Esbjornsson et al., 2014; Gottlieb et al., 2018; Faria et al., 2012).

Genome of HIV-2

HIV-1 and 2 share only a 55-48 % identity in the nucleotide level; the main structural genes also show comparable similarity (*gag*: 54 %, *pol*: 55 % and *env*: 35 %) (Motomura et al., 2008) (Li et al., 2015).

HIV-2 genes can be classified into three main groups: main structural genes: *gag*, *pol*, *env*; regulatory genes: *tat* and *rev*, and accessory genes: *vif*, *nef*, *vpr* and *vpx*. On both the 5' and 3' ends of the viral genome, the long terminal repeat (LTR) region is flanking, where the 5' LTR region acts as a promoter for transcription (Shah et al., 2014). Schematic representation and comparism between the two HIV genomes is provided in Figure 3.

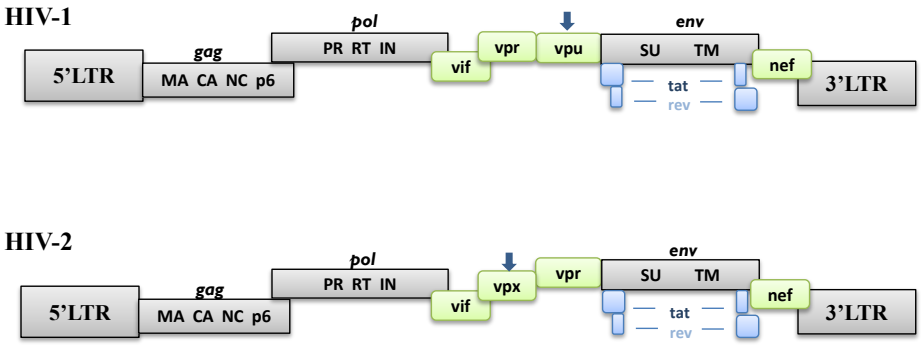

Figure 3. Genomic comparism of HIV viruses. The main difference between the two viral genome have been indicated by blue arrows.

Structural genes

Gag

HIV *gag* encodes a precursor protein, which is cleaved by the viral protease into matrix (MA), capsid (CA), nucleocapsid (NC) and p6 proteins (Bieniasz, 2009). MA domain consists of a myristoylated globular head and an α-helical stalk. The function of CA is to provide structural shell and protect the viral core (Campbell and Hope, 2015). NC is capable of interaction with RNA, and is important in the packaging of the viral genome (Bieniasz, 2009). The p6 domain, which is on the C-terminus of the precursor protein, is an anchor site of the endosomal sorting complexes required for transport (ESCRT) proteins (Bieniasz, 2009) (Usami et al., 2009).

Env

HIV-2 *env* gene encodes for a 140 kDa precursor protein (gp140), which is cleaved into gp125 (125 kDa) surface (SU) and gp36 (36 kDa) transmembrane (TM) proteins. SU contains 5 conserved (C1-C5) and 5 variable (V1-V5) regions (Reeves and Doms, 2002). Both HIV virions can bind CCR5 or CXCR4 co-receptors, though the V3 loop of envelope (Hu et al., 2000) (Döring et al., 2016).

The first step in the viral life-cycle is the interaction between gp125 and CD4 receptor, which initiates viral entry, trigerring the binding to the co-receptors (Engelman and Cherepanov, 2012). Although HIV viruses can bind to either CCR5 or CXCR4 co-receptors, binding to the CXCR4 co-receptor occurs when mutations in the V3 region change the charge of that region and new N-linked glycosylation sites appear (Döring et al., 2016). Changes in co-receptor utilization can provide a possible escape mechanism for the virus. For example, when CCR5 binding inhibitors are used, they result in a resistance to RANTES-induced inhibition (Nabatov et al., 2004) (Döring et al., 2016). Other variable regions also play a role in co-receptor usage: V1/V2 can interact with V3 loop, and mutations in the V1/V2 regions come about as a result of change in co-receptor utilization (Santos-Costa et al., 2014) (Nabatov et al., 2004).

Pol

Pol gene encodes for enzymes that are necessary for viral replication and infectivity. These are the protease (PR; p12), reverse transcriptase (RT, p51), RNase H (p15) and the integrase (IN, p32) (German Advisory Committee Blood, 2016).

HIV-2 protease is a homodimeric aspartyl protease that comprises 99- residues/monomer. HIV-2 PR shows 31 % asymmetry along its structure, particularly in the elbow and flap regions. The substrate binding site, with a highly conserved catalytic triad Asp-Thr-Gly, is located between the two subunits (Triki et al., 2018), and recognises the Gag and Pol polyproteins. While the exact timing of when the viral PR is active remains debatable, Mattei and his coworkers suggested that

the protease activates the Gag precursor protein by cleaving it in five sites, after maturation of the new virion (Mattei et al., 2018). Cleavage of the Gag polyprotein, results in release of the matrix, capsid, nucleocapsid and p6 proteins.

The reverse transcriptase of HIV has three main functions: RNA-dependent DNA polymerase, DNA-dependent DNA polymerase and endonuclease activity, mediated by the RNase H domain. RT can synthetize double stranded DNA from single stranded viral RNA template, and the RNA strands are degraded from the RNA-DNA complex by RNase H. The newly synthesized proviral DNA is then integrated into the host' s genome, a step catalyzed by the viral integrase (Coffin et al., 1997). RT of HIV-2 has lower activity than that of HIV-1s (75 %), furthermore, RNase H activity of HIV-1 is higher than that of HIV-2 (Boyer et al., 2006) (Boyer et al., 2012).

HIV integrase (IN) is derived from a Gag-Pol polyprotein though proteolytic cleavage by the viral protease. It contains three main domains: an N-terminal domain stabilized by a Zinc atom and involved in dimerization, a core-domain that is responsible for the catalytic activity, containing a conserved catalytic triad (DDE motif) forming a Mg-bivalent cation binging pocket (Esposito and Craigie, 1999) (Bercoff et al., 2010), and a C-terminal domain that contains the nuclear localization signal, and is involved in interaction with RT (Dar et al., 2009).

The first step of proviral DNA integration is a hydrolytic cleavage; also known as 3' processing, which is followed by a DNA strand transfer when the 3'-hydroxyl end of viral cDNA is covalently joined to the host DNA (Esposito and Craigie, 1999). Thereafter, host enzymes will „fill up" the gaps and ligate the viral DNA to host DNA.

IN shows only 40 % similarity at the nucleotide, and 65 % identity at the amino acid level between HIV-1 and 2 (Bercoff et al., 2010).

Regulatory genes

HIV genome encodes two regulatory proteins: the transactivator protein (Tat) and the RNA-splicing regulator protein (Rev). Both are equally vital to viral replication.

HIV Tat plays a crucial a role in the initiation of viral transcription. Tat protein of HIV-2 is longer compared to its counterpart, while HIV-1 Tat is comprised of 86-104 amino acids (Jeang et al., 1999) (Kurnaeva et al., 2019), depending on the group, on the other hand, Tat of HIV-2 is 130 amino acids long (Arya, 1993). Estimated molecular weight of HIV-1 Tat protein is 9 to 14 kDa, while the size of HIV-2 Tat ranges between 14 to 16 kDa (Bose et al., 2015) (Ruben et al., 1989). Both HIV-1 and HIV-2 Tat proteins are coded from two exons, and consist of six main domains; the first five domains are encoded by the first exon: an acidic N-terminal Pro-rich, a Cys-rich, a hydrophobic core, an Arg-rich basic, and a C-terminal Gln-rich domains, while the sixth domain is coded by the second exon (Clark et al., 2017) (Smith et al., 2003). Although the second exon is not implicated in transactivation, it is necessary for repressing MHC I expression and interaction with integrins (Smith et al., 2003) (Clark et al., 2017) (Weissman et al., 1998) (Barillari et al., 1999).

Tat proteins of HIVs share similarities in their function and amino acid sequence. The Cys-rich core and basic domains of HIV-2 Tat show homology with Tat protein of HIV-1. On the other hand, the N-terminal region of HIV-2 Tat is longer, and contains less proline than that of HIV-1. Overall, only 10 % homology is observed between the Pro-rich regions of the two Tat proteins (Pagtakhan and Tong-Starksen, 1997). Amino acid sequence similarity is provided in Figure 4.

HIV Tat proteins are multifunctional. One of the functions of Tat is the initiation of viral transactivation, wherein a member of the super elongation complex; Cyclin T, interacts with the Tat protein through its first 3 domains: Pro-rich, Cys-rich and core domains (Kalantari et al., 2008) (Schulze-Gahmen and Hurley, 2018). During the initiation of viral transcription; Tat interacts with several cellular factors: Tat binds to RNAP II elongation factor, P-TEFb (Zhu et al., 1999), inducing transcriptional elongation (Karn and Stoltzfus, 2012). This interaction induces conformational changes in CDK9 kinase (Tahirov et al., 2010). CDK9 then phosphorylates RNAP II, which leads to stimulation of elongation (Rice, 2017). Tat is also involved in the assembly of

super elongation complex, comprised of CDK9, Cyclin T1, ELL1/2, AF9 and AFF4, at the TAR RNA (Rice, 2017).

An important property of Tat is its capability of nuclear localisation, wherein the 4th and 5th domains of Tat interact with the nuclear import receptor; importin-α (Smith et al., 2017) (Kalantari et al., 2008). The third cardinal function of Tat is to induce elongation of proviral transcription, thus, heavily regulating the expression of the viral genome (Jones et al., 1994) (Lata et al., 2018). It is worth mentioning that HIV-1 Tat is capable of trans-activating LTRs of both HIV viruses, while HIV-2 Tat is not (Chang et al., 1992).

HIV Tat is one of the most polymorphic of the viral proteins. Although mutations in the acidic domain of HIV-1 Tat are well tolerated and have no effect on the transactivation activity of Tat (Ruben et al., 1989) (Rossenkhan et al., 2012) information about the effect of mutations in the acidic domain of HIV-2 Tat is still lacking. Schematic representation of HIV-2 Tat protein with the indication of different domains and its main interaction partners is presented in Figure 5.

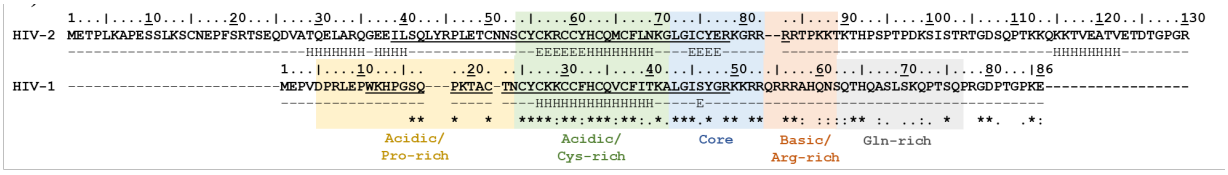

Figure 4. Amino acid sequence similarity between HIV-1 and HIV-2 Tat proteins. Domains were indicated based on Clark et al., 2017. Predicted secondary structures (H: α-helix, E: β-strand) and globular regions (underlined) are shown. Figure was constructed with the aid of Dr. János András Mótyán

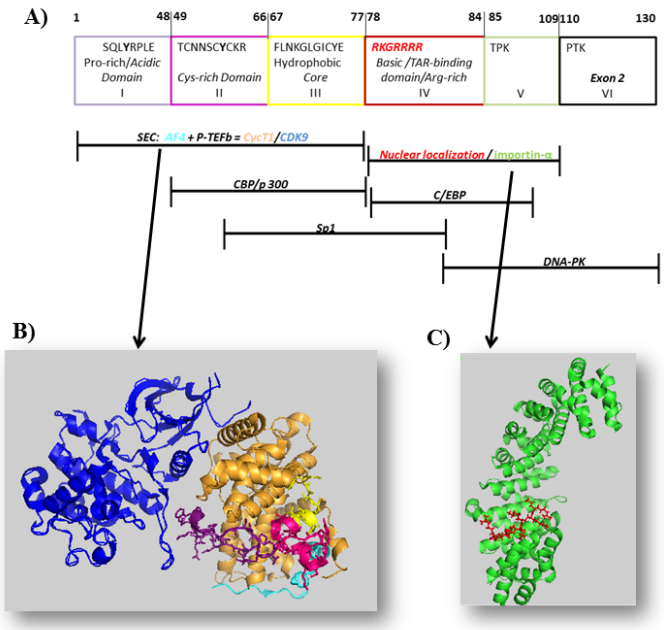

Figure 5. Schematic representation of HIV-2 Tat protein with locations of domains and indication of their potential interaction partners. A: Important amino acid residues are indicated within each domain. Y44 and Y55 residues highlighted in black. Interaction partners of HIV Tat are also represented (Luna et al.,2012). **B:** HIV Tat interacts with super elognation complex (SEC), which consists of FMR2 family member 4(AFF4)(cyan blue) and positive elongation factor b (P-TEFb), composed of Cyclin dependent kinase 9 (CDK9) (blue) and cyclin T1 (orange). Proline rich (purple stick), cyctein-rich (pink sticks and ribbon) and partial core (yellow ribbon) domains of HIV Tat involved in the interaction with SEC (PDB ID: 6cyt) (Schulze-Gahmen and Hurley, 2018). **C:** HIV Tat can be found in the nuclei of infected cells. Basic domain, also known as TAR binding domain, which contains the nuclear localization signal can directly interact with nuclear import receptor, importin-α (green). Amino acids of Tat required for the interaction are highlighted in red and represented in red sticks (PDB ID: 5svz) (Smith et al., 2017). Representation of interaction partners and domains was based on and modified from Luna et. al. (Luna et al.,2012), 6cyt protein sturcture was used to represent HIV Tat interaction with SEC (Schulze-Gahmen and Hurley, 2018), and 5svz stucture was used to show interaction between Arg-rich domain of Tat and improtin-*α* (Smith et al., 2017).

RNA-splicing regulator protein is encoded by *rev*. Rev transports the unspliced and singly-spliced viral RNAs from the nucleus of host cells to the cytoplasm (Blissenbach et al., 2010). Nuclear export signal is responsible for this function, which contains the ^{71}IQHLQGLTIQ^{82} motif (Szilvay et al., 1995). XPO1: in association with RBM14, interacts with Rev, and assists the export of vial RNAs (Budhiraja et al., 2010). During the transport, Rev binds to RRE segments of viral RNA (Coffin, 1997). Although HIV-1 Rev can facilitate the export of viral RNAs of both HIV viruses, HIV-2 Rev is unable to export viral RNAs of HIV-1 (Dillon et al., 1990).

Accessory genes of HIV-2

The genome of HIV-2 encodes four accessory genes: viral infectivity factor (Vif), negative regulatoring factor (Nef), viral protein R (Vpr) and viral protein X (Vpx), which play important roles in viral pathogenesis, budding and infectivity (German Advisory Committee Blood, 2016).

Vif

Viral infectivity factor (Vif) is expressed in the late stage of viral replication. Vif can facilitate reverse transcription, and is capable of the induction of proteosomal degradation of the cellular restriction factor APOBEC3G (Chougi and Margottin-Goguet, 2019). Interaction of Vif with the cellular E3 ubiquitin ligase complex; composed of Cullin-5, Elongin B and C and Rbx2, results in the polyubiquitination of APOBEC3G (Wolfe et al., 2010).

Vif contains a highly conserved ^{144}SLQLA^{149} motif; also known as the BC-box motif, which is responsible for the abolishment of the function of APOBEC3 proteins (Oberste and Gonda, 1992) (Yu et al., 2004). Serine at position 144 is one of the major phosphorylation sites, and is highly conserved in all lentiviruses (Barraud et al., 2008). S144A substitution is an inactivation mutation, which results in the loss of Vif's activity, suggesting that phosphorylation is required for enhanced viral infectivity (Oberste and Gonda, 1992) (Yang and Gabuzda 1998).

Nef

Negative regulatory factor (nef) is expressed in the late-phase of infection. The main function of Nef is the down-regulation of MHCI and CD4 receptor expression (Aiken et.al., 1994) (Das et al., 2005). It had been shown that in 10 % of HIV-2 infections, *nef* gene has deletions (Switzer et al., 1998), this is less commonly observed in HIV-1 infections (<1 %), being mostly noticeable in long-term non-progressors (Kirchhoff et al., 1995).

Vpr

Viral protein R (Vpr) of HIV-1 is a multifunctional protein, which induces G2 cell-cycle arrest in non-dividing cells, in order to benefit viral proliferation (Fletcher et al., 1996), and plays

a role in the nuclear transport of pre-integration complex (PIC) (Belshan and Ratner, 2003). These functions are shared between Vpr and Viral protein X in the case of HIV-2. Both Vpr proteins of HIV-1 and 2 contain a highly conserved arginine-rich domain, a repeated H(S/F)RIG amino acid motif (HIV-1 ^{70}HFRIGCHSRIGIIQ^{85} and HIV-2 ^{75}HFRAGCCGHSRIGQ^{88}), which can trigger cell grow arrest (Macreadie et al., 1995). Mutations in this domain affect the capability of cell-cycle arrest and LTR transcription activity (Sawaya et al., 2000).

Vpx

Viral protein X (vpx) is only present in HIV-2, and its ancestor SIVsmm. Similar to Vpr, it is incorporated into the viral particle *via* interaction with p6 Gag domain (Schaller et al., 2014). HIV-2 Vpx shares the same three-helix structure with Vpr (Chougi and Margottin-Goguet, 2019), and shows 22 % identity in the amino acid sequence to Vpr of HIV-2 gene, which suggests that HIV-2 *vpx* is supposedly a result of *vpr* gene duplication (Hanel et al., 2014) (Khamsri et al. 2006).

HIV-2 Vpx is important in the nuclear transport of PIC, wherein K^{68} and R^{70} residues of the protein mediate the main function (Belshan, 2002). The nuclear localization signal (residues 65-72) contains three main residues: K68, Y68 and R70 that are crucial for the infection of non-dividing cells (Belshan et al., 2006). Alanine substitutions of K68 and R70 residues lead to a complete loss of infection of cells (Belshan et al., 2006).

Another major function of Vpx is to counteract the antiviral effect of sterile α motif (SAM) domain and HD domain-containing protein 1 (SAMHD1), a human dendritic- and myeloid-cell – specific HIV-1 restriction factor (Laguette et al., 2011). SAMHD1 is able to block HIV replication by restricting reverse transcription, through maintaining low cellular free dNTP level in the early stage of infection (Goldstone et al., 2011) (Hollenbaugh et al., 2014). Vpx induces the proteosomal degradation of SAMHD1 by binding to the Cullin4-DDB1-DCAF1 E3 ligase

complex (Ciftci et al., 2015). K68 residue of HIV-2 Vpx is critical for Vpx-E3 ligase complex interaction, and the subsequent ubiquitation of SAMHD1 (Mcculley et al., 2012).

Vpx also neutralizes the effect of human silencing hub (HUSH) complex, by inducing proteosomal degradation of one member of the complex called transgene activation suppressor (TASOR), through the same mechanism used for the inactivation of SAMHD1. Vpx thereby induces the reactivation of HIV provirus through depletion of HUSH (Chougi and Margottin-Goguet, 2019). Schematic representation of HIV-2 Vpx induced proteosomal degradation of SAMHD1 and interaction partners of Vpx is presented in Figure 6.

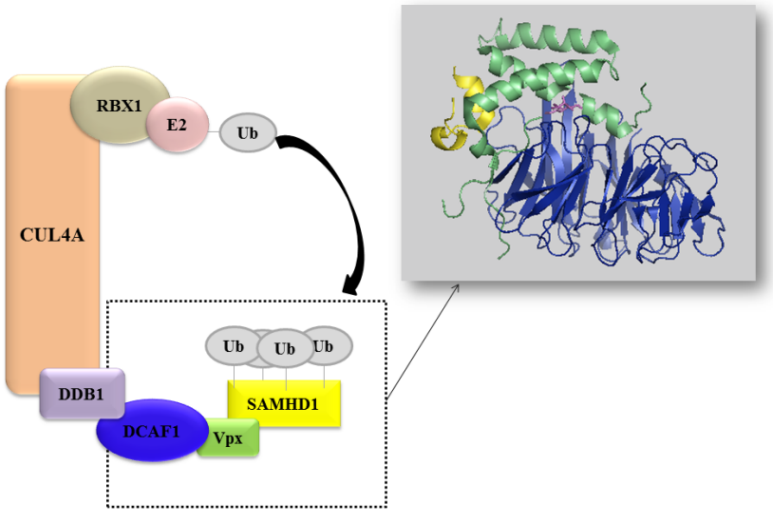

Figure 6. HIV-2 Vpx induces the proteosomal degradation of SAMHD1, a cellular restriction factor. Vpx (green) binds to Vpr-binding protein (DCAF1) (blue) through Q76 and K77 amino acids (highlighted in purple in the protein structure). DCAF1 interacts with DNA-damage binding protein 1 (DDB1) (purple) Cullin-RING Ligase 4 (CUL4A) (orange). CUL4A binding a RING-box protein 1 (RBX1) (brown), which interacts with the E2 ubiquitin-conjugating enzyme (E2) (light pink) and induces ubiquitination of SAMHD1 (yellow). (Chougi and Margottin-Goguet, 2019). Cartoon representation of DCAF1 (blue), Vpx (green) and SAMHD1 (yellow), where cylinders represents α-helix, amino acid residues binding to DCAF1: Q76 and K77 highlighted in purple (PDB ID: 4cc9) (Schwefel et al., 2014). Representation of interaction partners of Vpx was based on and modifed by using figure of Chougi G. and Margottin-Goguet F., and 4cc9 protein structure was used to show interaction partners (Schwefel et al., 2014).

Life-cycle of HIV viruses

Schematic representation of the life-cycle and structure of HIV is provided in Figure 7.

The life-cycle of HIV can be divided into two phases: early: from viral fusion to integration, and late phase: from beginning of proviral transcription to the release of the new virions) (Chougi and Margottin-Goguet, 2019).

Infection of the cell is initiated by the interaction between the viral envelope glycoproteins, CD4, and co-receptors. SU/TM binds to the CD4 receptor on the surface of target cells by forming a bridging site between the inner and outer side of the SU, which bare the co-receptor binding site (Engelman and Cherepanov, 2012). Following the interaction between SU/TM and the main receptor, a hydrophobic cavity is created (Kwong et al., 1998). Interaction with the co-receptors induces conformational changes in the TM domain of the viral envelope (Gallo et al., 2004) that leads to viral fusion.

HIV-2 has a lower binding affinity to CD4 receptor (Moore, 1990), moreover, it is capable of attachment to the cell surface in a CD4-independent manner, as SU is capable of interacting solely with co-receptors (Azevedo-Pereira and Santos-Costa, 2016). Another important difference between the two viruses, is that fusion between HIV-2 envelope and the cell membrane happens relatively faster than in the case of HIV-1 (Gallo et al., 2006).

After fusion between the cellular and viral membranes, the viral capsid is translocated into the cytoplasm. Following/or during de-capsidation, the RT mediated reverse-transcription creates double stranded viral DNA from a single-stranded viral RNA, which is then integrated into the host genome, by a reaction catalyzed by the viral integrase (Coffin et al., 1997) (Esposito and Craigie, 1999). Integration mostly occurs into actively transcribed genes (Chougi and Margottin-Goguet, 2019).

In the late phase of infection, host cells' machinery is used to transcribe viral genomic RNA and mRNAs. Spliced and partly-spliced mRNAs are transported from the nucleus to the

cytoplasm by the aid of Rev (Blissenbach et al., 2010). Following translation, the viral protease cleaves the precursor polyproteins: such as Gag precursor protein to MA, CA, NC and p6 proteins (Mattei et al., 2018) resulting in a fully functional proteins and infectious viral particles, which are released from infected cell by budding.

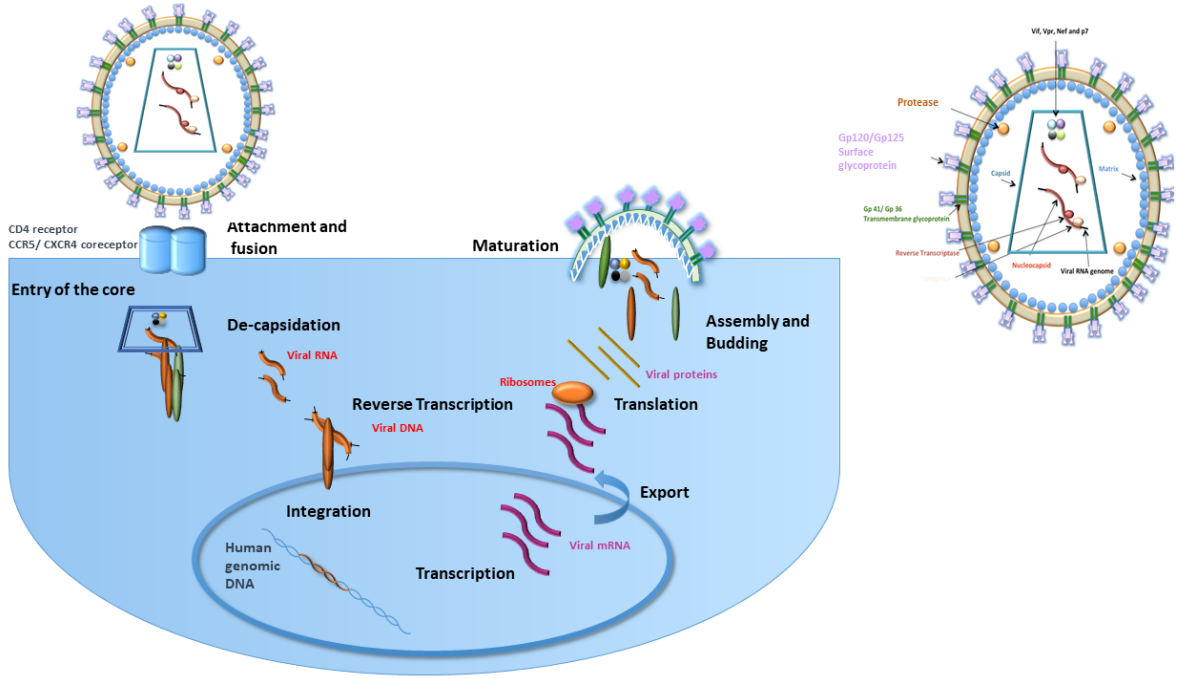

Figure 7. Life cycle of HIV viruses

Clinical manifestation of HIV-2 infection

A brief comparison between HIV-1 and HIV-2 in terms of characteristics is shown in Table 1.

Compared to its counterpart, HIV-2 appears to be initially less pathogenic. Previous studies reported that patients infected with HIV-2 have lower plasma RNA and mRNA loads compared to those observed in HIV-1 infection (Popper et al., 1999) (Popper et al., 2000) (Damond et al., 2002) (MacNeil et al., 2007). Plasma viral load is under the detection limit (10 copies / ml) in 39 % of HIV-2 infected individuals (Avettand-Fenoel et al., 2014), supporting the notion that HIV-2 viral load (VL) is 37-fold to 28-fold lower than that of HIV-1 (O'Donovan et al., 2000) (Andersson et al., 2000).

Modes of transmission for HIV-2 are the same as those for HIV-1; mainly through infected blood, sexual contact, and vertical, or postnatal transmission (Campbell-Yesufu and Gandhi, 2011). However, lower transmission rate has been reported for HIV-2 infection: mother to child transmission was significantly lower (O'Donovan et al., 2000) (Burgard et al., 2010) (Adjorlolo-Johnson et al., 1994). While vertical transmission rate of HIV-1 was 16-24 % (Newell et al., 1996) (O'Donovan et al., 2000), that of HIV-2 was ranging between 1.2-4 %. This finding can be explained by the lower maternal HIV-2 RNA level (O'Donovan et al., 2000) (Adjorlolo-Johnson et al., 1994). Viral RNA level in male genital secretions were found to be lower in HIV-2 infected patients compared to those infected with HIV-1 (Gottlieb et al., 2006).

Even without treatment, HIV-2 infection is associated with a slower decline of CD4+ percentage (% CD4+) (Van der Loeff et al., 2002). Higher percentage of CD4 + was detected in HIV-2 infection even in AIDS stage (median 8.2 % in HIV-1 infection *versus* median 18.2 % in HIV-2 infection) (Esbjörnsson et al., 2018). HIV-2 plasma VL correlates with CD4+ T cell count (Damond et al., 2002), total viral and integrated DNA and viral mRNA levels (MacNeil et al., 2007), and associates with a lower rate of transmission (Gottlieb et al., 2008). Lower plasma viral load is associated with decreased virus production and infection transfer (Popper et al., 2000).

AIDS-defining illnesses, such as tuberculosis, candidiasis, Kaposi's sarcoma, cytomegalovirus infection and HIV-associated nephropathy (HIVAN), were also reported in HIV-2 infections (Campbell-Yesufu and Gandhi, 2011). However, herpes virus 8-induced Kaposi's sarcoma and HIVAN are less frequent in HIV-2 infection than in HIV-1 (Ariyoshi et al., 1998) (Izzedine et al., 2006). An *in vivo* study showed that HIV-2 isolates have significantly reduced fitness; fitness dropped by 100-fold for HIV-2, as compared to HIV-1 strains (Ariën et al., 2005). This indicates a longer time to AIDS progression, and a longer survival time as well (De Cock and Brun-Vézinet, 1989) (Whittle et al., 1994) (Van der Loeff et al., 2002).

	HIV-1	HIV-2
Origin of different subtypes	SIVgor →HIV-1 P, O SIVcpz→HIV-1 M, N	SIVsmm→ HIV-2 A-I
Epidemiology	Worldwide	Endemic in West African countries and Portugal, Spain, France
Estimated number of infected individuals	38 million	undetermined (estimated 1-2 million in 2011) (Campbell-Yesufu et al., 2011)
Main difference in the clinical symptoms	• Higher transmission • Higher plasma RNA level	• Less transmission • Lower or undetectable viral load
Estimated time to AIDS phase in ART naive patients	5-10 years	10-20 years
Main difference in viral genome	*Vpu* (Viral protein U) gene only encoded in the genome of HIV-1 and SIVcpz (Huet et al., 1990) (Vanden Haesevelde et al., 1996)	*Vpx* (Viral protein X) gene encoded only in HIV-2 and its ancestors (Huet et al., 1990)
Coreceptor usage (in vivo)	CCR5, CXCR4	CCR5, CXCR4, Bob, Bonzo, CCR6, CCR2, CCR3 (several chemokine receptors)

Table 1. Comparison between HIV type 1 and type 2

Virus evolution and disease progression

Hepatitis B and RNA viruses such as hepatitis C and HIV-1, are mostly characterized by a high number of spontaneous mutations and genetic diversity (Perelson, 2002). A higher rate of spontaneous mutations may lead to faster evolution of the viruses, promotes eluding of neutralization, and indicates immune escape and the risk of disease progression (Krakoff et al., 2019) (Phillips et al., 1991).

Both HIV viruses evolve rapidly, due to high mutation and replication rates (Rambaut et al., 2004). Their rapid evolution is attributed to the lack of proofreading activity of the reverse transcriptase, and the editing of viral cDNA by the cellular cytidine deaminases of the A3 family (Andrews and Rowland-Jones, 2017) (Cuevas et al., 2015). It was previously shown that the error-prone nature of RT contributes 2 % of the mutations, while 98 % of the mutations are mediated by

the host cytidine deaminase (Cuevas et al., 2015). The mutation rate is extremely high for HIV-1: $(4.1 \pm 1.7) \times 10^{-3}$ per base per peripherial blood mononuclear cell (Cuevas et al., 2015), while no information exist about the mutation rate of HIV-2.

The association between HIV evolution and disease progression had been described in the literature (MacNeil et al., 2007) (Lemey et al., 2007). Although correlation between evolutionary rate and disease progression is well characterized for HIV-1 (Salemi, 2013), viral evolution of HIV-2; especially intra-patients evolution, is understudied. Some studies reported a lower rate of synonymous substitutions and evolutionary rate for HIV-2, compared to HIV-1 (MacNeil et al., 2007) (Lemey et al., 2007).

Env gene endures purifying selective pressure in both HIV virions (Barosso and Taveira, 2005) (Edwards et al., 2006). HIV-1 disease progression is mostly associated with positively selected sites in the viral envelope (Ross and Rodrigo, 2002). Skar *et al.*, observed a significantly higher evolutionary rate of HIV-2 in the gp125 and V3 regions of *env* gene, compared to that of HIV-1 (Skar et al., 2010). Mutations in the envelope proteins can lead to immune escape, as neutralizing antibodies become unable to effectively neutralize the mutant virions (Miller et al., 2018).

HIV-1 and HIV-2 dual infection

Where both HIV viruses circulate, patients can be dually infected. The estimated prevalence of HIV dual infection (HIV-D) is 0-3.2 % in West African countries (Hamel et al., 2007). In Guinea-Bissau where both HIVs are endemic, 0.5 % of HIV patients were dually reactive between 1990-1997 (Norrgren et al., 1999). Da Silva et al, have reported that the prevalence of dually infected individuals in Bissau and Guinea-Bissau was 0.5 % in 2006 (Da Silva et al., 2008). In Senegal; where less than 1.5 % of the population is infected with HIV, 8 % of the patients are dually infected, it is worth mentioning that the tendency of HIV-D infection did not change drastically since 1990 (Heitzinger et al., 2012). In a small cohort, 19 out of 47

individuals were diagnosed as dually infected (Gottlieb et al., 2003). In Cape Verde, 4.1 % out of registered HIV cases were dually infected (de Pina-Araujo et al., 2014).

Only few studies about the frequency of HIV-D infections in non-African countries exist. 0.2% of French HIV infected individuals were dually infected, (Barin et al., 2007); and in Spain, 32% of registered HIV-2 infected are also HIV-1 positive (de Mendoza et al., 2017). In some Asian countries such as India, 91 out of 553 (16.5 %) of HIV positive people showed dual seropositivity in 1994 (Grez et al., 1994), while 1.5 % of blood donors were co-infected (Kannangai et al., 2010).

Detection of CD4+ T-cell decline is one of the indicators of disease development. The percentages of CD4+ and CD8+ T-cells were significantly higher in dually seropositive cases, in comparison to HIV-1 mono-infected ones (Esbjörnsson et al., 2012). Moreover, in a cohort from Guinea-Buissau, a slower increase in the percentage of CD8+ T-cell was noticed in the case of dually infected patients, compared to HIV-1 mono-infected individuals, interestingly, this was only observed in individuals who were initially infected with HIV-2 followed by superinfection with HIV-1 (Esbjörnsson et al., 2012) (Esbjörnsson et al., 2014). CD4+ T cells count was also found to be higher in HIV-D, compared to HIV-1 mono-infection; however, the count was lower than that observed in HIV-2 mono-infection (Koblavi-Dème et al., 2004). Detection and monitoring of plasma viral load can provide information about disease progression, and point out the success of treatment. 25-40 % of HIV-2 infected patients have undetectable viral load (Gottlieb et al., 2018), similarly, in HIV-D, VL is undetectable in roughly half of the cases. Patients dually infected with both viruses have lower HIV-1 plasma viral load compared to HIV-1 mono- infected individuals, Additionally, they also have undetectable HIV-2 RNA load (Andersson et al., 2000) (Koblavi-Dème et al., 2004). Neither HIV-1 nor HIV-2 plasma RNA levels were detectable in 10 out of 11 cases of dually infected individuals (Landman et al., 2009).

HIV-2 mono-infection is mostly described by a lower mortality rate, and longer progression time to AIDS than HIV-1 mono-infection (Van der Loeff et al., 2002). Dually infected patients have slower progression to AIDS, compared to HIV-1 mono-infected individuals; time to development of AIDS was 104 months for HIV-D and 68 months for HIV-1 (Esbjörnsson et al., 2012). A meta-analysis however showed that no significant difference was observed in the mortality rate of HIV-1 mono- and dual infections (Prince et al., 2014).

The mechanism of dual infection with both HIV viruses remains poorly understood. Travers and his coworkers reported approximately 70 % protection against re-infection with HIV-1 in HIV-D patients (Travers et al., 1995), *Kanki et al.,* also reported a 64 % protection (Kanki et al., 1996), in other studies however, this HIV-2 mediated protection was not noted (Norrgren et al., 1999) (Greenberg, 2001).

HIV-2 was found to downregulate HIV-1 infection by blocking HIV-1 capsid and viral RNA production, in a dose-dependent manner, however, HIV-1 was not found to down-regulate HIV-2 (Al-Harthi et al., 1998) (Arya and Gallo, 1996). While HIV-2 is capable of utilizing a wide range of different co-receptors (*e.g.* CXCR6, GPR15 *etc*.), HIV-1 uses mostly CCR5 or CXCR4 *in vivo* (Blaak et al., 2005). Also, β-chemokines (natural ligands of CCR5 receptors) were found to be expressed at higher level during HIV-2 infection, compared to its counterpart (Akimoto et al., 1998), which could mediate blocking of R5-tropic HIV-1 during co-infection (Kokkotou et al., 2000). Moreover, T-cell activation by HIV-2 was found to differ from that of HIV-1; HIV-2 gp105 has a higher inhibitory effect on T-cell proliferation and activation than gp120 of HIV-1 (Cavaleiro et al., 2000).

In addition, Nef-mediated down-regulation of T-cell activation *via* down-modulation of TCR-CD3 was observed in the case of HIV-2 and its ancestors, while this function was diminished in HIV-1 (Schindler et al., 2006).

Anti-retroviral therapy for HIV-2 and HIV-D

Viral enzymes such as RT, IN, PR can be targeted by antiretroviral drugs. Nucleoside analogue reverse transcriptase inhibitors (NRTI) or non-nucleoside reverse transcriptase inhibitors (NNRTI) are the most commonly used RT inhibitors. HIV-2 shows natural resistance againts most of the NNRTIs, and zidovudine, as HIV-2 RT has I181Y substitution in the „NNRTI pocket" (Post et al., 2003) (Ren et al., 2002). HIV-2 is also resistant to enfuvirtide (fusion inhibitor), therefore, the use of NNRTIs and fusion inhibitor is highly discouraged in HIV-2 infection (Álvarez et al., 2018) (Witvrouw et al., 2004) (Poveda et al., 2004). However, NRTIs, integrase strand transfer inhibitors (INSTIs), and some protease inhibitors are effective against HIV-2.

An alternative way to inhibit viral replication is by blocking the coreceptor binding. Maraviroc and cenicriviroc; a CCR5 and CCR2 binding inhibitors, respectively, can effectively block R5 HIV-2 isolates, however, they are ineffective against X4 and R5/X4 strains (Visseaux et al., 2011) (Visseaux et al., 2015). In around 13 % of HIV-2 infections caused by X4-tropic viruses, the virus can switch to CCR4 or R5/X4 (dual) receptor usage (Visseaux et al., 2015). Another reason why co-receptor binding inhibitors may be ineffective against HIV-2, is the broad spectrum of co-receptor usage by HIV-2 (CCR5, CXCR4, CCR3, CCR2, CCR1, Bob (GPR15) and Bonzo (CXCR6)) (Mörner et al., 1999) (Blaak et al., 2005).

The recommended therapy for HIV-2 and HIV-D infection is an integrase inhibitor plus 2 NRTIs, or 2 NRTIs combinated with a boosted protease inhibitor (PR) (Darunavir / Lopinavir) (WHO guidelines).

In a 48-week trial, 40 % of ART naive patients showed positive response to Raltegravir-containing ART, no resistance mutations were detected in the RT region, and viral and total DNA levels were undetectable in most of the subjects (Matheron el al., 2018). In another trial that lasted for 1 year, HIV-2 patients receiving a combination of NRTIs and integrase inhibitor (elvitegravir + cobicistat + emtricitabine + tenofovir disoproxil fumarate) were followed. At the end of the

study, only one out of 29 participants had virological failure, as a result of multiple drug-resistance mutations in the RT (K65R) and IN (G140S + Q148R) regions (Ba et al., 2018). It is worth mentioning that IN G140S/Q148R mutations induced only 2 fold resistance to bictegravir in the case of HIV-1, while inducing a 34- and 110-fold resistance for HIV-2 (Smith et al., 2019).

Studies on the treatment of dually infected individuals are limited. One of the major hurdles of the therapy of HIV-D patients is the appearance of drug-resistance mutations in one or both of the viruses (Landman et al., 2009) (Rodés et al., 2005). Mutations commonly appear in HIV-2 RT (Q151M+ M184V or K65R+ I118V) and PR (I54M+ I82F or V47A) during treatment (Landman et al., 2009) (Rodés et al., 2005). Charpentier and his coworkers showed that 5 % of PI-resistant drug mutation are transmitted between individuals, and 69 % of HIV-2 infected patients on treatment carry the I54M and Y47A substitutions (Charpentier et al., 2013) (Charpentier et al., 2014).

Thus, frequent monitoring of both HIVs' viral loads and the continuous assay for treatment-associated mutations are vital during patient management. It is important to note that there are no guidelines for the treatment of HIV-D infection; treatment is usually similar to that of HIV-2: 2 NRTIs and an INSTI.

Scope of the study

Even though HIV-2 was discovered more than 30 years ago, relatively limited information exist about its pathomechanism and infectivity, compared to HIV-1. The two viruses share only a 40 % similarity in their genome. Each individual virus encodes for unique genes; such as *vpx* in HIV-2 and *vpu* in HIV-1; furthermore, some of the viral proteins are highly polymorphic, and substantially differ in their amino acid sequence between the two viruses; such as the transcriptional trans-activator protein (Kurnaeva et al., 2019), which may result in noticeable differences in their replication dynamics and the clinical manifestation of infection.

While mutations in the first domain of HIV-1 Tat have no effect on the transactivation activity of Tat (Ruben et al., 1989) (Rossenkhan et al., 2012), effect of substitutions in the acidic domain of HIV-2 Tat is unknown.

Secondly, although HIV-2 infection is associated with a slower rate to AIDS progression (Esbjörnsson et al., 2018), it has a high mutation rate, similarly to its counterpart (Rambaut et al., 2004). There are limited number of publications about the contribution of HIV-2 evolutionary rate to disease progression, of which most are phenotypic assays, performed on viral RNA or DNA from viruses reproduced in cell cultures, and not intra-patient studies, which would far more accurately represent the different circulating viruses in the population (Borrego et al., 2008) (MacNeil et al., 2007). Intra-patient studies are the key to understand viral evolution.

Moreover, although dual infection had been described in the literature, studies about its pathomechanism are widely lacking. Therefore, our aim was to carry out an in-depth study of HIV-D, in addition to characterizing inactivating mutations in HIV-2 Tat, and developing a sensitive and robust method for detection of HIV-2 DNA load.

Aim 1: Characterization of HIV dual infection in cell culture

1. To study the effect of inactivated HIV-2 protease, regulatory and accessory genes on HIV dual infection in HEK293T cells.

2. To study the effect of HIV-2 Vpx and its inactivation on HIV-1 superinfection in HEK293T cells, by quantification of HIV-1 2-LTR circle junctions, and measuring the activity of HIV-1 RT and p24 capsid production.

3. To optimize transfection and transduction of THP-1 cells, and study the transduction efficiency of HIV-1 in the presence of HIV-2 Vpx.

Aim 2: *In silico* and *in vitro* characterization of the effect of mutations in the acidic domain of HIV-2 Tat

1. Investigation of the destabilizing mutations of HIV-2 Tat using sequence- and structure-based *in silico* analysis.

2. Determine the effect of HIV-2 Tat mutation on HIV-2 capsid production, activity and expression of HIV-2 RT, and the efficiency of proviral transcription.

Aim 3: Development of a sensitive HIV-2 DNA quantification protocol

1. Optimalization and preparation of HIV-2 and PBDG standards for qPCR, to quantify the level of HIV-2 DNA load.

2. Optimalization of DNA extraction from whole blood of HIV-2, HIV-1 and HIV-naive individuals.

3. Quantify the sensitivity and specificity of HIV-2 DNA qPCR by using DNA from HIV negative and HIV-1 positive participants.

Aim 4: Investigation of differences in HIV-2 evolutionary rate between fast and slow HIV-2 progressors

1. Investigation of the association between HIV-2 disease progression and the evolutionary dynamics of HIV-2.

2. Analysis of the association between synonymous and non-synonymous nucleotide substitutions and viral evolutionary rate in faster and slower progressors.

3. Determination of the positively selected amino acids in slow progressors, and investigation of the association between envelope surface exposition and positively selected amino acids.

MATERIALS AND METHODS

Plasmids and vectors

2nd generation lentiviral vectors were used for HIV-1 and HIV-2 virion production. For production of HIV-1 pseudovirions, the following plasmids were used: psPAX$_2$ as a packaging plasmid; a kindly gift from Dr. D. Trono (University of Geneva Medical School, Geneva, Switzerland); pWOX-CMV-GFP transfer vector (Miklossy et al. 2008), which was modified to code for mCherry instead of Green Fluorescent Protein (GFP), and pMD.G; encoding for the envelope protein of vesicular stomatitis virus (VSV-G) (Figure 8). The following plasmids were used for HIV-2 pseudovirion production: HIV-2 CGP (a ROD based HIV-2 protein expression vector, which encodes for all HIV-2 genes except *nef* and *env*), a transfer plasmid CRU5SINCGW, which has a CMV promoter induced GFP expression cassette (Mahdi et al. 2014), and pMD.G plasmid. HIV-2-CRU5SIN-WPRE vector contains U5 regions and HIV-2 *gag*, lacking of *pol* and *env* (Figure 9). HIV-2 CGP and CRU5SINCGW plasmids were a kindly gift from Joseph P. Dougherty (Robert Wood Johnson Medical School, New Jersey, USA) (Mukherjee et al. 2007). pcDNA3.1-Vpx-NeGFP encodes for HIV-2 Vpx-GFP fusion protein, and the sequences of HIV-2 *vpx* gene is identical to that found in the HIV-2 CGP vector. pcDNA3.1-Vpx-NeGFP was obtained from Genscript services (Genscript Biotech Corporation (NJ, USA). As a mock plasmid, we created pcDNA3.1-NeGFP from pcDNA3.1-Vpx-NeGFP plasmid using KpnI and XbaI (New England Biolabs, MA, USA) restriction enzymes. pTY-EFeGFP was also used as a control vector in some experiments carried out in THP-1 cells (Chang et al. 1999).

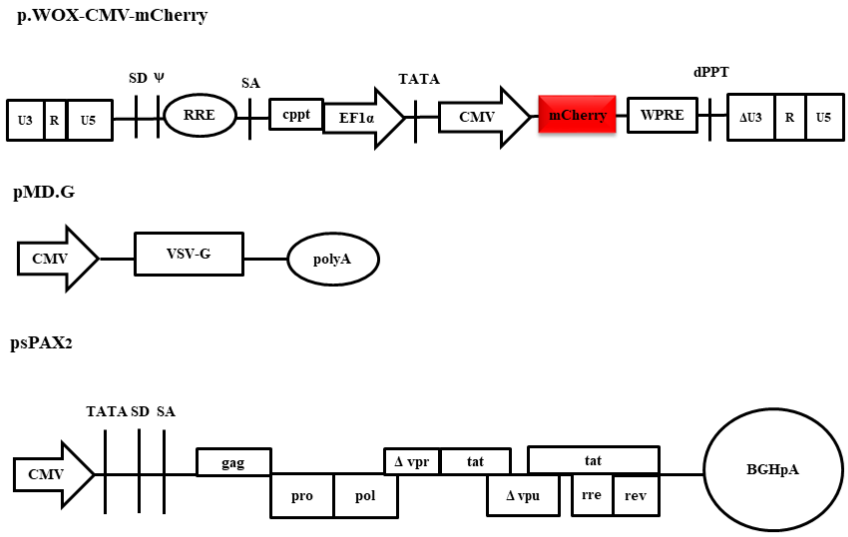

Figure 8. 2nd generation vector system for HIV-1 pseudovirion production

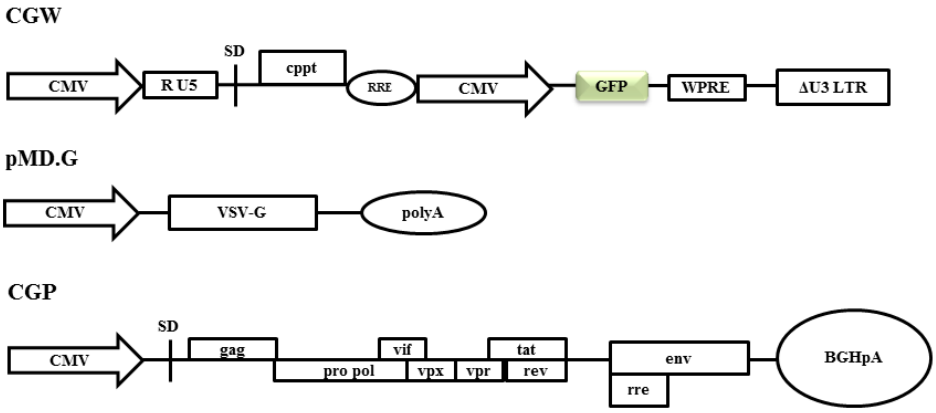

Figure 9. 2nd generation vector system for HIV-2 pseudovirion production

Mutagenesis

We used QuikChange II Site-Directed Mutagenesis and QuikChange Lightning Multi Site-Directed Mutagenesis Kits (Agilent Technologies, CA, USA) to carry out loss-of-function mutagenesis on HIV-2 protease and regulatory and accessory genes, using the primers listed in table 2. The following mutations were performed on the HIV-2 CGP plasmid. Protease: D25N, Tat: Y44A/ Y55A, Rev: H73R, Vif: S144A, Vpr: R78A, Vpx: K68A and R70A. Inactivating mutations of Vpx (K68A and R70A) were performed on the pcDNA3.1-Vpx-NeGFP vector. PCR sequencing was used to confirm the success of mutagenesis.

Name of primers	Sequence of primers
PR D25N	F: 5'-GTA GAA GTT TTG TTA AAC ACG GGA GCT GAC G-3' R: 5'-C GTC AGC TCC CGT GTT TAA CAA AAC TTC TAC-3'
TAT Y44A	F: 5'-CTC TCT CAG CTA GCC CGA CCC CTA GAA AC-3' R: 5'-GT TTC TAG GGG TCG GGC TAG CTG AGA GAG-3'
TAT Y55A	F: 5'-CA TGC AAT AAC TCA TGC GCC TGT AAG CGA TGC TGC TAC CAT TG-3' R: 5'-CA ATG GTA GCA GCA TCG CTT ACA GGC GCA TGA GTT ATT GCA TG-3'
REV H73R	F:5'-CC AGA CTA TAC AGC GTC TGC AGG GAC TTA C-3' R:5'-G TAA GTC CCT GCA GAC GCT GTA TAG TCT GG-3'
VPR R78A	F: 5'-TTC ACG CAC TTC GCA GCA GGA TGT GGC C-3' R: 5'-G GCC ACA TCC TGC TGC GAA GTG CGT GAA-3'
VIF S144A	F: 5'-GA GCC CAG GTA CCG GCA CTT CAA TTT CTG-3' R: 5'-CAG AAA TTG AAG TGC CGG TAC CTG GGC TC-3'
VPX K68A	F:5'GGG ATG TCA GAA AGT TAC ACA GCG TAT AGA TAT TTG TGC ATA ATA CAG-3' R: 5'-GCA CAA ATA TCT ATA CGC TGT GTA ACT TTC TGA CAT CCC-3'
VPX R70A	F: 5'-GT TAC ACA GCG TAT GCA TAT TTG TGC ATA ATA CAG-3' R: 5'-GTA TTA TGC ACA GCT ATG CAT ACT TTG TGT AAC 3'

Table 2. Mutagenesis primers for loss-of-function mutations. Underlined positions indicate the substitutions in the original gene. (F: Forward; R: Reverse)

In silico predictions of Tat mutations

For *in silico* predictions, sequence of HIV-2 Tat protein was downloaded from UniProt database (UniProt ID: P04605), and protein model structures were obtained from Swissmodel repository (Bienert et al. 2017) (SWISS-MODEL Template Library identifiers, SMTL IDs: 1tvs.1 and 1tvt.1) (https://swissmodel.expasy.org/repository/uniprot//P04605, date of download: 2017.03.27). For short disordered and structured region predictions, we used IUPred webserver (Dosztanyi et al. 2005). I-Mutant 2.0 server was used to calculate the point mutation-induced stability changes (Capriotti, Fariselli, and Casadio 2005). We also used JPred4 server for secondary structure predictions (Drozdetskiy et al. 2015). To estimate the effect of point mutations on Tat protein stability, we used SDM server (Pandurangan et al. 2017) and FoldX algorithm (Guerois, Nielsen, and Serrano 2002) structure-based predictions.

Full-length HIV-2 Tat sequences were downloaded from the Los Alamos National Laboratory HIV sequence database (https://www.hiv.lanl.gov/content/sequence/NEWALIGN/align.html, date of download: 2019.10.28). A multiple-sequence alignment of amino acid sequences (without any

gap) was made using ClustalW (https://www.genome.jp/tools-bin/clustalw) and the divergence of HIV-2 Tat sequences was schematically visualized using Weblogo for 1-70 residues of the first two domains (https://weblogo.berkeley.edu/logo.cgi).

Experiments on HEK293T cells to study HIV-1/2 dual infection

Production of HIV-1 and HIV-2 viral particles

293T human embryonic kidney (HEK293T) cells (Invitrogen, CA, USA) were used for pseudovirion productions. For production of HIV-1 pseudovirions, we used: psPAX$_2$, pWOX-CMV-mCherry, and pMD.G plasmids in a 3:2:1 ratio. For HIV-2 production, we used HIV-2 CGP, HIV-2 CRU5SINCGW, and pMD.G in a 1:1:1 ratio (Mahdi et al., 2018). HEK293T cells were seeded in T-75 flask and grown in 15 ml Dulbecco's Modified Eagle's Medium (DMEM) (Sigma-Aldrich, St. Louis, MO, USA) complemented with 10 % fetal bovine serum (FBS), 1 % glutamine and 1 % penicillin-streptomycin.

Cells were passaged in order to achieve around 70 % confluency (5-6×10^6 cells/ml) on the next day. For HIV-2, we used a total of 30 µg plasmid DNA, and a total of 36 µg plasmid DNA for HIV-1. Transfection was carried out using polyethylenimine (PEI) (Sigma-Aldrich, St. Louis, MO, USA) (Mahdi et al., 2014). HEK293T cells were incubated at 37°C, 5 % CO_2 in 5 ml antibiotics-free DMEM containing 1% FBS after adding the PEI-DNA solution for 5-6 hours. The media was then replaced by 15 ml DMEM supplemented with 10 % FBS, 1 % glutamine and 1 % penicillin-streptomycin, and the supernatant containing virions was collected and filtered through a 0.45 µm polyvinylidene fluoride filter (Merck Millipore, Darmstadt, Germany) on day 1, 2 and 3. The collected supernatant was then concentrated by ultracentrifugation (100 000 x g, 2 hours, 4°C), and the viral pellet was dissolved in 200 µl phosphate-buffered saline (PBS), portioned, and stored at -70°C. Reverse transcriptase (RT) activity and amount of HIV-2 capsid were then measured using ELISA-based colorimetric reverse transcriptase assay (Roche Applied Science, Mannheim,

Germany), and ELISA-based colorimetric p24 (for HIV-1) or SIV p27 (HIV-2) assay (Express Biotech International, Frederick, USA), according to the manufacturer`s protocols.

Transduction of HEK293T cells

24 hours before transduction, HEK293T cells were seeded in a 48-wells plate in 300 µl DMEM containing 10 % FBS, 1 % glutamine and 1 % penicillin-streptomycin to achieve around 50 % confluency ($2.5–3\times10^4$ cells/ml) on the next day. Cells were transduced with 10-30 ng RT-equivalent of HIV-1 or HIV-2 pseudovirions in 100 µl serum- and antibiotic-free media, complemented with 8 µg/ml polybrene. The day after transduction, cells were complemented with 200 µl of DMEM contains 20 % FBS, 2 % glutamine, 2 % penicillin-streptomycin, and were thereafter incubated at 37°C, 5 % CO_2 for 4 days. Media was then removed, and the cells were mechanically detached and suspended in 200 µl PBS. After centrifugation (5 min, 152 x g), PBS was discarded, and cells were suspended in 400 µl 1 % formaldehyde containing ice-cold PBS. Fluorescence-activated cell sorting (FACS) (FACSCalibur, BD Biosciences, Singapore) was used to determine the number of successfully transduced cells based on either GFP or mCherry fluoresence.

HIV-1 and HIV-2 dual transduction assays

Schematic representation of HIV-1 and HIV-2 dual transduction models is provided in Figure 10.

Simultaneous infection model

The day before transduction, 40,000 HEK293T cells were plated per well in 48-well plate. Cells were then infected with 30 ng RT-equivalent of HIV-1 and HIV-2 pseudovirions simultaneously. The cells were complemented with 100 µl of serum- and antibiotic-free media containing 8 µg/ml polybrene. We also prepared HIV-1 and HIV-2 mono-infection controls, where 30 ng RT-equivalent of HIV-1 or HIV-2 virions were used to infect the cells. On the next day, the cells were supplemented with 200 µl DMEM containing 20 % FBS, 2 % glutamine, and 2 % penicillin-

streptomycin, and were incubated for 4 days. FACS analysis was then performed to analyze infectivity (Figure 10 A).

"Superinfection" models

Similarly to simultaneous transduction, HEK293T cells were plated in 48-well plate a day before superinfection. For HIV-1 superinfection experiments, cells in 100 µl of serum- and antibiotic-free media containing 8 µg/ml polybrene were first infected with 30 ng HIV-2, after 24 hours incubation at 37°C, 5 % CO_2, 30 ng RT-equivalent of HIV-1 and 200 µl of DMEM medium containing 20 % FBS, 2 % glutamine and 2 % penicillin-streptomycin was added to the cells, followed by a 4 days incubation in the same conditions (Figure 10 B). HIV-2 "superinfection" was carried out similarly, with the exception that HIV-2 transduction was followed by transduction with HIV-1 (Figure 10 C). After 4 days incubation, FACS analysis was performed to quantify HIV-1 (mCherry) and HIV-2 (GFP) positivity in 5,000 cells.

To exclude the possible interference between mCherry and GFP fluorescent proteins, HEK293T cells were transduced with mCherry and GFP encoding HIV-1 pseudovirions, using the aforementioned protocol.

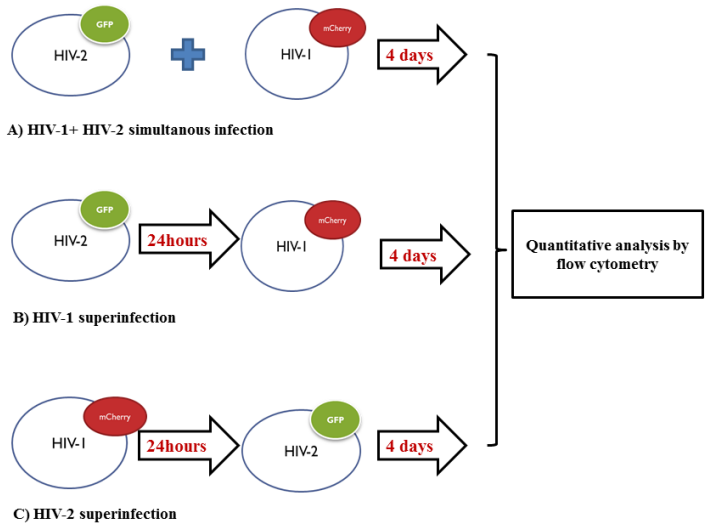

Figure 10. Schematic representation of simultaneous and HIV "superinfection" models in HEK293T cells.

HIV-1 transduction of HEK293T cells pre-transfected with wild-type and mutant HIV-2 CGP vectors

HEK293T cells were passaged in order to achieve ~ 70 % confluency on the next day. Cells were then transfected with 10 µg of HIV-2 CGP vectors carrying the wild-type, or the mutant gene of interest using PEI in T75 flasks, and similarly to the transfection protocol, cells were incubated and media was changed after 5-6 hours. After 30 hours incubation, transfected cells were deattached using trypsinization. Cells were then plated in 48-well plate (70,000 cells /well), and supplemented with 50 µl antibiotics- and serum-free DMEM containing 8 µg/ml polybrene. 30 ng (RT-equivalent) HIV-1 pseudovirions were used to infect the cells, thereafter incubated for 24 hours, and 200 µl DMEM containing 20 % FBS, 2 % glutamine and 2 % penicillin-streptomycin was added to the cells, followed by further incubation at 37°C, 5 % CO_2 for 3 days. Cells were then mechanically scraped and suspended in 500 µl PBS containing 1 % formaldehyde. Flow cytometry analysis was used to detect the percentage of HIV-1 positivity (mCherry) in 5,000 cells.

HIV-1 transduction of HEK293T cells transfected with Vpx

Representation of methods used to study the effect of HIV-2 vpx on the infectivity of HIV-1 is provided in Figure 11.

Using the previously mentioned transfection protocol, HEK293T cells were transfected with 10 µg of pcDNA3.1-Vpx-NeGFP plasmid. After 30 hours incubation, Vpx-transfected cells were seeded in 48-well plate (70,000 cells/well) and transduced with 20 ng RT-equivalent of HIV-1 pseudovirions. After 4 days incubation (at 37°C, 5% CO_2), cells were mechanically scraped off, and HIV-1 mCherry positivity was analyzed in 5,000 cells using flow cytometry.

For control experiments, non-transfected, HIV-1 transduced cells, pcDNA3.1-NeGFP vector, and K68A-R70A functionally restricted mutant Vpx was used to transfect cells, followed by transduction with HIV-1.

Western blotting of of HIV-2 Vpx expressed in HEK293T cells

Western blotting was used to verify the presence of HIV-2 Vpx. HEK293T cells were transfected with 10 µg of HIV-2 CGP, pcDNA3.1-Vpx-NeGFP or pcDNA3.1-NeGFP in T75 flasks using PEI, and incubated at 37°C, 5 % CO_2 for 6 hours. Thereafter, the medium was changed to DMEM containing 10 % FBS, 1 % glutamine and 1 % penicillin-streptomycin, and cells were incubated for 30 hours. After that, the media was discarded, and cells were scraped in 5 ml ice cold PBS. The cells were a centrifuged for 10 minutes at 152 x g at 4°C, then dissolved in 1 ml lysis buffer (50 mM Tris-HCl, 250 mM NaCl, 0.5 % NP-40, 5 mM EDTA, 50 mM NaF, pH 7.4) and left on ice for 30 minutes, while vortexed every 10 minutes. The cells were also disrupted by short sonication (Branson Sonicator, 10 seconds at 40 % energy, 4°C), and the lysate was then centrifuged for 30 minutes at 14000 x g, 4°C. Protein was detected on 14 % SDS polyacrylamide gel from 30 µl of the supernatant (normalized to capsid level). HIV-2 Vpx monoclonal antibody (Kappes et al., 1993) was used as a primary antibody, followed by a secondary anti-mouse IgG (Sigma-Aldrich, St. Louis, MO, USA) to detect the presence of viral protein X. HIV-2 Vpx Monoclonal Antibody (6D2.6) was obtained through the NIH AIDS Reagent Program, Division of AIDS, NIAID, NIH: from Dr. John C. Kappes. β-actin antibody (Covalab, Villeurbanne, France) was used as a primary antibody, followed by anti-mouse IgG, used for normalization of total protein. Blots were detected with SuperSignal West Pico Chemiluminescent substrate (Thermo Fisher Scientific, MA, USA).

Quantitative real-time PCR analysis of vpx transfected, HIV-1 transduced cells

Isolation of viral DNA from vpx-transfected, HIV-1 transduced cells

HEK293T cells were pre-transfected with pcNDA3.1-Vpx-NeGFP plasmid, then transduced with HIV-1 pseudovirions using the aforementioned protocol. For control, we used HEK293T cells only transduced with HIV-1 virions. After 3 days incubation, medium of the cells was replaced by

4 ml ice-cold PBS and cells were scraped. After centrifugation for 10 minutes at 1500 x g, 4°C, the pellet was suspended in 500 µl ice-cold PBS, and DNA was extracted using Qiagen Blood and Cell culture DNA Mini Kit (Qiagen, Hilden, Germany), following the manufacturer's protocol. Concentration of eluated DNA was measured using NanoDrop 2000 spectrophotometer (Thermo Scientific, Massachusetts, USA).

Real-Time PCR for quantification of 2-LTR circle junction

Real-time polymerase chain reaction of HIV-1 2-LTR circle junction was used to analyze the change in HIV-1 infectivity (transduction efficiency) as a result of pre-transfection of cells with HIV-2 Vpx (see Figure 11). qPCR was carried out with an initial denaturation step at 95°C for 10 minutes, followed by 45 cycles of 95°C for 1 minute, and 60°C for 1 minute (Prasad and Kalpana, 2008). pWOX-CMV-mCherry plasmid was used as a standard, as it encodes for the long terminal repeat region. For quantification, a series ten-fold and two-fold dilution of pWOX-CMV-mCherry corresponding to 10^7 to 5 copies of DNA was used as a standard. HIV-1 DNA was normalized to the expression of PBDG (porphobilinogen deaminase) housekeeping gene using 600 nM of PBDG forward and reverse primers. 15 µl SYBR Green Master Mix containing ROX (Thermo Scientific, Massachusetts, USA), and 100 ng template and the same PCR cycling conditions were used as for HIV-1 U3 LTR amplification. Sequences of primers are listed in Table 3.

Name of primers	Sequence of primers
HIV-1 U3 LTR F	5’ TGA TAT CGA GCT TGC TAC AAG GGA 3’
HIV-1 U3 LTR R	5’ AAG TAG CCT TGT GTG TGG TAG ATC C 3’
PBDG F	5’AGG GAT TCA CTC AGG CTC TTT CT 3’
PBDG R	5’GCA TGT TCA AGC TCC TTG GTA A 3’

Table 3. qPCR primers used for quantification of 2-LTR circle junctions. (PBDG: porphobilinogen deaminase) (F: Forward; R: Reverse)

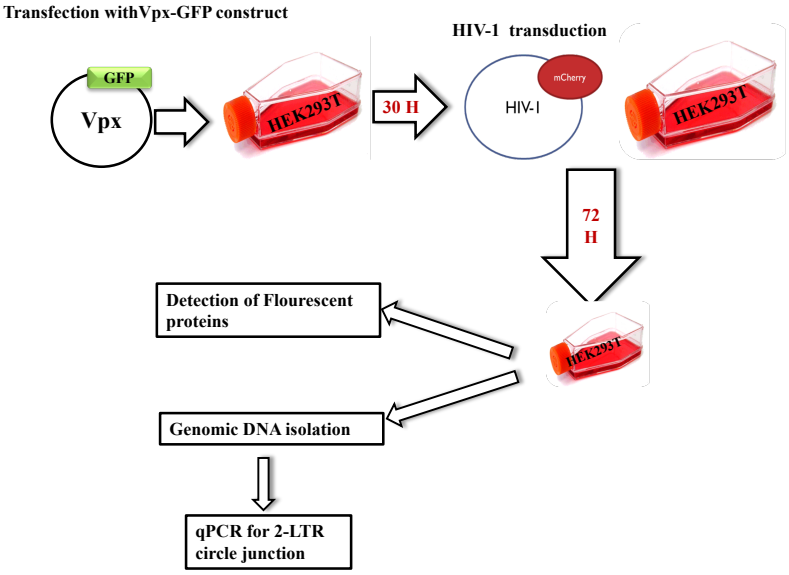

Figure 11. Representation of methods used to study the effect of pre-transfection of cells with HIV-2 vpx on HIV-1 superinfection

Detection of HIV-2 Vpx incorporation into HIV-1 pseudovirions

Schematic representation of methods used to detect the incorporation of Vpx into HIV-1 is provided in Figure 12.

Firstly, HEK293T cells were transfected with 10 µg of pcDNA3.1-Vpx-NeGFP vector in T75 flasks using PEI. After 30 hours of incubation (37°C, 5 % CO_2), the transfected cells were also transfected with 36 µg of plasmids used for HIV-1 ($psPAX_2$, pWOX-CMV-mCherry, and pMD.G in 3:2:1 ratio) using the abovementioned transfection protocol (see protocol in the section of *"Production of HIV-1 and HIV-2 viral particles"*). Pseudovirion-containing medium was then collected and filtered every 24 hours for 3 days, thereafter concentrated by ultracentrifugation (100 000 x g, 2 hours, 4°C). For control experiments, pTY-EFeGFP (a lentivector-based plasmid) was used instead of the pcDNA3.1-NeGFP plasmid in the co-transfection experiments. ELISA-based colorimetric RT assay was used to detect the reverse transcriptase activity from the harvested pseudovirions.

To detect the presence of Vpx in the harvested pseudovirions, western blot analysis was performed. Pseudovirions were lysed in pH 7.8 lysis buffer (50 mM Tris, 80 mM KCl, 25mM DTT, 0.75 mM EDTA, 0.5 % Triton X-100) and incubated for 30 mins at room temperature. 40 µl of the lyzed virions was loaded onto 14 % SDS polyacrylamide gel, then anti-Vpx monoclonal antibody (Kappes et al., 1993) and anti-p24 monoclonal antibody (Chesebro et al., 1992) were used as primary antibodies, and anti-mouse IgG (Sigma-Aldrich, St. Louis, MO, USA), was used as a secondary antibody. Blots were detected using SuperSignal West Femto Chemiluminescent substrate (Thermo Fisher Scientific, MA, USA) and the amount of pseudovirions was normalized to p24 capsid. (The following reagent was obtained through the NIH AIDS Reagent Program, Division of AIDS, NIAID, NIH: HIV-2 Vpx Monoclonal Antibody (6D2.6) from Dr. John C. Kappes, and anti-HIV-1 p24 Monoclonal (183-H12-5C) from Dr. Bruce Chesebro and Kathy Wehrly).

The harvested pseudoviorions were also used to transduce HEK293T cells using the previously mentioned transduction protocol referred to in the "*Transduction of HEK293T cells*" section. Fluorescence microscopy was used to detect positively transduced cells (EVOS FLoid Cell Imaging Station).

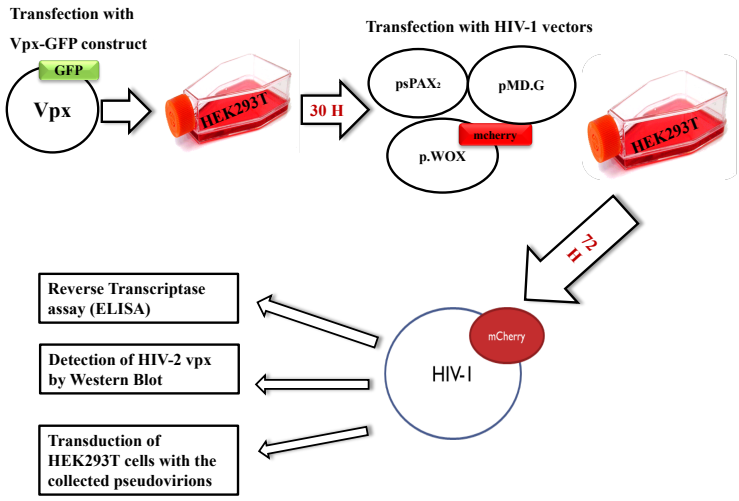

Figure 12. Schematic representation of methods used to detect HIV-2 Vpx incorporation into HIV-1 pseudovirions.

Experiments on THP-1 cells

Simultaneous and "superinfection" assays in THP-1 cells

THP-1 cells (ATCC Number: TIB-202) were plated for transduction in 96-well plate (5,000 cells/well) in 200 µl serum and antibiotic-free RPMI media containing 8 µg/ml polybrene. Cells were transduced with 10 ng RT-equivalent HIV pseudovirions. The day after the transduction, cells were complemented with 150 µl of RPMI containing 20 % FBS, and 2 % glutamine and incubated for 3 days. For HIV-1 superinfection, cells were plated in 50 µl of serum- and antibiotic-free RPMI media in 96-well plate, and then transduced with 10 ng of HIV-2 in the presence of 8 µg/ml polybrene, followed by incubation for 30 hours. Cells were then superinfected with 10 ng RT-equivalent HIV-1 virions, and supplemented with 200 µl of RPMI containing 20 % FBS and 2 % glutamine. After 3 days incubation, FACS analysis was carried out. HIV-1 or HIV-2 mono-infections were used as controls

Activation, transfection and transduction of THP-1 cells

50 nM phorbol 12-myristate 13-acetate (PMA) was used to activate THP-1 cells. ~ 15,000 cells per well were plated in 48-well plate in RPMI containing only 10 % FBS. After the addition of 50 nM PMA, the cells were incubated for 2 days. Differentiation of monocytes to adherent macrophages was detected by optical microscopy. Activated cells were transfected with 500 ng pcDNA3.1-Vpx-NeGFP or pcDNA3.1-NeGFP (mock) vectors using Lipofectamine LTX Reagent (Thermofisher Scientific, Massachusetts, USA), following instructions of the manufacturer, and incubated for 30 hours at 37°C, 5 % CO_2. Thereafter, the supernatant was changed to a fresh 300 µl RPMI medium, and cells were infected with 13 ng RT-equivalent of HIV-1. This was followed by 3 days of incubation, and fluorescent cells were detected using EVOS FLoid Cell Imaging Station and by flow cytometry.

Studying the effect of HIV-2 Tat Y44A mutation

Experiments in HEK293T cells

Detection of HIV-2 RT and Tat by Western-blot

HEK293T cells were transfected with HIV-2 CGP plasmid encoding for the wild-type or Y44A mutant Tat, HIV-2-CRU5SIN-CGW, and pMD.G plasmids as described in the "*Production of HIV-1 and HIV-2 viral particles*" section. As control, HEK293T cells were transfected only with 10 µg of HIV-2 CGP carrying wild-type HIV-2 *tat* using PEI.

To detect the presence of HIV-2 RT and Tat by Western-blot in pseudovirions, 1 ng of HIV-2 pseudovirions (normalized for p27 capsid) were suspended in lysis buffer (50 mM Tris, 80 mM KCl, 25 mM dithiothreitol (DTT), 0.75 mM EDTA, 0.5 % Triton X-100, pH 7.8), thereafter, incubated for 30 minutes at room temperature. 40 µl of the lysate was then loaded onto 12 % SDS polyacrylamide gel. After blotting of the proteins onto nitrocellulose membrane, the membrane was incubated either with Tat antiserum (Echetebu and Rice, 1993), anti-HIV-2 RT (Klutch et al., 1993), or anti-p24 monoclonal primary antibodies, followed by the use of secondary anti-rabbit IgG (BioRad, Hercules, CA, USA) for anti-Tat, and anti-RT antibodies and anti-mouse IgG; for anti-p24 monoclonal antibody (Sigma-Aldrich, St. Louis, MO, USA). SuperSignal West Pico Chemiluminescent substrate (Thermo Fisher Scientific, MA, USA) was used to detect the bands. (The following reagent was obtained through the NIH AIDS Reagent Program, Division of AIDS, NIAID, NIH: antiserum to HIV-2 Tat (466) from Dr. Bryan Cullen; and anti-HIV-2 ROD RT Polyclonal (Antigen 2) from Dr. Judith Levin).

To detect intracellularly expressed RT and Tat, HEK293T cells were transfected with 10 µg of HIV-2 CGP plasmid coding for either the wild-type or Y44A mutant HIV-2 Tat. 24 and 72 hours after transfection, transfected cells were mechanically scrapped in 5 ml ice cold PBS, then centrifuged for 10 minutes at 152 x g, and the pellet was suspended in 1 ml ice cold PBS. After a

brief sonication (Branson Sonicator, 3x2 minutes, 4°C), the cell lysate was centrifuged for 30 minutes (13,500 x g, 4°C). 30 µl of the supernatant (normalized to β-actin) was then loaded onto 10 % SDS polyacrylamide gel. HIV-2 Tat antiserum or anti-HIV-2 RT primary antibodies were used, followed by the use of secondary anti-rabbit IgG, and the SuperSignal West Pico Chemiluminescent substrate was used for detection.

Proximity Ligation assay (PLA)

For PLA assay, HEK293T cells were plated on polylysine pre-coated 8-well ibidi chambers (30,000 cells/well) (Ibidi GmbH, Gräfelfing, Germany) in 300 µl DMEM supplemented with 10 % FBS, 1 % penicillin-streptomycin and 1 % glutamine. At ~50 % confluency, cells were transduced with 2 ng (normalized for p27) of wild-type and Y44A Tat mutant HIV-2 pseudovirions, in 200 µl serum- and antibiotic-free media, supplemented with 8 µg/ml polybrene. Cells were incubated for 1 hour (37°C, 5 % CO_2), then the supernatant was discarded and the cells were washed with 100 µl PBS, and fixed with 8 % formaldehyde (Thermo Fisher MA, USA) for 30 minutes at room temperature. Cells were then washed twice with 100 µl PBS, and permeabilized with PBS containing 0.5% Triton-X 100 for 10 minutes at room temperature. The PLA protocol was performed according to the manufacturer's recommendations (Duolink ™ PLA Kit (Sigma-Aldrich, St. Louis, MO, USA) using anti-Vpx and anti-Tat antibodies in 1:100 dilutions. Interaction was detected by fluorescence microscopy using EVOS FLoid Cell Imaging Station.

Experiments in GHOST cells

Production of viral particles for transduction of GHOST cells

In regards to experiments on GHOST(3) parental cells (cat nb.: 3679) (Mörner et al., 1999) GHOST(3) Parental Cells (3679) were obtained through the NIH AIDS Reagent Program, Division of AIDS, NIAID, NIH: from Dr. Vineet N. Kewalramani and Dr. Dan R. Littman). We used HIV-

2 CGP as an expression vector, HIV-2-CRU5SIN-WPRE as a transduction vector, instead of HIV-2-CRU5SIN-CGW, and pMD.G. Pseudovirion production was performed using a slightly modified protocol: HIV-2 CGP, HIV-2-CRU5SIN-WPRE, and pMD.G plasmids were used in a 1:1:1 ratio. Preparation of HEK293T cells, collection of supernatant, virus concentration and detection of RT and capsid concentration was performed as described in the "*Production of HIV-1 and HIV-2 viral particles"* section.

Transduction of GHOST cells

GHOST cells were seeded in a 12-well plate (100,000 cells / well) in 1 ml DMEM supplemented with 7.5 % FBS, 1 % glutamine and 1 % penicillin-streptomycin the day before transduction. On the next day, the indicator cells were transduced with 5 ng (normalized for p27) HIV-2 virus in 1 ml serum- and antibiotic-free DMEM, augmented with 2 µg/ml polybrene, and incubated at 37°C, 5 % CO_2 for 2 hours, thereafter, 500 µl of DMEM containing 7.5 % FBS, 1 % glutamine, 1 % penicillin-streptomycin was added to the cells, followed by incubation at 37°C, 5 % CO_2 for 3 days. The medium was then removed and the cells were mechanically detached and suspended in 200 µl PBS. After short centrifugation (152 x g, 5 min), the PBS was changed to 500 µl PBS containing 1 % formaldehyde. To quantify the percentage of LTR-induced GFP positive cells, FACS analysis was performed (FACSCalibur, BD Biosciences, Singapore). Protocol of GHOST cell transduction was adopted and modified from *Vodros and Fenyo* (Vodros and Fenyo 2005).

Dot Blotting

1 ng (normalized for HIV-2 capsid) pseudovirions carrying wild-type or mutant (Y44A or Y55A) Tat were lyzed using the following lysis buffer: 50 mM Tris, 80 mM KCl, 25mM DTT, 0.75 mM EDTA, 0.5 % Triton X-100, pH 7.8; and incubated for 30 minutes at room temperature. 20 µl of the lysed pseudoviruses were loaded onto nitrocellulose membrane and detected using HIV-2 Tat anti-serum as a primary antibody, followed by the use of secondary anti-mouse IgG.

SuperSignal West Femto Chemiluminescent substrate (Thermo Fisher Scientific, MA, USA) was used to detect the blots.

Dot-blotting of the cell lysate was performed as follows: GHOST(3) indicator cells were transduced with 5 ng (normalized for p27) of wild-type or Y44A / Y55A mutant Tat HIV-2 pseudovirions, as mentioned above. After 3 days incubation, the medium was discarded, and cells were mechanically scraped in 3 ml of ice-cold PBS. Cells were then centrifuged for 6 minutes at 152 x g, and the pellet was dissolved in 500 µl lysis buffer (50 mM Tris-HCl, 250 mM NaCl, 0.5 % NP-40, 5 mM EDTA, 50 mM NaF, pH 7.4). and incubated on ice for 30 mins, while vortexed in every 10 minutes. Cells were then disrupted with sonication and centrifuged in the same conditions mentioned previously. 20 µl of supernatant was loaded onto nitrocellulose membrane. HIV-2 Tat anti-serum (Echetebu and Rice ,1993), followed by secondary anti-rabbit IgG (BioRad, Hercules, CA, USA) were used to detect HIV-2 Tat in the cell lysate. β-actin was used as a control (primary antibody: β-actin antibody (Covalab, Villeurbanne, France) and secondary anti-rabbit IgG). SuperSignal West Pico Chemiluminescent substrate (Thermo Fisher Scientific, MA, USA) was used to detect the dot blots.

Quantification of HIV-2 DNA in Whole Blood

DNA extraction from PM1, U1 cells and Whole Blood

DNA was extracted from 5 x 10^6 PM1 cells (modified CD4+ T-cell clone) (Lusso et al., 1995) and 5 x 10^6 U1 cells (subclones of U937 chronically HIV-1 infected cells) (Folks et al., 1987) using Qiagen QIAamp DNA Mini Kit according to the manufacturer's instructions. U1 cells were used as control to detect the specificity to HIV-2. Viral DNA was extracted from 200 µl of whole blood in the presence of 5 µg carrier RNA to increase the effiency of extraction using Qiagen QIAamp Blood DNA Mini Kit (Qiagen, Hilden, Germany) according to the manufacturer's instruction.

Preparation of HIV-2 standard for Real-Time PCR

Firstly, RNA was extracted from 1.44 x 10^{11} RNA-copies/ml of electron microscopy-counted HIV-2 particles using Qiagen miRNeasy micro Kit according to the manufacturer's instructions with minor modifications: extraction was performed in the presence of 5 µl carrier RNA (1 µg/ µl) (Qiagen, Hilden, Germany), increased volume of chloroform (200 µl), and the RNA was eluted in 30 µl of RNase-free water.

Secondly, cDNA synthesis was performed using SuperScript III One-Step RT-PCR System (Thermo Fisher Scientific, MA, USA) and Platinum Taq DNA polymerase (Thermo Fisher Scientific, MA, USA). Reactions were prepared in 25 µl solution containing: 2x reverse transcription buffer (0.4 mM of each dNTP, 3.2 mM $MgSO_4$), 1 µl of eluted total RNA (5,000 copies/µl), 100 ng forward and reverse primers (Forward Primer BEN_740F and BEN_1640R reverse primer) (100 ng/µl), 1 µl SuperScript™ III One-Step RT-PCR System with Platinum™ Taq DNA Polymerase (Thermo Fisher Scientific, MA, USA), and RNase/DNase–free sterile water up to the final volume. RT-PCR was carried out with an initial cDNA synthesis step for 30 min at 50 °C, followed by initial denaturation for 2 min at 94 °C, 35 cycles of 15 s at 94 °C, 30 s at 50 °C, 45 s at 68 °C, and a final elongation step for 5 min at 68 °C. PCR protocol of *Damond et al.* (2002) was used for HIV-2 qPCR with minor modifications. Product was visualized on 1% agarose gels stained with Gel Red, and was purified using QIAquick PCR purification Kit (Qiagen, Hilden, Germany) according to the manufacturer's instruction; concentration was then verified using NanoDrop ND-1000 spectrophotometer.

Preparation of PBDG standard for Real-Time PCR

PBDG fragment was amplified using two steps PCR (an outer and a nested PCR). The reaction was prepared in 25 µl solution. For outer PCR, the reaction contained 10 ng eluted DNA of PM1 cells, 0.125 µl Dream Taq DNA polymerase (5 U/µl), 5 mM dNTP mix and 100 ng primers (PBGD-

CF1 and PBGD-CR2). For nested PCR, the reaction contained 1 µl of outer PCR product, 0.125 µl Dream Taq DNA polymerase (5 U/µl), 5 mM dNTP mix and 100 ng primers (PBGD-CF1 and PBGD-CR1). Products were visualized on 1% agarose gels stained with Gel Red. Nested and outer PCRs were carried out with an initial denaturation of 2 min at 94 °C followed by 35 cycles of 30 s at 94 °C, 30 s at 55 °C, 45 s at 72 °C and a final elongation step for 5 min at 72 °C. PCR product was purified using QIAquick PCR purification Kit according to the manufacturer's instruction, then quantified using NanoDrop ND-1000 spectrophotometer. Sequences of primers for HIV-2 and PBDG standards are listed in Table 4.

HIV primers used for standard preparation			**Relative position of HIV-2**	
Name	Sequence of primers	bp	Start	End
BEN_740F	5'-GTG TTC CCA TCT CTC CTA GTC-3'	20	740	760
BEN_791F	5'-AAC AAG ACC CTG GTC TGT TAG-3'	20	791	811
BEN_1640R	5'-GAT TTC AGG CAC TCT CAG AAG-3'	20	1620	1640
PBDG primers used for standard preparation			**Relative position of PBDG**	
Name	Sequence of primers	bp	Start	End
PBDG-CF1	5'-TGC TCC CAG TTC TGA AGG TGC T-3'	22	4891	4913
PBDG-CR1	5'-AGG CTC CAC CAC TGA AGT AGA G-3'	22	5645	5666
PBDG-CR2	5'-ACT GCC CTA GGC TCC ACC ACT G-3'	22	5638	5659

Table 4. Primers used for HIV and PBDG standard preparation. HIV-2 BEN was used as a reference strain (GenBank accession number M30502), PBDG (porphobilinogen deaminase) was used a host gene for normalization (GenBank accession number M95623). (Bp: base pair; F: Forward; R: Reverse)

Quantitative real-time PCR analysis for detection of HIV-2 DNA

Reactions were prepared in 30 µl solution containing: 15 µl Thermo Fisher Maxima probe qPCR Master Mix (Thermo Fisher Scientific, MA, USA), 4 µM of probe, 100 ng/µl of each primer (Damond et al., 2002) and 8 µl of template DNA (concentration ranging between 800-1000 ng). Sequences of primers and probes were obtained from *Damond et al*. (Damond et al., 2002). Reactions were also prepared in the presence of 1 µg PM-1 cell's DNA in the same conditions as mentioned above. qPCR was carried out with an initial denaturation step at 95°C for 10 minutes,

followed by 40 cycles of 95°C for 15 seconds, 60°C for 30 seconds and extension at 72 °C for 30 seconds. For quantification, a series of ten-fold and two-fold dilution of the HIV-2 *gag* fragment corresponding to 10^6 to 1 copies DNA was used as a standard (see Figure 13).

HIV-2 DNA was normalized to the expression of PBDG housekeeping gene using 2 µM of probe, 50 ng/µl primers (sequences have been obtained from Mbisa et al. (2009)), 12.5 µl Thermo Fisher Maxima probe qPCR Master Mix, and 3 µl of template DNA (extracted DNA of uninfected and infected individuals). For quantification, a series of ten-fold of the PBDG fragment corresponding to 10^6 to 100 DNA copies was generated. The same PCR cycling conditions were used as mentioned previously for HIV-2 *gag* fragment.

HIV-2 DNA concentrations were firstly calculated as HIV-2 DNA copies/µl obtained from the qPCR reaction. Copy number of HIV-2 DNA was then normalized to PBDG. Finally, the results were reported as the number of copies/10^5 cells, using the following formula: (HIV-2 DNA copies per µl)/(PBDG copies per µl/2 chromosomes per cell) x 10^5 cells = HIV-2 DNA copies per 10^5 cells. Limit of detection (LOD) and limit of quantification (LOQ) were calculated using a formula described by *Schwarz et al.* (2004).

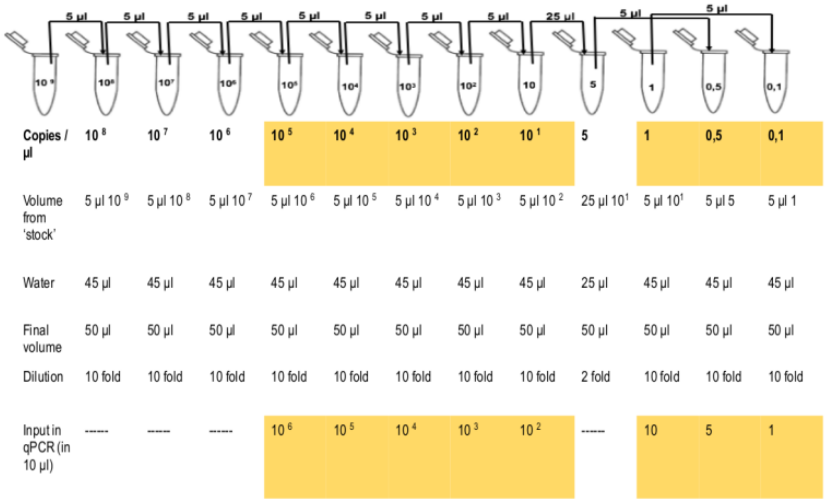

Figure 13. Schematic representation of the serial dilution of HIV-2 standard. Serial dilution of standard was prepared in 1.5 ml Eppendorf tubes by pipetting 5 µl from 10^9 'stock' to 10^8 copies/µl tube and adding 45 µl water. Yellow highlight indicates dilutions used to prepare the HIV-2 standard curve.

Ethical approval of HIV-2 DNA quantification from patient samples

Quantification of HIV-2 DNA was approved by the ethical committees of the National Health Ethics Committee in Guinea-Bissau (Ref 038/CNES/INASA/2016) and the Regional Ethical Review Board, Lund University, Sweden (Dnr 2016/426). All participants had received information about the study before inclusion, and provided oral and written informed consent. To ensure confidentiality, all study data were managed under code.

Analysis of the association between $CD4^+$ T-cell level and HIV-2 evolutionary rate

Population study of cohort in Guinea-Bissau

Samples were collected from a large cohort of police officers in Guinea-Bissau by members of the SWEGUB CORE group. The cohort was started in 1990 and continued until 2011 (Mansson et al., 2009) (Norrgren et al., 1995) (Esbjörnsson et al., 2012). Plasma samples were collected from selected individuals in 2013 as well. The cohort included 438 seroincident HIV-2 infected individuals. 83 members of the cohort had an estimated date of infection. It is worth mentioning that due to low viral RNA levels in HIV-2 infection, amplification of viral RNA was only successful in a few samples.

V1-C3 region of HIV-2 *env* was amplified from 53 samples collected from 16 individuals of a cohort of police officers in Guinea-Bissau (Mansson et al., 2009) (Norrgen et al., 1995). Median observation time of 16 participants was 19,2 years (interquartile range [IQR]: 15.0-20.8); median time between the first and last amplified sequence of participants was 7.9 years (IQR: 5.2-14.0).

Information of samples and individuals are presented in in Table 5, whereas AIDS have been defined by WHO stage 4 and CDC stage C (Hare, 2006) (Anonymous, 1999).

Individual	Date of infection	Observation time(months)	Sample date	Visit no*	AIDS†	ART†	Clones‡
DL3405	26-Jun-1999.	188	2001-10-20	IV	N	N	**11**
			2004-06-26	V	N	N	**8**
			2008-10-07	VII	N	N	**9**
DL3542	NA	241	1994-11-07	II	N	N	**9**
			2013-09-25	X	Y	N	**8**
DL2051	NA	252	1996-02-12	IV	N	N	**7**
			1997-09-26	V	N	N	**5**
			2002-07-31	VI	N	N	**11**
			2006-11-28	IX	N	N	**5**
			2009-10-07	X	N	N	**2**
DL2876	NA	174	1995-12-28	IV	N	N	**6**
			1996-12-19	V	N	N	**6**
			2000-08-23	VII	N	N	**9**
DL3654	02-Jul-1997	238	1998-02-04	III	N	N	**7**
			2013-09-27	IX	N	N	**7**
DL2533	NA	201	1991-04-19	I	N	N	**10**
			2001-12-04	V	N	N	**7**
			2002-07-24	VI	N	N	**4**
			2006-11-14	VII	N	N	**12**
DL2316	NA	149	2001-10-21	IX	N	N	**10**
			2002-07-22	X	Y	N	**7**
DL2794	12-Jun-2000	154	1993-11-10	II	N	N	**10**
			1996-04-08	IV	N	N	**7**
			2004-06-26	VIII	Y	N	**5**
DL3941	NA	226	2004-12-08	IV	N	N	**12**
			2008-09-18	V	N	N	**5**
			2010-03-10	VI	N	N	**8**
			2013-09-23	VII	Y	N	**6**
DL2381	NA	278	2003-03-13	VIII	N	N	**7**
			2004-06-10	IX	N	N	**11**
			2009-09-28	XI	N	N	**12**
DL2335	NA	278	2002-07-16	IV	N	N	**9**
			2003-11-14	V	N	N	**12**
			2004-11-05	VI	N	N	**12**
			2007-10-11	VII	N	N	**7**
			2009-09-29	VIII	Y	N	**2**
DL3647	NA	196	2001-06-25	IV	N	N	**9**
			2006-11-11	VII	Y	N	**5**
			2010-03-19	VIII	Y	N	**7**
DL3646	NA	238	1996-04-08	II	N	N	**9**
			2006-11-10	VII	N	N	**6**
			2008-10-04	VIII	N	N	**9**
			2009-10-19	IX	N	N	**10**
			2010-05-11	X	N	Y	**6**
DL3222	18-May-1994	178	1997-02-06	IV	N	N	**9**
			2001-07-26	V	N	N	**11**
DL3740	10-Jul-2004	236	2007-10-24	IV	N	N	**7**
			2009-03-30	V	N	N	**8**
			2009-10-23	VI	N	N	**4**
			2013-09-16	VII	N	Y	**9**
DL2386	29-Jul-1995	278	2008-10-16	VI	N	N	**5**
			2010-02-19	VII	N	N	**6**
			2013-09-26	**VIII**	**N**	**N**	**4**

Table 5. Characteristics of participants with successfully amplified HIV-2 env gene.

* Visit number are indicated in roman numerals; † Samples collected after patients developed AIDS or initiated antiretroviral therapy (ART)(N=no, Y=yes). AIDS was interpreted by WHO stage 4, when CD4+ T cell count is < 200 cells/µl and/ or CD4% < 14%. ‡ The number of clones from each sample.

Amplification and sequencing of V1-C3 region of HIV-2 *env*

HIV-2 RNA was extracted from plasma samples using Qiagen miRNeasy micro kit according to the manufacturer's instructions. Extraction and sequencing was performed by members of the Department of Laboratory Medicine, University of Lund. Viral RNA was extracted from 200 µl of plasma in the presence of 15 µg carrier RNA.

cDNA synthesis was performed from extracted RNA using SuperScript III One-Step RT-PCR System and Platinum Taq DNA polymerase, KH2_OF, and TH2_OR primer pairs. This was followed by a semi-nested PCR using Platinum Taq High Fidelity, KH2_OF, and KH2_OR primer pairs (MacNeil et al., 2007) (Barroso and Taveira, 2005). Sequences of primers are shown in Table 6.

One-step and nested-PCRs were carried out with an initial cDNA synthesis step for 30 min at 50 °C, followed by initial denaturation for 2 min at 94 °C, 40 cycles of 15 s at 94 °C, 30 s at 50 °C, 60 s at 68 °C, and a final elongation step for 5 min at 68 °C.

Amplified fragments were cloned into pCR2.1 TOPO cloning system, and then 12 individual clones were picked for subsequent sequencing.

HIV-2 V1-C3 region of *env* sequences were edited using CodonCode Aligner v1.5.2 and MEGA5 using the Clustal algorithm (Tamura et al., 2011).

HIV primers used for HIV-2 two-step PCR		
Name	Sequence of primers	bp
KH2_OF	5´-GAG ACA TCA ATA AAA CCA TGT GTC -3´	24
TH2_OR	5´-TTC TGC CAC CTC TGC ACT AAA GG-3´	23
KH2_OR	5´-ACC CAA TTG AGG AAC CAA GTC A-3'	22

Table 6. Primers used for amplification of HIV-2 *env*. HIV-2 BEN was used as a reference strain (GenBank accession number M30502), (Bp: base pair; F: Forward; R: Reverse)

Survival and phylogenetic analysis

Survival and phylogenetic analyses were performed by members of the Department of Laboratory Medicine, University of Lund. Kaplan-Meier analyses were performed for AIDS progression time, and log rank test was used for statistical comparisons.

To determine the non-significant interactions between covariates, Cox proportional-hazards model was used. PHI test was used to identify intra-patient recombinants (Bruen et al., 2006), then Maximum-likelihood (ML) phylogenetic trees were used to reconstruct the inferred model using Garli v2.0 (Zwick).

Internal branches were identified by Maximum-likelihood-based approximate likelihood ratio test (aLRT) Shimodaira-Hasegawa (SH)-like branch support, in PhyML 3.0, where SH-values of > 0.9 were significant (Guindon et al., 2010) (Anisimova et al., 2011). Subtype analysis was performed using reference sequences from Los Alamos database and Clustal algorithm (Tamura et al., 2011), then phylogenetic analysis was performed.

Evolutionary rate analysis of HIV-2 envelope

Evolutionary rate analyses were performed by members of the Department of Laboratory Medicine, University of Lund. BEAST v1.7.5 was used to reconstruct time-measured and Bayesian rooted phylogenetic trees. All analyses were performed by Markov Chain Monte Carlo (MCMC) $50x10^6$ generations with sampling every 2500-5000 generation, and effective sample sizes >100 and inspection of traces, as assessed in Tracer v1.6 (available from http://beast.bio.ed.ac.uk/software/tracer/), For every participant, two different clock models were used to estimate the nucleotide substitutions (uncorrelated lognormal relaxed and strict clock), and two different demographic models were also used for substitutions: Bayesian skyline plot and constant size.

To estimate the rate of substitutions, the Hasegawa, Kishino and Yano (HKY) substitution

model was used (Hasegawa et al., 1985), and exploratory analyses were performed by single analysis of $50x10^6$ MCMC generations. Results of duplicate analyses were combined in LogCombiner v1.7.5 (Drummond and Rambaut, 2007). Nucleotide (HKY) and codon (GY94 codon model) substitution rates were estimated for V1-C3 regions of HIV-2 *env* (Hasegawa et al., 1985) (Goldman and Yang, 1994). BEAST v1.7.5: hierarchical phylogenetic model (HPM) was used to compare the evolutionary rate between slow and fast disease progressors (Drummond and Rambaut, 2007) (Edo-Matas et al., 2011), and Bayes Factors (BFs) >3 were considered as a significant association (Kass and Rafter, 1995).

Absolute rates and divergence plots

The indicator of selection and molecular adaption is the ratio of nonsynonymous and synonymous rates (dN/dS rate ratio), which cannot be used to detect the simultaneous increases and decreases (Seo et al., 2004), thus, every branch in the tree of the substitution rate needs to be differed into expected nonsynonymous (E[N]) and synonymous (E[S]) substitution rates (Lemey et al., 2007). Analysis of expected nonsynonymous (E[N]) and synonymous (E[S]) substitutions and divergence plots were performed by members of the Department of Laboratory Medicine, University of Lund, based on publication of Lemey et al. (Lemey et al., 2007). For each individual, 200 random trees generated by HPM analysis were used to define the [N] and E[S] rates in HyPy 2.2.0 (Pond et al., 2005).

Analysis of selected sites of HIV-2 env

BEAST v1.8.1 (Drummond and Rambaut, 2007) was used to approximate the ratio of nonsynonymous (E[N]) and synonymous (E[S]) substitution at each codon, and identify the differences under positive and negative selection (Lemey et al., 2012), when dN/dS is equal to 1, there is a neutral selection, when the ration is >1 it suggests positive, when is it less then 1 it suggest a negative selection. The analysis was performed by Patrik Medstrand and his coworkers.

Analysis was carried out using strict clock model with HKY nucleotide substitution model (Hasegawa et al., 1985) and constant population size model.

Conservation analysis of HIV-2/SIVsmm envelope

For conservation analysis, reference sequences of HIV-2 and SIVsm *env* (N=61 and N=54) were downloaded from Los Alamos database, and Clustal algorithm was used for alignment. When amino acid positions showed 100 % identity, it was considered as conserved amino acid in HIV-2 and SIVsm *env* as well.

Surface accessibility of envelope protein

To quantify solvent-accessibility surface area of the HIV-2 gp125 (PBD ID:5cay), DSSP running web server was used (http://www.cmbi.ru.nl/xssp/) (Touw et al., 2015). Relative solvent accessibility (RSA) was calculated as described by Tien et al (Tien et al 2013). Residues were considered to be exposed on the surface when residues of RSA of ≥5% (Miller et al., 1987). HIV-2 envelope protein (PBD ID: 5cay) was used to visualize the surface exposed positively selected amino acids, by Chimera programe (https://www.cgl.ucsf.edu/chimera/).

Statistical analysis

One-way ANOVA analysis was performed to compare RT activities, transduction efficiencies and LTR-induced GFP positivity of wild-type and Tat mutant HIV-2 transduced GHOST cells, using GraphPad Prism 7.0.

For analysis of dual infection experiments: statistical analysis using One-way ANOVA analysis of variance for independent samples were used to show the difference of HIV-1 infectivity when a wild-type or mutant HIV-2 CGP vector, and when wild type or mutant Vpx coding pcDNA3.1-Vpx-NeGFP vector was used.

Regarding the phylogenetic analysis: IBM SPSS Statistics 21 was sued to perform statistical analyses for cohort study: two-tailed Mann-Whitney U test, two-tailed Fisher's Exact Test, Friedman's test for compare multiple groups and Spearman's rho for correlation analyses. Bonferroni corrected Wilcoxon signed rank test was performed after significant Friedman's tests.

RESULTS

Inhibitory effects of HIV-2 Vpx on the replication of HIV-1

Simultaneous or pre-transduction of cells with HIV-2 decreases the transduction efficiency of HIV-1 in HEK293T cells

Transfection and transduction efficiency of HIV-1 and HIV-2 vectors and pseudovirions was first optimized. Viral titers were determined by colorimetric reverse-transcriptase (RT) assay, and ranged from 1-3 ng RT / µl. Transduction efficiency of 10 ng RT-equivalent HIV in HEK293T cells ranged between 15-25 % for HIV-2 and 25-40% for HIV-1 (Figure 14 A and B). In the case of fluorescence transduction experiments, HIV-1 related fluorescency was significantly decreased by more than 60%, compared to HIV-1 mono-infected cells (P-value = 0.001), while HIV-2 related fluorescent signal did not change significantly (P-value = 0.7) (Figure 14 C-E and Figure 15 A). When HIV-2 transduced HEK293T cells were superinfected with HIV-1, the HIV-1 related fluorescent signal decreased by more than 80 % (P-value $\leq$ 0.01).This is indicating a protective nature of HIV-2 againts HIV-1 “superinfection” (Figure 15 B). To exclude that the observed difference is due to interference between the fluorescent proteins encoded by the pseudovirions, we carried out concominant dual transduction experiments, using HIV-1 virions coding for mCherry and GFP proteins. No significant difference was observed in the fluorescence signal of mCherry (Figure 15 C).

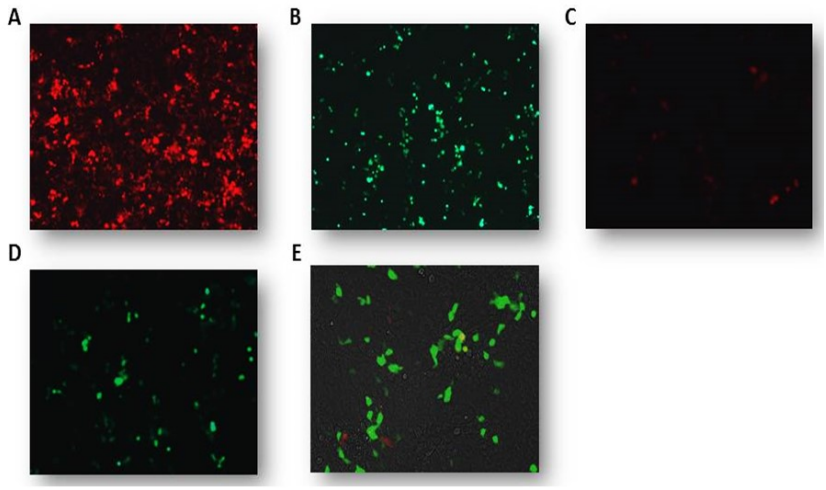

Fig 14. **Analysis of transduction efficiency**. Fluorescence microscopy was used to detect cells positively infected with HIV-1 (mCherry) and HIV-2 (GFP). **A:** Cells transduced with HIV-1, **B:** cells transduced with HIV-2, **C:** Simultaneous HIV-D (HIV-1), **D:** Simultaneous HIV-D (HIV-2) and **E:** an overlay of mCherry and GFP fluorescence in HIV-D.

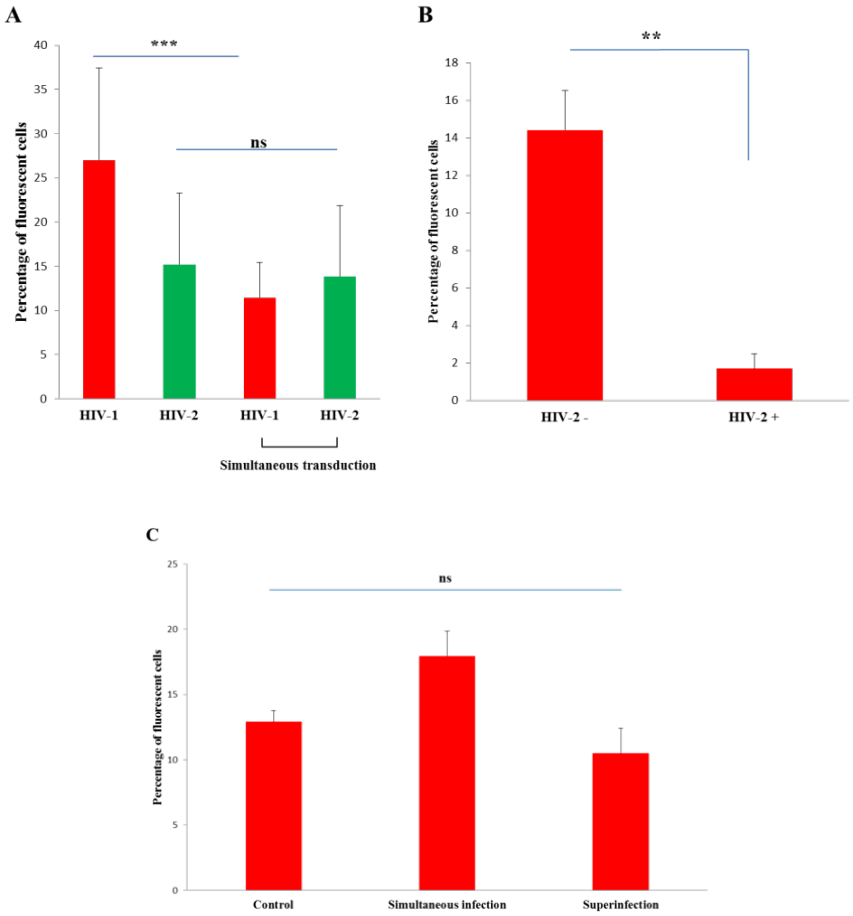

Figure 15. Analysis of HIV-1 and HIV-2 dual "infections". HIV-1 (mCherry) and HIV-2 (GFP) related fluorescent signals were affirmed by flow cytometry. **A:** Simultaneous transduction: HIV-1 fluorescence decreased by 60% (*** P-value = 0.001), while that of HIV-2 remained unaltered (P-value = 0.7). **B:** HIV-1 "superinfection": 80% decrease of mCherry fluorescence in HIV-1 positive cells (** P-value ≤ 0.01). **C:** Effect of Fluorescent proteins on dual transduction, when dual "infection" was repeated using only HIV-1 pseudovirions, where one encodes mCherry, and the other coding for GFP. Results show the positivity of mCherry detected after simultaneous dual transduction (P-value= 0.18), and supertransduction (P-value=0.36).

HIV-2 Vpx protects cells against "superinfection" with HIV-1

Based on the findings of dual transduction experiments, we aimed to determine which HIV-2 protein plays a role in the inhibitory mechanism of HIV-2 against HIV-1 "superinfection". HEK293T cells were transfected with CGP plasmid carrying defective HIV-2 genes, and the cells were "superinfected" with HIV-1 pseudovirions. A CGP vector coding for an active-site mutant HIV-2 protease was used to study the effect of the lack of Gag and Gag-Pro-Pol processing effect on HIV-2 induced inhibition of HIV-1.

Following transfection of cells with HIV-2 CGP vector coding for a defective protease, Rev, Tat, Vpr and Vif, HIV-1 transduction efficiency decreased by 40 %, 30 %, 51 %, 36 % and 45 %, respectively (Figure 16). The decrease in HIV-1 "infectivity" was comparable to that observed when HEK293T cells were pre-transfected with the wild-type CGP plasmid. This was statistically proven using One-Way analysis of variance of independent samples (P-values = 0.02-0.04). HIV-1 "infectivity" was not altered when cells were pre-transfected with the control HIV-2-CRU5SIN-WPRE vector; a minimal HIV-2 vector with GFP expression cassette lacking viral enzymes and regulatory and accessory genes. However, when cells were first transfected with HIV-2 CGP vector encoding a functionally restricted Vpx, HIV-1 "infectivity" was restored (* P-value ≤ 0.05), reaching levels similar to those obtained in mock-transfected cells (P-value = 0.32). These findings suggest that the presence of an active Vpx may be involved in the inhibition of superinfection by HIV-1.

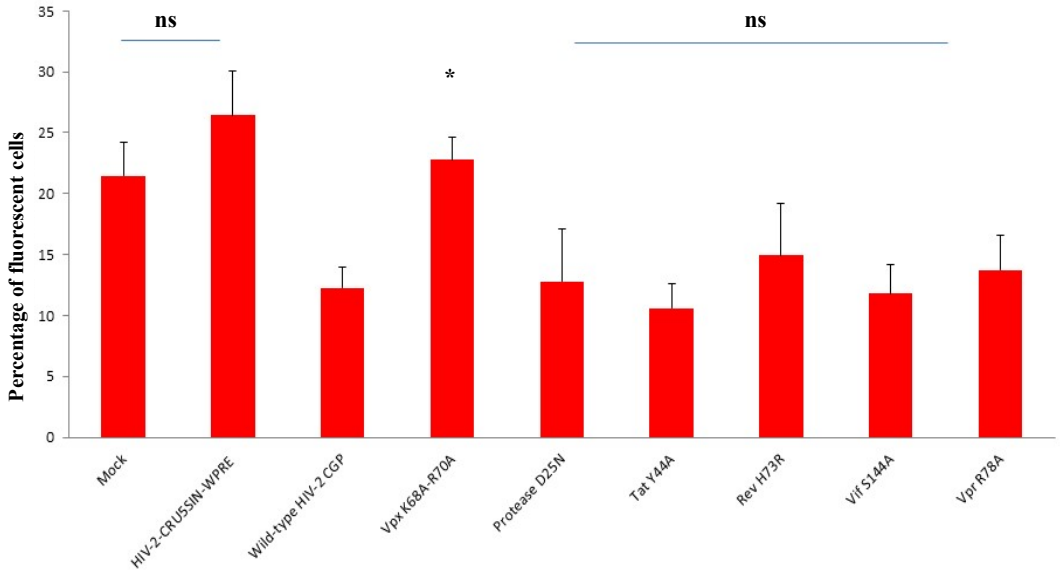

Figure 16. HIV-1 transduction of HEK293T cells pre-transfected with mutant HIV-2 protease/ regulatory (tat and rev) / accessory (vif, vpx, vpr) genes. HEK293T cells were transfected with CGP (HIV-2 based vector) carrying defective accessory/regulatory/ protease, followed by transduction with 15 ng HIV-1 (RT-equivalent). Results show percentage of HIV-1-infected cells from triple measurements. (ns: non-significant) (* P-value ≤ 0.05).

HIV-1 transduction of GFP-Vpx expressing cells

Based on the previous findings, HEK293T cells were transfected with pcDNA3.1 vector coding for HIV-2 Vpx in fusion with Green fluorescent protein (GFP) (pcDNA3.1-Vpx-NeGFP), followed by transduction with HIV-1. The sequence of the encoded *vpx* gene is identical to that found in the wild-type HIV-2 CGP vector. A mock vector was designed by restriction of the *vpx* coding sequence from the pcDNA3.1 plasmid using KpnI and XbaI restriction endonucleases. Transfection efficiency of pcDNA3.1-Vpx-NeGFP and the mock vector was measured by flow cytometry, and was found to be > 90 %. In the presence of HIV-2 Vpx, HIV-1 infectivity (transduction efficiency) was reduced by more than 80 % compared to the control transduction (Figure 17 A). Furthermore, HIV-1 transduction of HEK293T cells pre-transfected with a functionally restricted (K68A-R70A) mutant Vpx did not resulted in reduction of HIV-1 transduction efficiency (see Figure 17 B). Western blotting was used to detect the intracellular expression of Vpx following transfection with pcDNA3.1-Vpx-NeGFP and HIV-2 CGP vectors

(see Figure 17 C). These results indicate that HIV-2 Vpx plays a crucial role in the inhibition of HIV-1's replication.

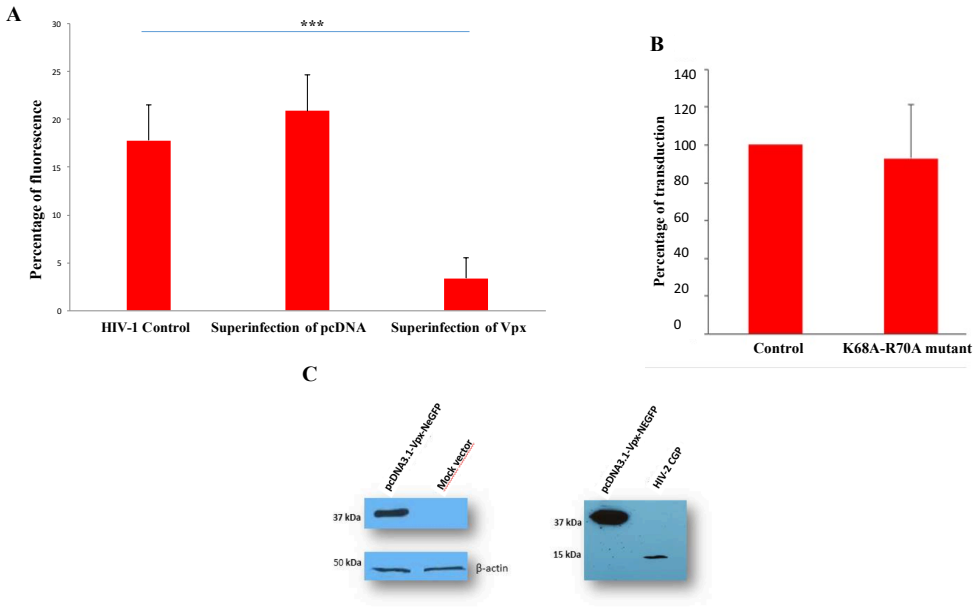

Figure 17. Transduction analysis in HEK293T cells. A: Western blotting of HIV-2 Vpx. Estimated molecular weight of HIV-2 Vpx was found to be ~ 13 kDa. Cells transfected with vectors coding for HIV-2 Vpx were lysed, and an anti-Vpx monoclonal antibody was used to detect expression of the protein. Mock vector used was a pcDNA3.1-NeGFP vector devoid of HIV-2 *vpx*. **B:** HIV-1 transduction of Vpx-transfected cells. Cells were first transfected with HIV-2 Vpx-GFP fusion protein followed by transduction with HIV-1. Results show percentage of positive HIV-1 cells from triplicate measurements (*** P-value ≤ 0.001). As a mock transfection, cells were transfected with pcDNA3.1-NeGFP plasmid devoid of the *vpx* gene. **C:** HIV-1 transduction of K68A-R70A mutant Vpx-transfected cells. Cells were first transfected with a vector coding for a functionally restricted Vpx, thereafter transduced with HIV-1 pseudovirions. Results show that a functionally restricted Vpx did not alter infectivity of HIV-1. Percentage of fluorescence was adjusted to allow for comparison with HIV-1 transduction of native cells.

Effect of Vpx on the replication of HIV-1

To characterize the inhibitory effect of HIV-2 Vpx on HIV-1, we performed qPCR of HIV-1 2-LTR junctions from isolated DNA. When HEK293T cells were first pre-transfected with a Vpx-GFP coding plasmid, followed by transduction with HIV-1 pseudovirions, the copy number of 2-LTR circle junctions were reduced by > 40 % (P-value < 0.01) (Figure 18). Furthermore, p24 capsid production and RT-activity were hampered (Figure 19 A and B). pTY-EFeGFP lentiviral vector was used as a control vector (see Figure 19 C).

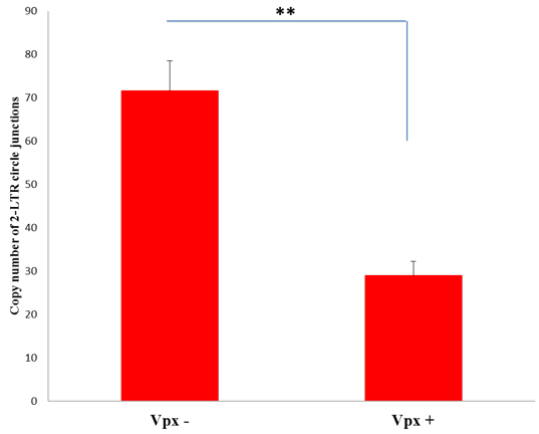

Figure 18. qPCR analysis Vpx transfected and HIV-1 transduced cells. 2-LTR circle junctions were decreased by more then 40% in the presence of Vpx (** P-value ≤ 0.01), compared to HIV-1 transduced HEK293T cells. Results show 2 LTR circle quantity from triplicate measurements.

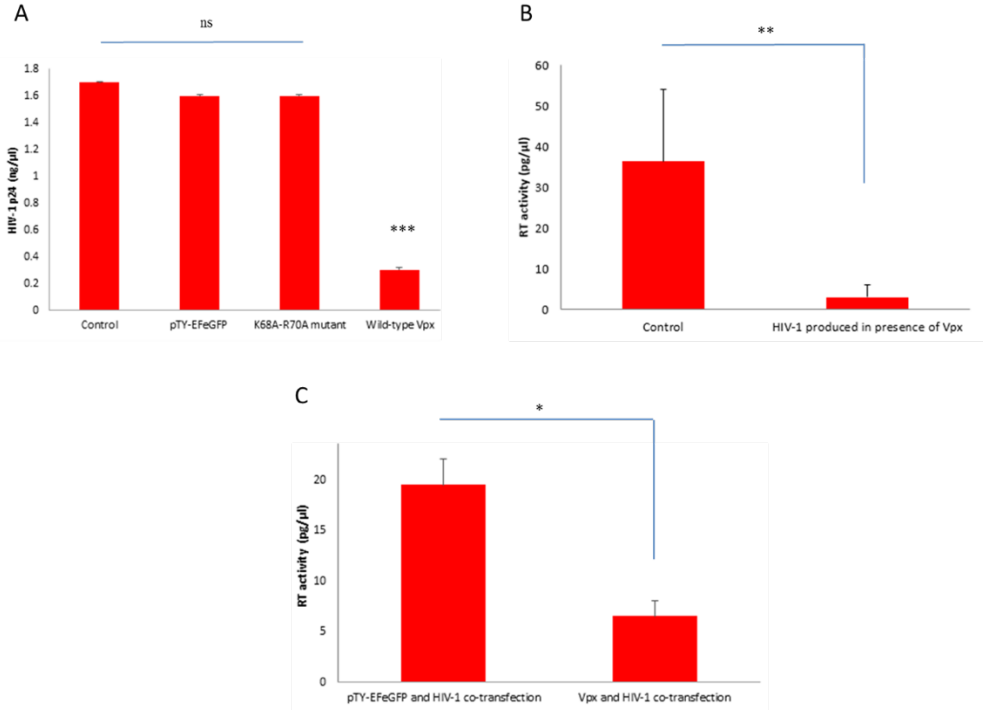

Figure 19. HIV-1 and Vpx co-transfection experiments. A: Quantification of HIV-1 p24 production. When HIV-1 pseudovirions were produced in the presence of wild-type Vpx, level of p24 capsid was significantly decreased compared to HIV-1 control virus production. (*** P-value ≤ 0.001). In the presence of functionally restricted K68A-R70A Vpx mutant and mock plasmid pTY-EFeGFP, amount of p24 protein level did not change significantly. **B:** HIV-1 RT activity was also decreased in the presence of Vpx (** P-value ≤ 0.01). **C:** pTY-EFeGFP vector was used in our control experiments, and RT activity of harvested virions were significantly changed in the presence of wild-type Vpx compared to mock vector co-transfected virions (* P-value ≤ 0.05).

Vpx-GFP incorporation into HIV-1 pseudovirions

We studied whether or not Vpx-GFP is incorporated into HIV-1 pseudovirions. For this, HIV-1 pseudovirions were produced and collected from cells pre-transfected with a plasmid coding for Vpx-GFP. Western blotting was used to detect the presence of the 37 kDa Vpx-GFP fusion protein

from lyzed pseudovirions, and p24 capsid was used for normalization (Figure 20 A). The harvested virions were used to transduce HEK293T cells, and the presence of Vpx-GFP was confirmed using a fluorescent microscope (see Figure 20 B).

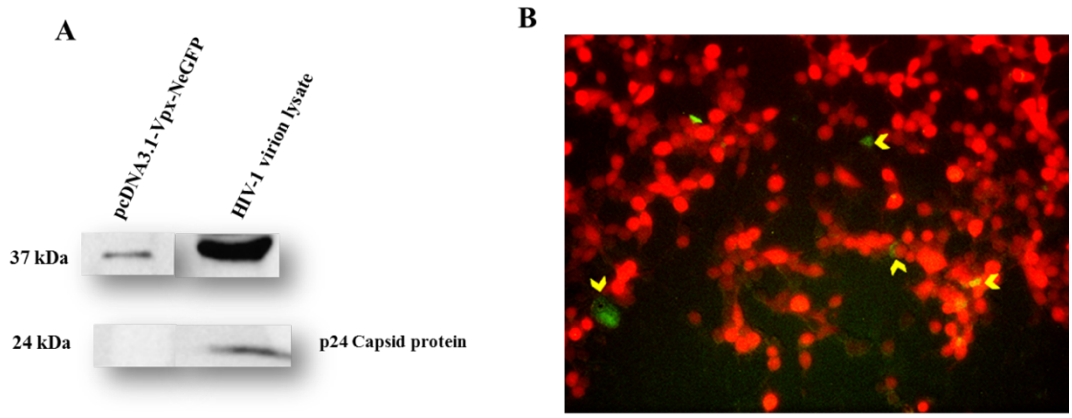

Figure 20. **Vpx incorporation into HIV-1 pseudovirions A:** Western blotting of HIV-1 virions produced in Vpx-transfected HEK293T cells. Anti-Vpx antibody was used to detect the approximately 37 kDa sized Vpx-GFP fusion protein from lysed pseudovirions and anti- HIV-1 p24 antibody was used as a control. **B:** These previously mentioned virions were used to transduce HEK293T cells, and then infection related fluorescency was detected by using fluorescence microscopy. Yellow arrowheads indicate the presence of Vpx-GFP protein.

Experiments on THP-1 cells

Protocols were optimized for transduction of THP-1 cells by HIV-1 and HIV-2 pseudovirions. Transduction efficiency of HIV-2 was higher compared to that of HIV-1 (less then 5 % for HIV-1). This decreased efficiency of HIV-1 transduction is attributed to the presence of a cellular restriction factor, SAMHD1 in cells of monocytic lineage (Uhlen et al., 2015). When THP-1 cells were transduced with both HIV-1 and 2 pseudovirions concomitantly, or when HIV-1 "superinfection" followed pre-transduction with HIV-2, the transduction efficiency of HIV-1 did not change significantly (Figure 21 A). To minimize the interaction between Vpx and SAMHD1, THP-1 cells were activated and differentiated into macrophages using phorbol 12-myristate 13-acetate (PMA). This was then followed by transfection with the pcDNA3.1-Vpx-NeGFP plasmid encoding for the Vpx-GFP fusion protein. Transfection efficiency was confirmed by flow cytometry and fluoresce microscopy, and resulted in 15-20 % fluoresence. It is worth mentioning that when THP-1 cells were first pre-transfected with Vpx-GFP, and then transduced by HIV-1;

HIV-1-related mCherry fluorescence was restored, indicating increased transduction efficiency, which may be the result of proteosomal degradation of SAMHD1 by Vpx (Figure 22 D).

In activated THP-1 cells, similarly to results obtained in HEK293T cells, pre-transfection with wild-type Vpx decreased the transduction efficiency of HIV-1 (* P-value ≤ 0.05) (Figure 21 B).

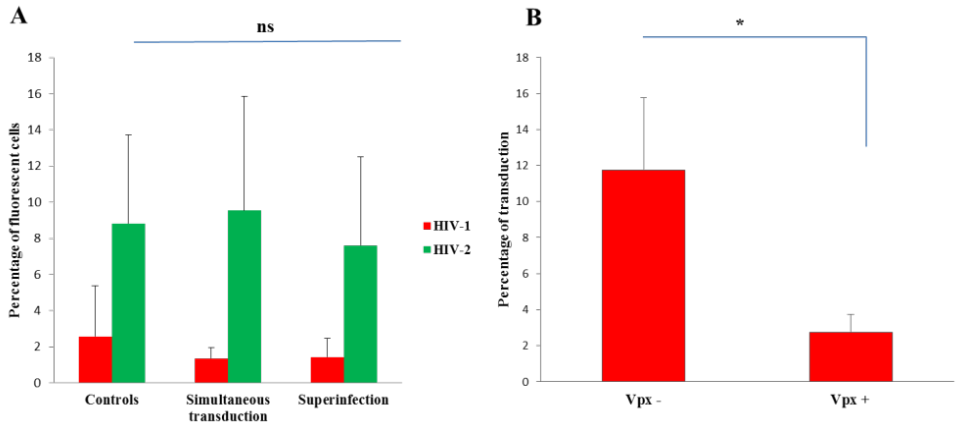

Figure 21. Transduction of THP-1 cells. A: Simultaneous and HIV-1 "superinfection" in undifferentiated THP-1 cell line. No significant reduction was observed in the transduction efficiency of HIV-1 in either the dual or sequential transductions. **B:** HIV-1 transduction of Vpx pre-transfected differentiated THP-1 cells. When HIV-1 transduction was performed on Vpx-transfected macrophages, HIV-1 infectivity was significantly reduced (* P-value ≤ 0.05).

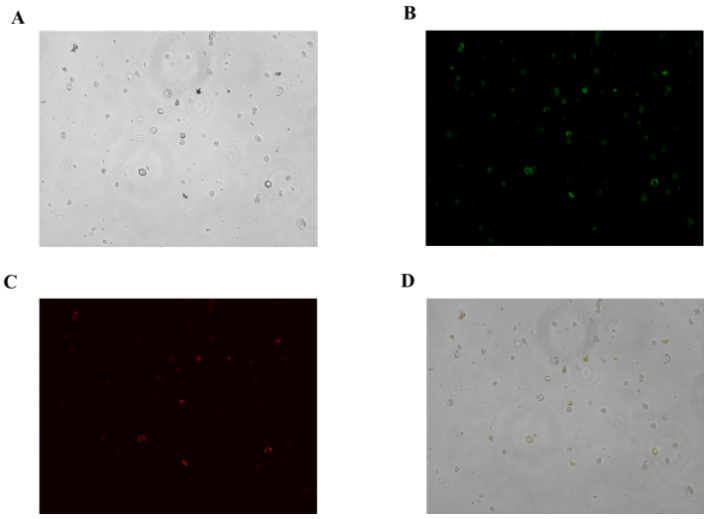

Figure 22. **Fluorescence microscopy of transfected and transduced THP-1 cells**. THP-1 cells were pre-transfected with pcDNA3.1-Vpx-NeGFP vector, and thereafter transduced with HIV-1 pseudovirions. **A**: native picture of THP-1 cells, **B**: Vpx-related GFP fluorescence of transfected cells, **C**: HIV-1 transduction-related mCherry fluorescence, and **D**: superimposed picture of GFP and mCherry fluorescence.

Effects of Y44A mutation in the acidic domain of HIV-2 Tat on the expression and activity of RT, and the transactivation of proviral genome

In silico characterization of HIV-2 Tat mutations

Effects of mutations in HIV-2 Tat protein focusing on the acidic domain were examined by *in silico* methods. Sequence- and homology model structures were used to predict and identify a residue to destabilize the Tat protein. Disorder predictions show that while the central region (39-78 residues) of the protein has a globular nature, both N- and C-termini are unstructured. It is worth mentioning that Cys-rich domain of HIV-1 Tat have a flexible nature (Bayer et al., 1995), our predictions of the Cys-rich domain of HIV-2 Tat show that it may be structured (see Figure 4).

SWISS-MODEL repository was used to map potentially destabilizing mutations, as no crystal or NMR structures are available for HIV-2 Tat. Since homology models are not available for the full-length, only for truncated proteins, we chosed those models which are predicted to be globular for the entire region. To map possible inactivating mutations, structure-based methods were performed. Alanine-scanning was performed using FoldX algorithm and SDM server. Changes in stabilities upon point mutations were calculated for the full-length protein, with the exception of A7, A28, and A33 residues. Mutations which showed destabilizing nature of alanine-substitution by both methods were found to be within, or near the globular region of the protein (see Figure 23A). Mutations of these residues (G36, L40, Y44, L47, L72, and G80); mainly in the central region of the protein, may induce changes in the structure and stability of the protein, which was proven using sequence-based prediction by I-Mutant server (see Figure 23 B). Except for Y44; which is a hydrophilic sidechain, the predicted residues are hydrophobic. Substitution of this large polar Tyr sidechain to a small hydrophobic Ala may result in loss of potential hydrogen bond interactions. Based on these results of stability analyses, I-Mutant 2.0 was used to predict the effect of substitutions at the 44th Tyr, and Y44A mutation was predicted to be the most destabilizing on protein structure (Figure 23 C).

Previous studies on SIV and HIV-1 Tat proteins reported that Tyr to Ala substation leads to the inactivation of the protein (Verhoef et al., 1997) (Das et al., 2007). Both Tyr residues at position 44 for HIV-2 and 55 for SIV are located in the N-termini of the proteins, and Y55 is equivalent to the Y26 in HIV-1. Stability analyses were used to compare the effects of the point mutations (Y44A and Y55A) on protein stability (see Figure 23 D). By using three different methods for prediction, a destabilizing nature of Y44A mutation in both analysed model structures was shown. IUPred2A and Jpred4 servers were used to predict the effect of Y44A and Y55A mutations in the secondary structure of HIV-2. Based on our secondary structure predictions for Y44A and Y55A in HIV-2, both mutations indicate disruption of the α-helix at the N-terminal part of the globular region, and in the case of Y44A substitution, a higher probability for helical arrangement of the Cys-rich domain was observed (Figure 24).

Both Y26 (for HIV-1) and Y55 (for SIV) residues are highly conserved, based on available data in the HIV Sequence Compendium (2018; https://www.hiv.lanl.gov). Polymorphism analysis of the first two domains of HIV-2 Tat protein was performed on sequences from different subtypes, based on data available in the HIV Sequence Compendium (Table 7). Similarly to its counterpart, HIV-2 Tat also contains conserved Tyr residue in the Cys-rich domain (Y55), and the Tyr residue in the 44th position also shows high conservation (Figure 25 A), especially in group B (Figure 25 C), however, His and Phe variations were observed in epidemic and non-epidemic strains (Figure 25 B and D).

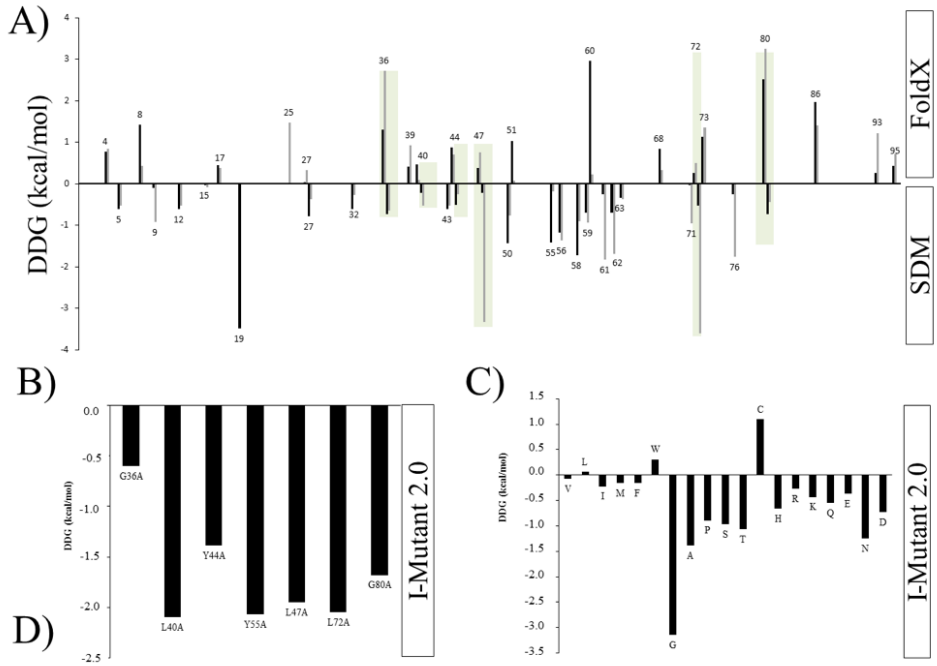

Prediction type	Method	Y44A				Y55A			
		ΔΔG (kcal/mol)			change of stability	ΔΔG (kcal/mol)			change of stability
		1tvs.1	1tvt.1	average		1tvs.1	1tvt.1	average	
Structure-based	FoldX	0.875	0.709	0.792	decreased	-1.721	0.059	-0.831	increased
Structure-based	SDM	-0.51	-0.26	-0.39	decreased	-1.41	-0.19	-0.80	decreased
Sequence-based	I-Mutant 2.0	-1.39		-	decreased	-2.07		-	decreased

Figure 23. Mapping of destabilizing mutations. A: Alanine-scanning of HIV-2 Tat performed by FoldX and SDM. Wild-type and mutant proteins have been compared based on the free energy levels (DDG, kcal/mol) and residues regarded to be destabilizing for both model structure (by black and grey for 1tvs.1 and 1tvt.1 models, respectively) were plotted on the graph. For FoldX server Ala substitutions causing DDG > 0 kcal/mol change, while in SDM DDG < 0 kcal/mol change in stability are considered to be destabilizing. Mutations in the globular regions are highlighted in green. **B**: Residues selected considered to destabilize the protein (see figure part A) have been analyzed by I-Mutant 2.0 to predict the effect of alanine-substitutions. Negative values (kcal/mol) indicate decreasing nature of the mutations. **C:** Effect of substitution in Y44 residue was predicted by using I-Mutant 2.0 server. **D:** Comparison of predicted effect of Y44A and Y55A mutations. Values obtained for both homology model structures are shown (SMTL IDs: 1tvs.1 and 1tvt.1). Stability change was considered to be increased or decreased, based on average values. Figure was constructed with the aid of Dr. Mótyán János András

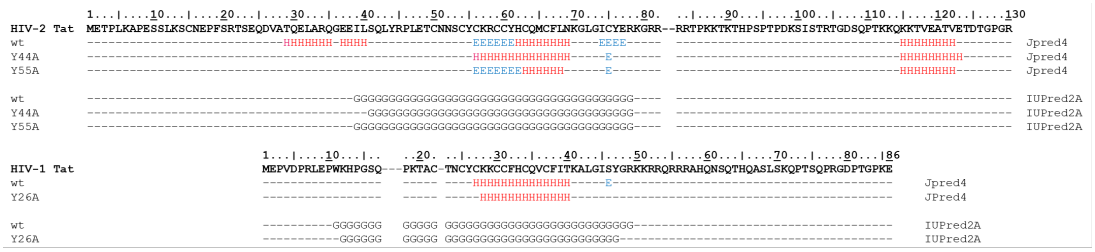

Figure 24. Effects of Y44A and Y55A substitutions on secondary structure and globular regions. For predictions, amino acid sequences of the wild-type HIV-1 and HIV-2 Tat proteins were used. Jpred4 was used to predict secondary structures for the wild-type and mutant proteins, where H stands for α-helices and E indicates β-strands. And IUPred2A was used for residues predicted to constitute globular regions are shown by G. Figure was constructed with the aid of Dr. János András Mótyán.

Accession number	Name	Subtype	Isolation year	Isolation country	Protein ID
U38293	A.CI.88.UC2	A	1988	Cote d'Ivoire	AAB47786.1
M30502	A.DE.x.BEN	A	1990	Germany	AAB00741.1
U22047	A.DE.x.PEI2_KR_KRCG	A	1995	Germany	AAA64580.1
KY025539	A.FR.93.LA37	A	2000	France	APJ01780.1
Z48731	A.GW.x.MDS	A	2006	Guinea-Bissau	CAA88625.1
MF595856	A.NL.01.RH2.13	A	2001	Netherlands	ATU79188.1
EU980602	A.IN.07.NNVA	A	2007	India	ACH73025.1
DQ307022	A.IN.95.CRIK_147	A	1995	India	ABC39622.1
AB731742	A.JP.08.NMC786_clone_41	A	2008	Japan	BAM76177.1
AF082339	A.PT.x.ALI	A	1998	Portugal	AAC95345.1
M15390	A.SN.85.ROD	A	1985	Senegal	AAB00768.1
L17625	B.CI.88.UC1	B	1988	Cote d'Ivoire	AAA43940.1
AB485670	B.CI.x.20_56	B	2009	Cote d'Ivoire	BAH97699.1
U27200	B.CI.x.EHO	B	1994	Cote d'Ivoire	AAC54471.1
KY025545	B.FR.00.LA44	B	2000	France	APJ01830.1
KY025544	B.FR.98.LA43	B	1998	France	APJ01822.1
AB100245	B.JP.01.IMCJ_KR020_1	B	2001	Japan	BAC79371.1
KP890355	F.US.08.NWK08	F	2008	United States	ALA65441.1
AF208027	G.CI.92.Abt96	G	1992	Cote d'Ivoire	AAF82033.1
EU028345	AB.CM.03.03CM_510_03	AB	2003	Cameroon	ABV83030.1
L36874	H2_01_AB.CI.90.7312A	H2_01_AB	1990	Cote d'Ivoire	AAL31357.1
AB731738	H2_01_AB.JP.04.NMC307_20	H2_01_AB	2004	Japan	BAM76141.1
AB731740	H2_01_AB.JP.07.NMC716_01	H2_01_AB	2007	Japan	BAM76159.1
AY530889	U.FR.96.12034	U	1996	France	AAT37067.1

Table 7. Sequences of HIV-2 Tat used in polymorphism analysis for the first two domains of the protein. Data regarding sequences include accession numbers, the isolation year, country of isolation, protein ID and sequence name.

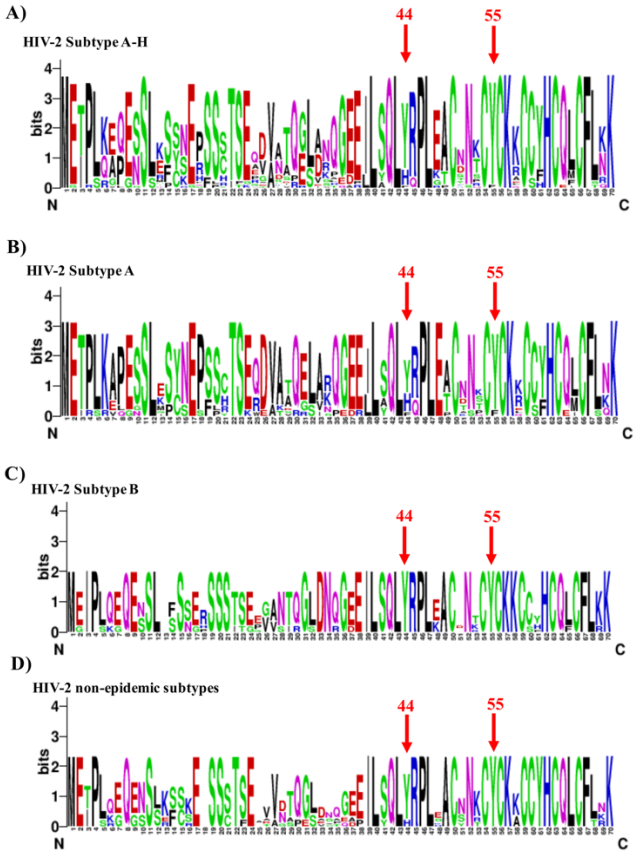

Figure 25. Genetic diversity of N-terminal domains of HIV-2 Tat. HIV-2 Tat sequences of epidemic (group A and B) and non-epidemic groups were collected from the Los Alamos National Laboratory (LANL) HIV sequence database (2019. 10. 28). ClustalW was used to align multiple amino acid sequences, and divergence of sequences was schematically visualized using Weblogo until the 70th residue. **A:** Sequence logo showing the Tat amino acid diversity observed until position 70 in all HIV-2 groups, **B** and **C:** Diversity in epidemic groups A and B and **D:** polymorphism represented in non-epidemic groups of HIV-2. Red arrows indicate positions of 44th and 55th amino acids.

In vitro characterization of HIV-2 Y44A mutant Tat

To confirm the predicted destabilizing nature of the designed amino acid substitution, and to explore the effects of Y44A mutation on the function of Tat and activity of RT, HIV-2 vector carrying the modified *tat* gene was prepared and used for *in vitro* experiments. Furthermore, Y55A mutant was also studied for comparison in some of the experiments. HIV-2 *tat* was inactivated in the CGP vector using site directed mutagenesis.

ELISA-based colorimetric SIV p27 (capsid) assay was used to determine the viral titers, which yielded 16-18 ng/mL for wild-type and mutant pseudovirions. HIV-2-CRU5SIN-WPRE was used

to produce HIV-2 pseudovirions for experiments performed on GHOST HIV indicator cells, and no difference in capsid amount was observed between the mutant and wild-type virions

Transduction efficiency of the wild-type and mutant Tat HIV-2 pseudovirions in HEK293T cells using 6 ng of viruses (normalized for capsid) was confirmed by flow cytometry, and no significant difference in GFP expression was observed between the wild-type and mutant pseudovirions (P values 0.95 and 0.44, respectively) (Figure 26). This observation was expected, since GFP expression in the HIV-2-CRU5SIN-CGW is driven under a CMV promoter. A pseudovirion carrying an inactivating mutation in the active site of the protease (D25N) was used as a negative control, which resulted in a complete abolishment of viral infectivity.

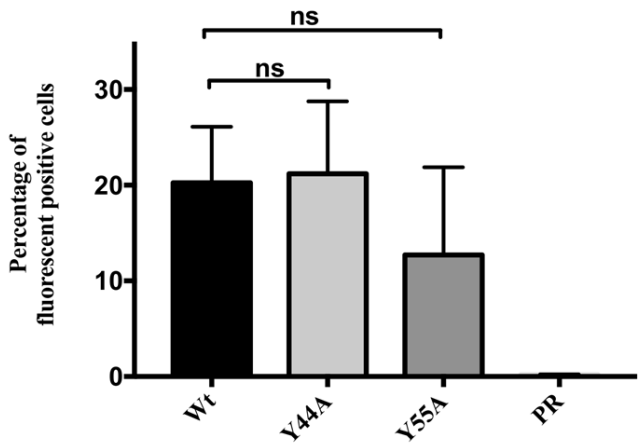

Figure 26. Effect of Y44A and Y55A Tat mutations on transduction efficiency of HEK293T. HEK293T cells were transduced with 6 ng of pseudovirions (normalized by capsid ELISA) (n=3). Percentage of fluorescent positive cells was measured by flow cytometry. In the presence of Y44A and Y55A mutations, percentage of transduction efficiency did not change significantly compared to the wild-type HIV-2. Wt: wild-type, PR: active-site protease mutant.

Experiments in GHOST(3) cells

GHOST(3) cells contain a *tat*-dependent HIV-2 LTR-GFP construct, and a GFP fluorescence is obtained in response to transduction with a functional Tat. To examine the effect of Tyr mutations on Tat-induced HIV LTR transactivation, HIV indicator cells were infected with 5 ng (normalized for p24 capsid) of virions. GFP fluorescence signal was significantly decreased by more than 93 % and 91 % in the presence of HIV-2 Tat Y44A and Y55A mutations, respectively

(P value < 0.0001), compared to that of the wild-type (Figure 27 A). The pseudovirions used were produced using the HIV-2-CRU5SIN-WPRE transducing vector instead of the HIV-2-CRU5SIN-CGW, thus, the fluorescence obtained was only attributed to Tat-induced LTR transactivation, since the HIV-2-CRU5SIN-WPRE vector did not contain a CMV driven GFP expression. Furthermore, dot-blotting was used to confirm the presence of HIV-2 Tat from cell lysate, following transduction, and also in the virions (Figure 27 B and C).

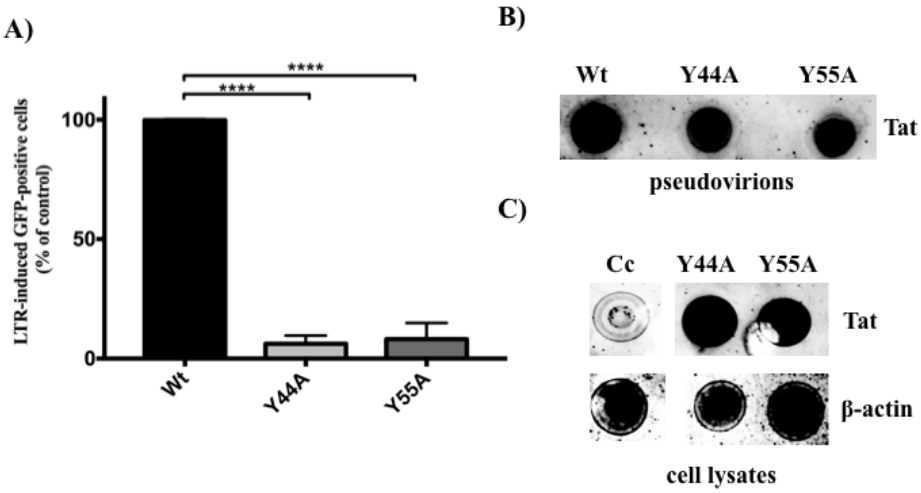

Figure 27. Experiments on HIV-indicator GHOST cells. A: GHOST(3) cells were transduced using equal amounts of p27-containing wild-type and Tat mutant virions (5 ng as determined by capsid ELISA) , then HIV LTR-induced GFP expression was measured by flow cytometry. GFP-positivity measured for GHOST(3) cells that were transduced with wild-type HIV-2 pseudovirions was considered to be 100%. LTR-induced GFP percentage was significantly decreased in the presence of Y44A and Y55A mutations (P value < 0.0001) (n=9). Error bars show SDs. Wt: wild-type. **B:** Dot-blotting was used to demonstrate the presence of Tat protein in the virions. Equal amount of pseudovirions (1000 pg) were lysed, and anti- HIV-2 tat serum was used to detect the presence of the protein. **C:** GHOST(3) cells were transduced with 5 ng p27-containing pseudovirions (determined by capsid ELISA) and Dot-blotting was used to detect the presence of HIV-2 Tat from cell lysate. *β-actin* was used as control. *Cc, uninfected GHOST(3) cells.*

Effects of Tat mutations on RT

RT activity was determined from viral supernatant using an ELISA-based colorimetric assay. In the presence of Y44A and Y55A mutations, HIV-2 reverse transcriptase activity was significantly reduced, compared to that of the wild-type pseudovirions. RT activity was decreased by 97% for Y44A and by 96% for Y55A *tat* mutations, compared to the wild-type HIV-2 (P-values < 0.0001), implying a detrimental effect of the mutations on the activity of RT (Figure 28).

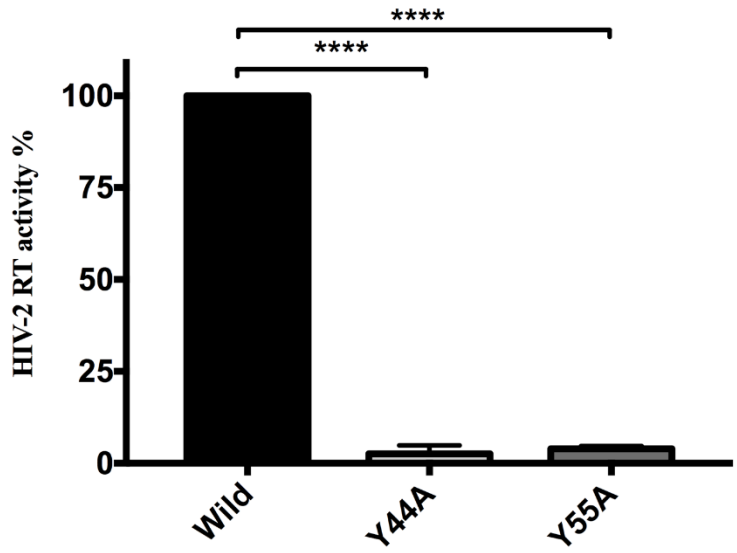

Figure 28. Effect of Tat mutations on HIV-2 RT activity. Quantification of HIV-2 RT activity. Activity of HIV-2 RT was significantly decreased in the presence of Tat mutations. Amount of pseudovirions were normalized to capsid. Error bars represent SD (n=6), **** P value < 0.0001, Wt: wild-type.

Western-blot was carried out to qualitatively determine whether the Y44A Tat mutation had any effect on the quantity of RT packaged into the pseudovirions. Surprisingly, RT was undetectable in the presence of Y44A mutant Tat from the lysate of pseudovirions (Figure 29 A). This finding may explain why RT activity was abolished, while the amount of capsid and Tat in the pseudovirions was not affected by the mutation.

To explore the changes in RT as a result of the mutation, HEK293T cells were transfected with wild-type and Y44A mutant Tat coding HIV-2 CGP plasmids, and changes in RT quantity were then followed by Western-blotting of transfected cell lysate over a period of 3 days. After 24 hours of transfection, the amount of RT was lower in the presence of Y44A mutation compared to that found in the wild-type, and after 3 days, RT was undetectable (Figure 29 B). *β-actin* was used as a control.

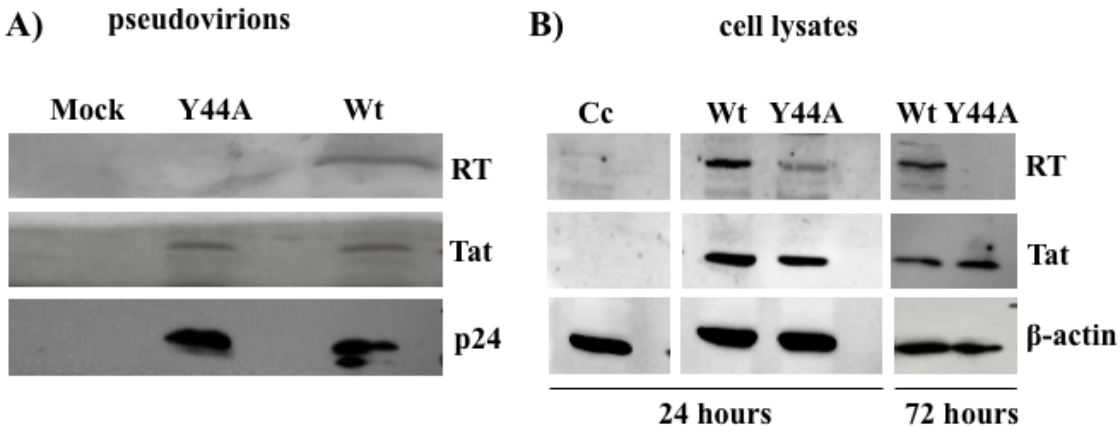

Figure 29. Effect of Y44A Tat mutation on the expression of HIV-2 RT. A: Western-blot analysis of RT, Tat and p24 in HIV-2 virions. Pseudovirions were concentrated by ultracentrifugation, and pelleted viruses were lysed and viral proteins were loaded onto SDS-PAGE and transferred onto nitrocellulose membranes. For protein detection, polyclonal antibodies against HIV-2 Tat or HIV-2 RT or monoclonal anti-p24 (capsid) were applied. **B:** HEK293T cells were transfected with HIV-2 CGP vector, then lysed after 24 and 72 hours. Polyclonal anti-Tat serum and polyclonal HIV-2 RT antibodies were used to detect HIV-2 Tat and RT from transfected cell lysate. β-actin was used as control. The results are representative of 3 separate experiments. *Cc, non-transfected HEK293T cells.*

Detection of HIV-2 Tat in pseudovirions

Incorporation of Tat into the pseudovirions was analyzed by proximity ligation assay (PLA). Using anti-Tat and anti-Vpx antibodies, the fluorescence signal indicating interaction between the two viral proteins was detected. Since HIV-2 Vpx is known to be incorporated into virions (Baldauf et al., 2017), this suggested that HIV-2 Tat was similarly packaged (Figure 30 A). Incorporation was detected for Y44A mutant virions, as well (Figure 30 B). Tat To explore whether or not exosomal expression of Tat might have interfered with our assay, a mock transfection of HEK293T cells with a wild-type *tat* coding HIV-2 CGP plasmid was performed. Following collection, filtration and ultracentrifugation of the supernatant, Western-blotting in this case failed to detect the Tat protein (see Figure 29 A).

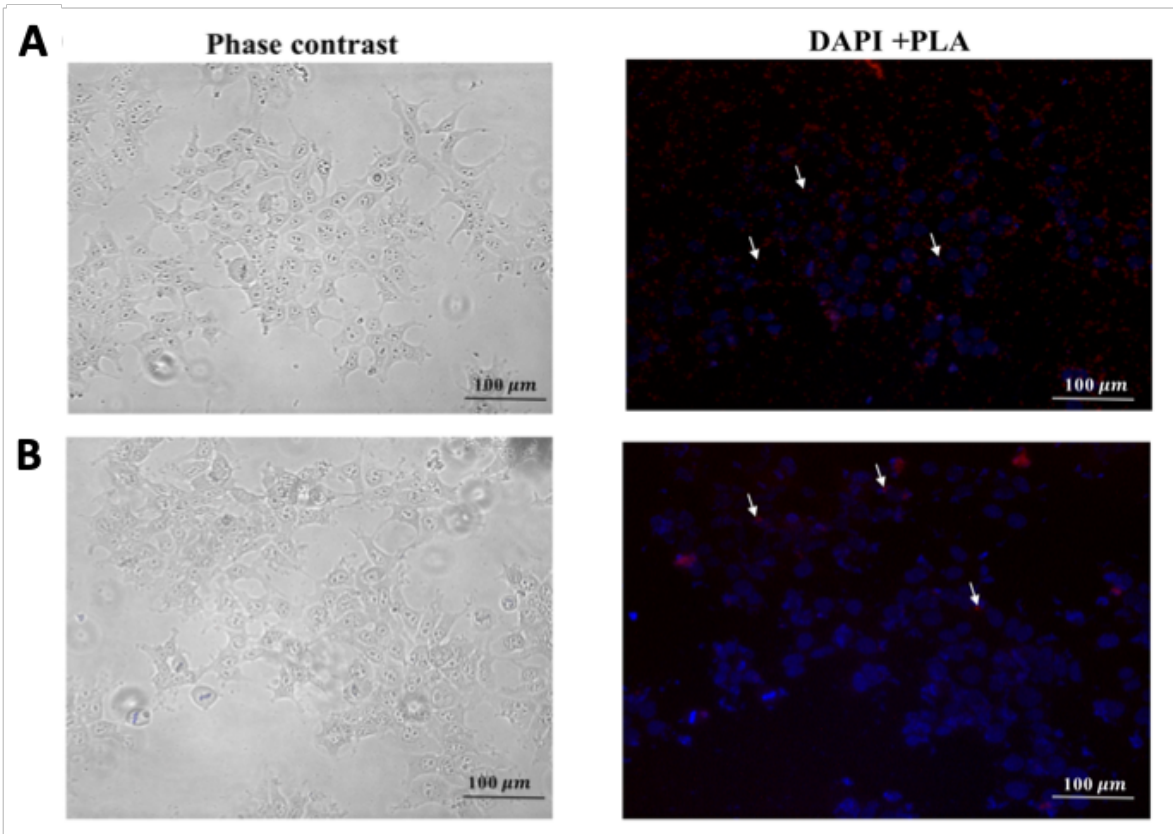

Figure 30. Detection of HIV-2 Tat incorporation into pseudovirions using PLA. HEK293T cells were transduced with 19 ng (normalized for p27, capsid**) A:** wild-type HIV-2, or **B**: mutant (Y44A) HIV-2. After one hour incubation, cells were fixed, permeabilized and processed for PLA. Cells nuclei were stained with DAPI. Scale bar: 100 µm. Each red spots represent an interaction between HIV-2 Tat and Vpx proteins. For representation, some of the PLA signals are indicated by white arrows. Phase contrast of both HIV-2 Tat (wild-type and mutant) is represented.

Quantification of HIV-2 DNA

HIV-2 standard was prepared using extracted RNA of HIV-2 particles counted by electron microscopy. Plus strand of HIV-2 *gag* with an estimated size of 850 base pair was then visualized on 1% agarose gel (see Figure 31).

For quantification, a series of ten-fold dilutions of the HIV-2 *gag* fragment was used, and was normalized to purified PBDG. The linear regression analysis between the quantities of HIV-2 *gag* gene and Ct values is represented in Figure 32. Regression equations were calculated with y = -3.305 + 38.692, R^2 = 0.999. Linear regression analysis between the quantities of PBDG and Ct values is represented in Figure 33. Regression equations were calculated with y = -3.483 + 39.893, R^2 = 0.999.

During qPCR reactions, several different controls have been used to establish the specificity: extracted DNA from U1 cells (subclone of cronically HIV-1 infected U937 cells) (Folks et al., 1987), DNA from HIV-1 infected patients, and DNA from negative participants. None of the control samples gave positive results, thus, specificity was 100%. Sensitivity of our assay was 100% at five copies/reaction (detected in 14/14 runs, 0.69 $\log_{10}$ with SD 0.44), while 78% at one copy/reaction (11/14 runs).

Limit of detection (LOD, respectively) was found to be 1 copies/reaction (11/14 runs), and the median correlation coefficient was 0.999 (range: 0.998-1.000), and limit of quantification (LOQ, respectively) was 5 copies/reaction at CT 33 (SD: 0.9). Median slope was -3.15 (range: -3.004--3.373) and median efficiency was 97% (range: 98.44% to 98.50%). Overall, detection limit of proviral DNA was 0.5 copies/10^5 leukocytes.

To exclude the possibility that human DNA contamination might have any effect on the sensitivity of our assay, qPCR was also performed in the presence of 1 µg PM-1 cell's DNA. Linear regression analysis between the quantities of HIV-2 *gag* fragment and Ct values in the presence of human DNA is presented in Figure 34. Regression equations were calculated with y = -3.305 +

38.692, R^2 = 0.999. It is worth mentioning that no effect was observed in the presence of background DNA. A sample calculation used to quantify the concentration of HIV-2 DNA is presented in Figure 35.

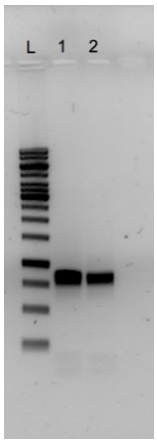

Figure 31. Detection of cleaned PCR product of HIV-2 gag PCR. An example of successful of PCR purification is visualised on 1% Agarose gel stained with Gel red. L: 1Kb DNA ladder, 1-2: Sample 1 and 2.

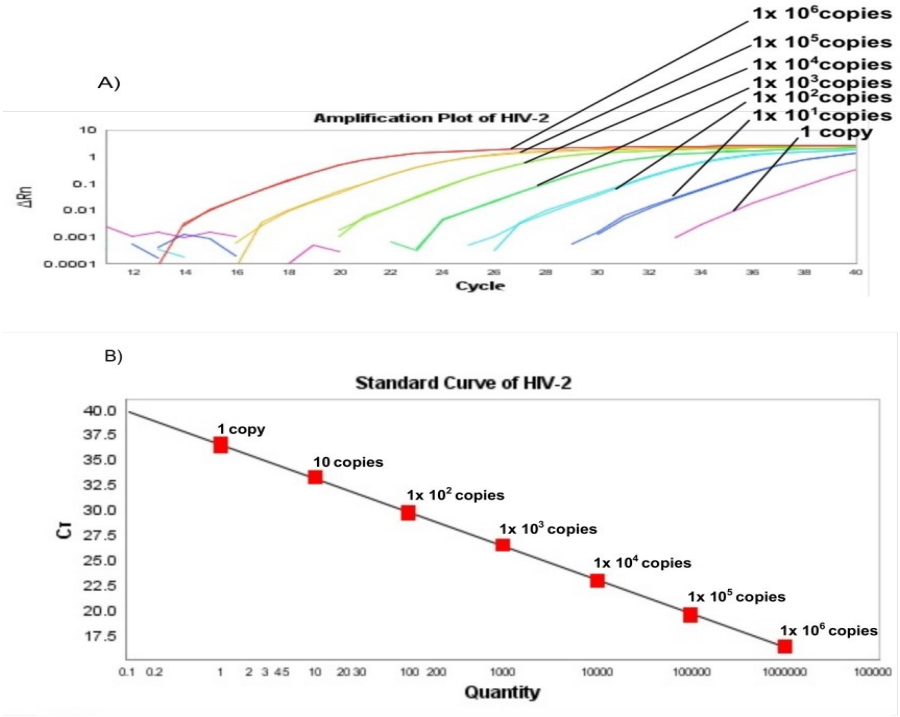

Figure 32. Standard curve of HIV-2 *gag* fragment. A: Sensitivity test for TaqMan probe for HIV-2 *gag* gene. Amplification plot shows the results of the tenfold dilution series of *gag* gene (from 10^6 to 1 DNA copies). **B:** The linear regression analysis between the quantities of HIV-2 *gag* and Ct values. Red box represents Ct values of *gag* fragment.

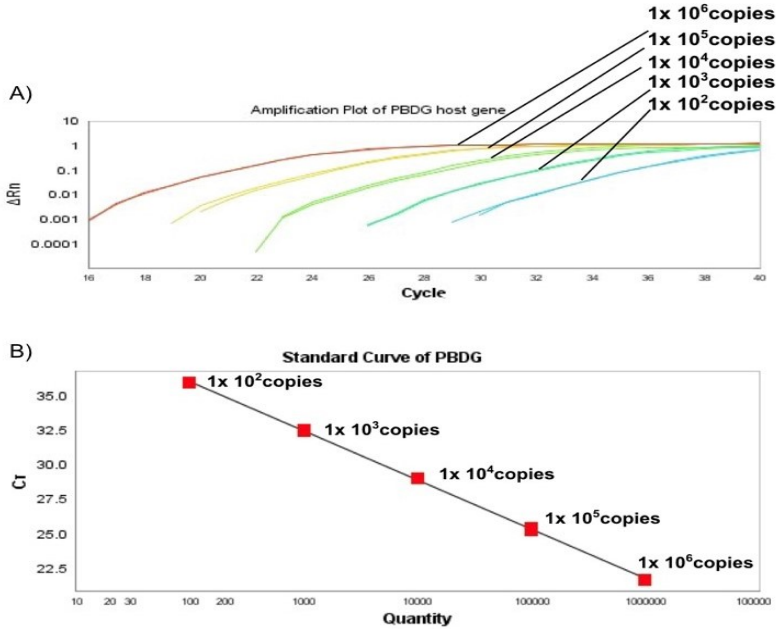

Figure 33. **Standard curve of PBDG. A:** Sensitivity test for TaqMan probe for PBDG. Amplification plot shows the results of the tenfold dilution series of host gene (from 10^6 to 100 DNA copies). **B:** The linear regression analysis between the quantities of host gene and Ct values. Red box represents Ct values.

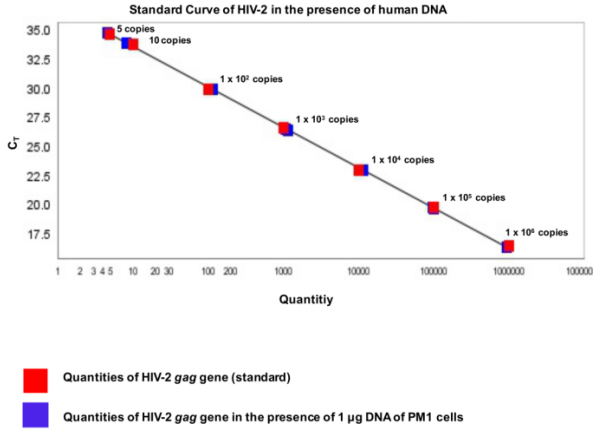

Figure 34. **Standard of HIV-2 *gag* in the presence of 1 µg human DNA of PM1 cells.** To exclude that human DNA has an inhibitory effect: reactions were set up in the presence of 1µg DNA of PM1 cells. The linear regression analysis is presented between the quantities of HIV-2 *gag* gene and Ct values in the presence of DNA of PM1 cells. Red box represents Ct values of HIV-2 gag without, and blue box represents Ct values in the presence of human DNA.

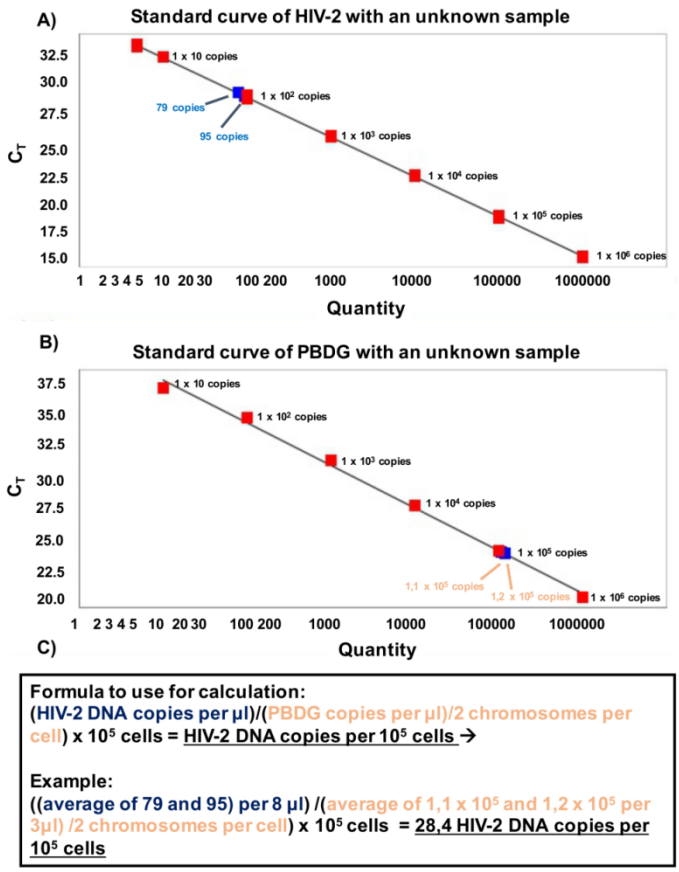

Figure 35. Example for a sample calculation used to quantify the concentration of HIV-2 DNA. A: Standard curve of HIV-2 *gag* fragment (red box) with the HIV-2 copy number of unknown sample (blue box). Red box represents Ct values of HIV-2 standard and blue box represents HIV-2 *gag* Ct values of unknown sample. **B:** Standard curve for PBDG (red box) and unknown sample (yellow box). **C:** Formula used to calculate the results to HIV-2 DNA copy number per 10^5 cells.

Low postseroconversion $CD4^+$ T-cell level is associated with faster disease progression, and higher viral evolutionary rate in HIV-2 infection

Phylogenetic analysis of V1-V3 region of *env* sequences

Maximum likelihood analysis was performed on 409 *env* sequences collected from 16 study participants. For each participants, in each time-point, a median of 7 clones were sequenced, in total, 528 sequences, however, for evolutionary analyses, 119 recombinant sequences were removed, thus, only 409 sequences were used. Phylogenetic analyses also showed that all the sequences are subtype A. Phylogenetic tree of sequenced samples is shown in Figure 36.

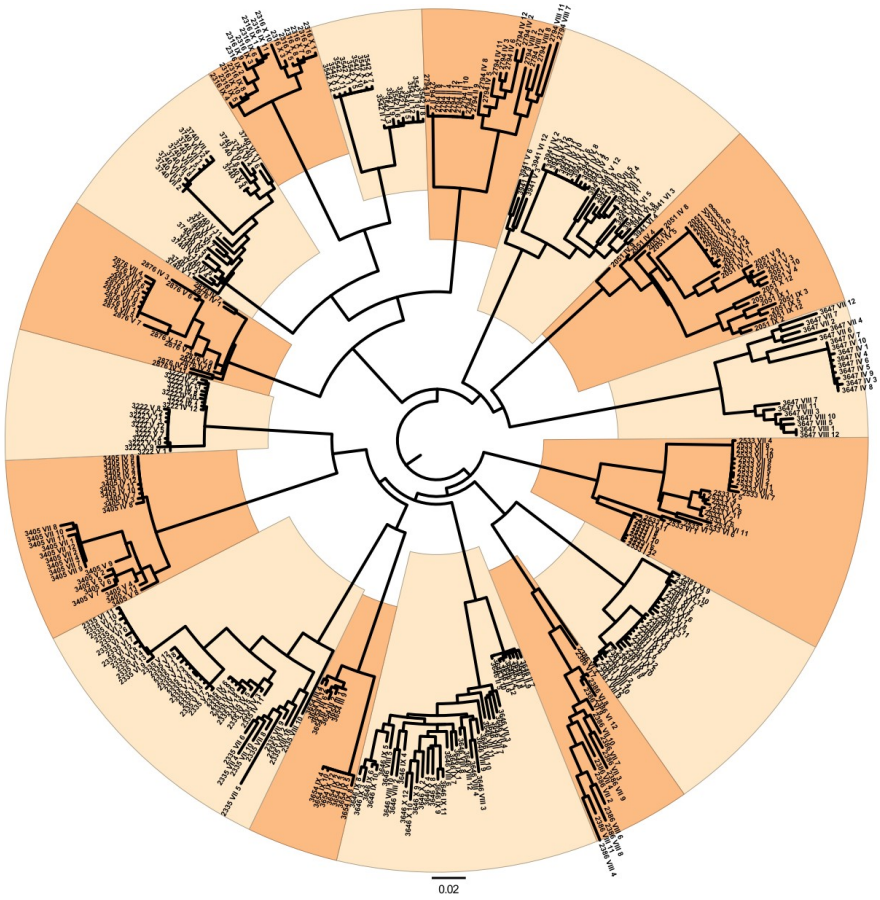

Figure 36. Maximum likelihood phylogenetic analysis of V1-V3 region of *env* sequences. In total 409 V1-V3 region of *env* sequences were collected in different time-points from 16 participants. Every monophylogenetic clade is formed from the sequences collected from a corresponding participant. Length of horizontal bar is 0.02 nucleotide substitutions per site. Name of sequences consist of the patient's number, followed by the number of visit in roman numerals and the clone number. Figure was constructed with the aid of Prof. Patrik Medstrand.

Classification of HIV-2 infected participants into faster and slower progressors

Classification of study participants into different group of progressors was based on the dynamics of longitudinal CD4+ T-cells. All HIV-2 infected cohort members were classified into two groups: faster and slower disease progressors.

As decline of CD4 T-cells is an indicator for disease progression, a minimum two CD4 % was recorded for all seropositive patients.

To define faster and slower progressors, 3 stratifications were used: the decline rate of CD4 %, the level of CD4% at the midpoint between the first and last records, and the combination of the decline rate and the level of CD4 % (Figure 37).

Firstly, the decline rate of CD4 % was resented. 111 patients were categorized as slower progressors, and 81 patients were classified as faster progressors. Mean CD4 % decline rate was 2,7% /year (SD: 2.6), and the median time to AIDS was 11.7 years (95% CI 7.3-16.1) for faster progressors, from the first recorded CD4%. Mean CD4% decline was 0.5% / year (SD: 1.6) and the median time to AIDS was 16.8 years (CI 12.3-21.3) for slower progressors, from the first recorded CD4 % (Figure 37 A, p=0.008, log-rank test).

The second stratification shows the level of CD4 % at the midpoint between the first and last recorded CD4 % levels, using the regression line generated in the first stratification. Based on the second stratification, 87 patients were faster progressors with a mean CD4% level of 21.0% (SD 4.3), and the median time to AIDS was 9.4 years (CI 6.7-12.1), with a low CD4 % level. While 105 participants were classified as slower progressors with a mean CD4 % level of 35.0% (SD 5.7), and the median time to AIDS was 15.5 years (CI 14.3-16.6) with a high CD4 % loads. (Figure 37 B, p<0.001, log-rank test).

In the third stratification, the decline rate and the level of CD4 % was combined (Figure 37 C). Based on this, 85 patients were faster progressors, where the median time to AIDS was 8.6 years (95% CI 6.5-10.8) from the first recorded level of CD4 %, and 107 participants were slower

progressors with 18.7 years (CI 13.6-23.8) median time to AIDS (Figure 37 C, $p<0.001$, log-rank test). Accordingly, the study participants were classified into faster or slower disease progressors (Table 8).

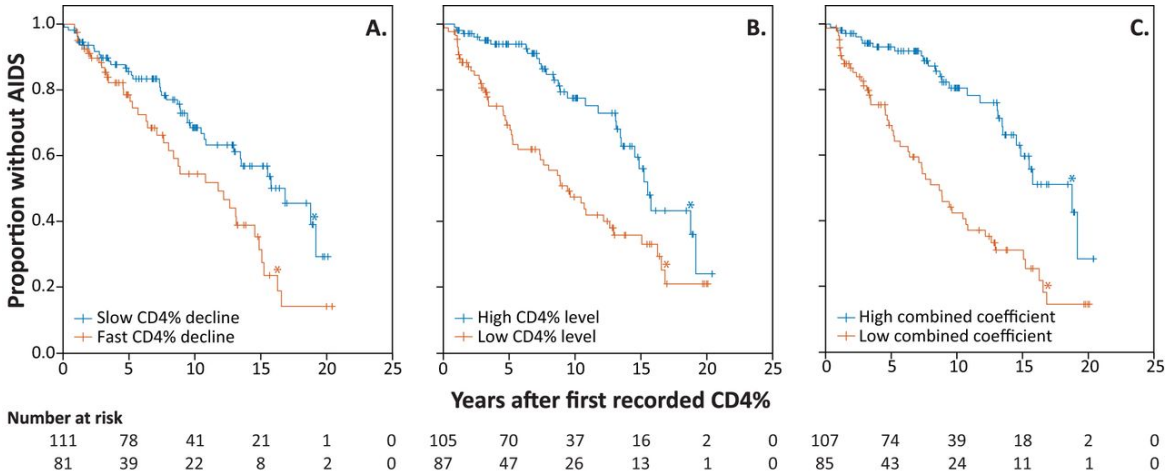

Figure 37. Kaplan-Mayer curves of latency period based on level and decline rate of CD4 %. A: Decline rate of CD4 % **B:** Level of CD4 % at the midpoint between the first and last recorded CD4 % levels. **C:** Combined effect of CD4% and decline rate. Asterisks indicate the time points, when 5 individuals were at risk of AIDS development and the number of participants at that time point is shown under the panels. Faster progressors are represented in orange, while data from slower progressors are represented in blue. Figure was constructed with the aid of Prof. Patrik Medstrand.

	CD4% decline rate /year		CD4% level		Combined coefficient	
Individual	**Value**	**Progressor†**	**Value***	**Progressor†**	**Value*,‡**	**Progressor†**
DL3405	-1.46	Slow	33.95	Slow	1.00	Slow
DL3542	0.69	Fast	32.73	Slow	0.74	Slow
DL2051	1.61	Fast	31.11	Slow	0.62	Slow
DL2876	0.55	Fast	28.91	Slow	0.67	Slow
DL3654	-0.15	Slow	27.74	Slow	0.70	Slow
DL2533	-1.10	Slow	23.96	Slow	0.68	Slow
DL2316	1.10	Fast	23.45	Fast	0.50	Fast
DL2794	-0.11	Slow	20.99	Fast	0.53	Fast
DL3941	3.40	Fast	20.65	Fast	0.29	Fast
DL2381	1.17	Fast	20.62	Fast	0.44	Fast
DL2335	0.58	Fast	20.41	Fast	0.47	Fast
DL3647	0.73	Fast	19.63	Fast	0.44	Fast
DL3646	0.33	Slow	19.32	Fast	0.46	Fast
DL3222	-0.88	Slow	19.25	Fast	0.53	Fast
DL3740	-0.69	Slow	17.57	Fast	0.48	Fast
DL2386	1.61	Fast	16.29	Fast	0.32	Fast

Table 8. Disease progression of all individuals based on stratifications for CD4 %. Individuals have been classified into slower or faster progressors based on the three different stratifications (n=16).

HIV-2 evolutionary rate association with the level of CD4 %

Evolutionary rate of HIV-2 was evaluated within hierarchical phylogenetic modelling (HPM) framework. Evolutionary rate of V1-C3 region was $23.5x10^{-3}$ codon substitutions/site/year.

When participants were classified based on the decline rate of CD4 % (Bayes Factor [BF]=0.3), there was no association between disease progression and evolutionary rate. Although, when classification was based on CD4 % level or a combination of CD4 % decline rate and level, the mean evolutionary rate was significantly higher for faster disease progressors ($28.6x10^{-3}$ codon substitutions /site/year, HPD: $24.2x10^{-3}$-$33.5x10^{-3}$). Evolutionary rate on the other hand was only $14.9x10^{-3}$ codon substitutions/site/year for slower progressors (Table 9).

Also, strong association was found between disease progression and evolutionary rate in the first variable regions (V1V2) (BF=11.8), and the conserved domains of Env (C2 (BF=28.4); C3 (BF=6.1)).

To find out the difference in evolutionary rate between different disease progressors, ratio of non-synonymous to synonymous substitution rates (the dN/dS rate ratio) were estimated. The dN/dS rate ratio shows if the region of a gene goes under positive (dN/dS>1), negative selection (dN/dS <1) or just naturally developed (dN/dS=1). While there was a negative selection of the entire V1-C3 region of Env (dN/dS rate ratio=0.56), there was no statistical difference between the two classified groups (BF=1.3). Although region-specific analyses showed that V1/V2 (dN/dS rate ratio=1.27) and C3 (dN/dS rate ratio=0.94) regions developed naturally, C2 (dN/dS rate ratio=0.22) and V3 (dN/dS rate ratio=0.41) regions were under strong negative selection. When dN/dS rate ratios were compared between the different groups for different regions, only the C2 regions was found to be strongly negatively selected in faster progressors, compared to slower progressors (BF=3.7) (Table 10).

While dN/dS ratio evaluates the selective pressure of the specific region, expected non-

synonymous (E[N]) and synonymous (E[S]) substitution rates can provide information about viral replication (Lemey et al., 2007). E[N] and E[S] divergences were plotted as accumulated derivation over time (see Figure 38). E[N] and E[S] substitutions increased relatively rapidly in the faster progressors during the asymptomatic phase. Median E[N] rate was $3.0x10^{-3}$-$6.6x10^{-3}$ nucleotide substitutions/site/year for faster progressors, and $1.4x10^{-3}$-$4.6x10^{-3}$ nucleotide substitutions/site/year for slower progressors (*P*=0.005, two-tailed Mann-Whitney U test [M-W]). This suggests the overall higher evolutionary rate for faster progressors compared to slower progressors.

CD4%stratification							
***env* region**	**Individuals**	**CD4% decline**			**CD4% level and Combination**		
		Fast*	**Slow†**	**BF**	**Fast***	**Slow†**	**BF**
V1-C3	23.5 (20.3-26.6)§	24.7 (20.1-29.6)	21.9 (19.1-24.9)	0.3	28.6 (24.2-33.5)	14.9 (12.2-17.6)	20.3
V1V2	29.5 (25.1-34.2)§	30.1 (24.6-36.0)	28.8 (23.7-34.0)	0.3	35.4 (28.9-42.2)	19.6 (14.8-24.7)	11.8
C2	18.0 (15.2-20.7)§	18.6 (15.3-21.9)	16.7 (13.9-19.5)	0.3	21.5 (17.6-25.7)	12.0 (9.2-15.2)	28.4
V3	21.2 (17.0-25.7)§	21.6 (16.5-26.8)	20.8 (15.7-25.9)	0.3	24.1 (18.0-30.6)	16.5 (11.0-22.2)	2.4
C3	26.6 (22.6-31.1)§	27.0 (22.0-32.4)	26.0 (21.6-30.6)	0.2	30.4 (24.3-27.0)	20.2 (15.2-25.8)	6.1

Table 9. Evolutionary rate of HIV-2 envelope using hierarchical phylogenetic model. BF= Bayers factor, which is stands for the association between disease progression and codon substitution rate. When BF is more than 3, it is considered as a significant association.

CD4% stratification				
***env* region**	**Individuals**	**CD4% decline**		
		Fast*	**Slow†**	**BF**
V1-C3	0.56 (0.49-0.63)	0.47 (0.41-0.53)	0.71 (0.56-0.87)	1.3
V1V2	1.27 (0.84-1.80)	0.94 (0.68-1.22)	1.84 (0.93-3.11)	1.4
C2	0.22 (0.18-0.27)	0.18 (0.14-0.23)	0.29 (0.20-0.39)	3.7
V3	0.41 (0.27-0.57)	0.35 (0.22-0.51)	0.50 (0.26-0.79)	1.2
C3	0.94 (0.70-1.22)	0.90 (0.65-1.19)	1.00 (0.62-1.43)	0.5

Table 10. Ratio of non-synonymous to synonymous substitution rates (the dN/dS rate ratio) in V1-C3 regions of envelope in faster and slower progressors.

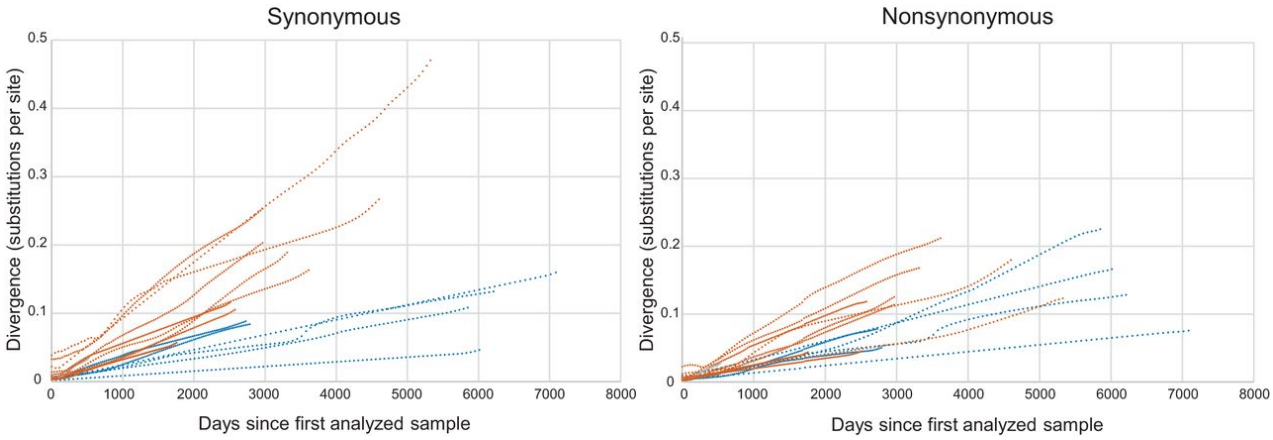

Figure 38. E[N] and E[S] divergences over time. Estimated Synonymous and non-synonymous **(**E[N] and E[S]) divergences over time in V1-C3 regions of HIV-2 *env*. Faster progressors are represented in orange, data from slower progressors are shown in blue. Figure was constructed with the aid of Prof. Patrik Medstrand.

Positive selection in conserved sites of HIV-2 envelope in slower disease progression

To estimate the number of residues that go under positive selection during disease progression, a renaissance counting procedure was used to estimate the dN/dS rate ratio at each codon site (Figure 39).

The number of positively selected sites was similar in the V1/V2, V3 and C3 regions in both groups. C2 region of Env in slower progressors has a higher number of positively selected sites, compared to that in faster progressors (35 vs 20 sites; P=0.026, two-tailed Fisher's Exact Test [FET]). C2 and C3 regions of HIV-2 env are exposed and under negative selection, thus, positive selection of amino acids in these regions may negatively affect the viral fitness (Barroso et al., 2011).

Some of the amino acids of Env, which are critical to viral fitness, and are conserved in HIV-2 and SIVsm, have been identified. Among the 246 amino acids, 84 were conserved in SIVsm and HIV-2 V1-C3 regions, and 20 conserved amino acids showed positive selection in slower progressors, compared to only 5 in faster progressors (P=0.002, FET). Positive selection was mostly observed in C2 region between the two groups, (12 sites for slower and 3 sites for faster progressors, respectively, P=0.021, FET).

Protein structure of HIV-2 gp125 (Barroso et al., 2011) (Davenport et al., 2015) was used to visualize the surface exposition of positively selected amino acids, the majority (15 of 22) were surface-exposed (Figure 40). Furthermore, surface accessibility of amino acids showed that the positively selected amino acids were associated with solvent-exposed surfaces in the C2 region (29 out of 68 AAs, P=0,04), FET).

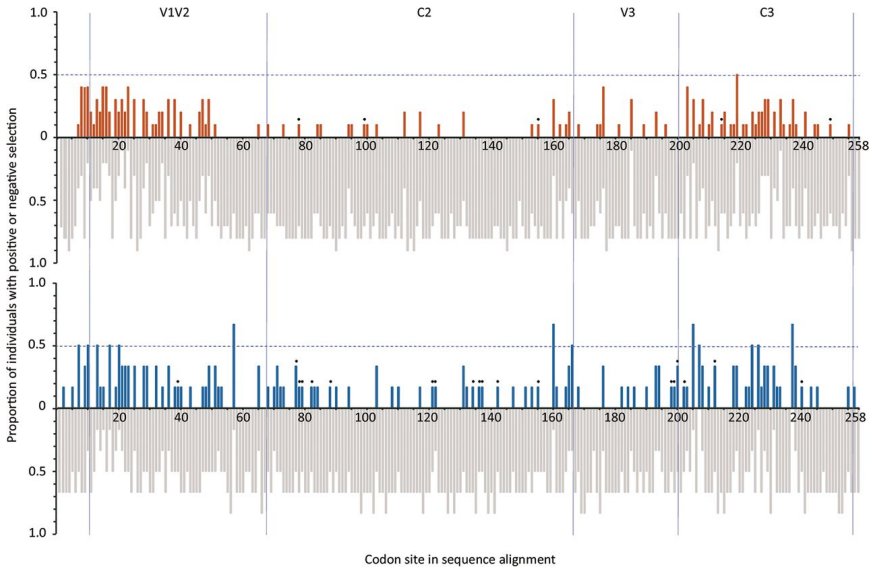

Figure 39. Codon-specific selection pressure of V1-C3 region of HIV-2 *env* for faster and slower progressors. Y axis shows the proportions with positive selection (faster progressors are represented in orange and slower ones in blue colour) or negative selection (gray colour) of the codon sites in the sequence alignments (x axis). The upper graph shows the selection for faster, and the lower graph shows the selection for slower progressors in different regions of HIV-2 envelope gene. Figure was constructed with the aid of Prof. Patrik Medstrand.

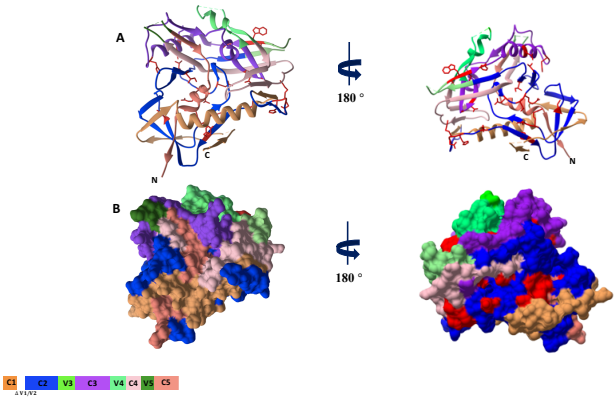

Figure 40. Ribbon and surface representation of HIV-2 gp125 monomer. A: Ribbon representation of constant and variable regions of envelope protein. N- and C-terminal region are indicated by N and C, and each regions are colour coded, and codes are indicated on the left side of the diagram. **B:** Surface representation of HIV-2 gp125 monomer, structure is rotated by 180°, positively selected amino acids are coloured in red.

DISSCUSSION

HIV-1 and HIV-2 share a common ancestral origin, and a similar replication cycle; however, HIV-2 differs from its counterpart in many aspects. Infection by HIV-2 is mostly characterized by lower pathophysiology and reduced transmissibility (Azevedo-Pereira and Santos-Costa, 2016). While most HIV-2 infected patients were registered in West African countries (Sousa et al., 2016), the incidence of HIV-2 infection had been on the rise in many European countries; such as Portugal, France, UK, Spain, Belgium and Italy; and also, in America and Asia, as well (Soriano et al., 2000) (Barin et al., 2007) (Dougan et al., 2005) (de Mendoza et al., 2014) (Ruelle et al., 2008) (D'Ettorre G et al., 2013) (Makroo et al., 2011) (Torian et al., 2010).

As previously described, patients can be dually infected with both HIV viruses. The mechanism of dual infection is poorly understood. While Travers and his colleagues suggested protection of HIV-2 against HIV-1 infection (Travers et al., 1995), other studies did not reach this conclusion (Norrgren et al., 1999) (Greenberg, 2001), and it is yet unclear, whether or not HIV-2 accessory and/or regulatory proteins are involved in this prolongation of the asymptomatic phase of infection.

Our goal was to construct an *in vitro* model to study HIV dual infection, and determine whether HIV-2 regulatory and accessory proteins might have any interfering role in HIV-D. In our dual infection assays, simultaneous infection of HEK293T cells with both HIV virions resulted in a decrease in the infectivity of HIV-1 by more than 60 %, while that of HIV-2 had not changed, "superinfection" of HIV-2 pre-transduced cells by HIV-1 resulted in a 90 % decrease of HIV-1 related fluorescence signal. Based on our findings, we carried out dual sequential transduction assays, using functionally restricted accessory/ regulatory HIV-2 proteins, in order to determine the protein responsible for the decrease of HIV-1's infectivity. All of the loss–of–function mutations were described previously in the literature, with the exception of Tat Y44A mutation.

Our results showed that in the presence of a functionally restricted Vpx, HIV-1 infectivity was restored, similarly to those obtained in mock-transfected cells. To prove that HIV-2 Vpx might have an inhibitory effect on the infectivity of HIV-1, we carried out experiments using a vector

coding only for a Vpx-GFP fusion protein, results of which showed that the infectivity of HIV-1 decreased by more than 80 %.

As Vpx plays an important role in the transport of PIC (Belshan, 2002), we hypothesized that this interference with HIV-1 happened in the early phase of the viral life-cycle. 2-LTR qPCR was then used to analyse this hypothesis. In the presence of Vpx, the 2-LTR circle junctions amount of HIV-1 was significantly reduced by > 40 %. We also found that Vpx has an inhibitory effect on HIV-1 capsid production and RT activity. When HIV-1 pseudovirions were produced in the presence of Vpx, RT activity and p24 quantity were significantly lower. Additionally, Vpx incorporation into HIV-1 pseudovirions was also demonstrated using Western blotting. How Vpx was able to protect cells against HIV-1 infection, however, remains obscure, and elucidation of the pathomechanism is currently underway.

When we experimented in immune cell line, HIV-1 superinfection of Vpx- pre-transfected native THP-1 cells appeared to promote the entry of HIV-1 virions into the cells. This is perhaps a result of an interaction between HIV-2 Vpx and SAMHD1, which is a cellular restriction factor that is highly expressed in cells of monocytic lineage.

To attenuate the interaction between Vpx and SAMHD1, we repeated our HIV-1 superinfection experiments on differentiated THP-1 monocytes. It was shown that the level of SAMHD1 is decreased in monocyte-derived macrophages (MDMs) (Laguette et al., 2011), thus, PMA was used to activate and differentiate THP-1 monocytes into macrophages. When we carried out our experiments on MDMs, HIV-1 related fluorescency was decreased by > 80 % in the presence of Vpx, which was similar to that observed in HEK293T cells. Therefore, after down-regulation of SAMHD1; as a potential interaction partner of Vpx, we could conclude that Vpx was detrimental to HIV-1.

Moreover, another aim was to study the effect of mutations in the acidic domain of HIV-2 Tat *in silico* and *in vitro,* given the lack of studies on this particular region in HIV-2. Our sequence-

based analysis showed that even though HIV-2 Tat shares common and highly conserved sequences with Tat protein of HIV-1, amino-terminal region of the two proteins shows only 10 % homology. Despite the fact that HIV Tat is a highly polymorphic protein, mutations in the Pro-rich domain of HIV-1 Tat are well tolerated, and do not affect its functions (Ruben et al., 1989). On the other hand, mutations in the core and basic domains of HIV-1 Tat negatively affect reverse transcription (Ulich et al., 1999). The effect of mutations in the Pro-rich region of HIV-2 Tat, however, are yet to be been defined.

Using sequence-based predictions and stability analysis, we found that Y44A substitution may inactivate the protein. Based on our *in silico* analyses, we assumed that Y44A mutation may inactivate HIV-2 Tat or negatively affect its function. We carried out a series of *in vitro* experiments to study the inactivating nature of the Y44A mutation. Previous publications about SIV (Y55A) and HIV-1 (Y26) Tat proteins show that Tyr to Ala substitution in the Cys-rich domain abolishes the transcription activation function of the protein (Das et al., 2007) (Verhoef et al., 1997). For comparison, Y55A Tat mutation was also studied, since Y55 residue of HIV-2 Tat corresponds to the Tyr in the 26th position of HIV-1 Tat.

To determine the effect of the Y44A and Y55A Tat mutations on transactivation of the proviral genome, we carried out experiments in GHOST (3) HIV indicator cell line. When GHOST cells were transduced with HIV-2 pseudovirions carrying mutant Tat (Y44A or Y55A), LTR-induced GFP signal was significantly decreased by more than 90 %, compared to that observed for wild-type HIV-2 Tat. This was expected for Y55A mutation, since HIV-1 Tat Y26A mutant was shown to reduce the Tat mediated HIV LTR activation (Verhoef et al., 1997). Our finding is in good agreement with the previous studies, which showed that the 38-48 region is crucial for transactivation of the LTRs in HIV-2. Furthermore, deletion in the amino-terminal region (30-47 residues) drastically reduced the LTR activation function of the protein (Arya, 1993) (Pagtakhan and Tong-Starksen, 1997).

HIV-1 Tat interacts with both subunits of RT *in vitro*, and this interaction can stimulate the activity of RT (Apolloni et al., 2007). To examine whether HIV-2 Y44A mutation has any effect on the activity and expression of RT, we carried out a series of experiments *in vitro*. Our findings showed that RT was undetectable in pseudovirions carrying the Y44A mutant Tat. It is possible that the Y44A mutation negatively affected the stability and packaging of RT (Lin et al., 2015). We carried out further experiments to detect the changes in RT in transfected cell lysate by Western-blot. While RT was still detectable in day 3 post-transfection in the case of wild type, it was undetectable in day 3 in the presence of Y44A Tat mutant. Our findings indicate that Tat plays an important role in the stabilization of RT, and perhaps, Y44A Tat mutation may have induced the degradation of HIV-2 RT in a ubiquitination-dependent, or -independent manner.

As our *in silico* and *in vitro* results were concurrent, our findings imply that the applied methods can be used for mutation analysis and design, however, the possible uncertainties of the models; caused by relatively lower target-template identity, need to be considered, and sophisticated experimental approaches may be applied in future studies to confirm the predicted changes. The Y44A mutation was predicted to alter the structure of an ordered region, thereby inactivating the protein. This indicated that the Pro-rich domain has a main role in the transactivation function of HIV-2 Tat, unlike Tat protein of its counterpart. Also, the findings of this study suggest that the first domain of HIV-2 Tat is involved in the regulation and stability of RT and reverse transcription, in addition to Tat-dependent LTR transactivation.

While plasma viral load of the two viruses differ, proviral DNA load was reported to be similar for both viruses (Popper et al., 1999) (Popper et al., 2000). We aimed to develop a sensitive cellular HIV-2 DNA quantification method using whole blood. HIV-2 DNA load was normalized to PBDG host gene, and both specificity and sensitivity of the assay was 100 %. Furthermore, we were able to detect viral DNA in participants with undetectable viral RNA.

It was previously shown that the decline of T helper cells is associated with disease progression of in HIV-2 infection (Jaffar et al., 1997). Even though HIV-2 infection is mostly characterized by a long asymptomic phase, infection in some patients can rapidly progress, similarly to HIV-1 infection (Van der Loeff et al., 2010). To determine the association between evolutionary dynamics of HIV-2 and disease progression, firstly, we classified participants of a cohort into groups of faster and slower progressors based on longitudinal $CD4^+$ T-cell datas. Then, the level and decline rate of CD4+ T cells in association with progression to AIDS was determined in three stratifications. We found that CD4 % level or the combined CD4 % level/decline rate stratifications were associated with the evolutionary rate of HIV-2 infection, and it was almost twice as high in the case of fast disease progressors, compared to slower progressors. To specify which regions of HIV-2 envelope undergoes selection during the development of the disease, 528 HIV-2 *env* V1-C3 sequences were analysed from longitudinal plasma samples of 16 individuals during a median observation time of 7.9 years, and we found that both non-synonymous and synonymous substitutions accumulated at a higher rate in faster progressors, indicating that the evolutionary rate is higher for faster progressors. We could also determine that slower progressors had more residues that underwent positive selection in the C2 region of *env,* compared to faster disease progressors. These positively selected amino acids in the C2 region; which are conserved in the envelope of HIV-2/SIVsm, are surface exposed.

In conclusion, our analyses of dual infection with both of HIVs, and experiments on the association between viral evolutionary rate and disease progression of HIV-2, may help to understand the clinical manifestation of HIV-2 and dual infection with HIV-1 and HIV-2 viruses. Our findings may provide new insights into associations between pathogenesis and evolution of HIV-2 virus, and may provide a base to understandwhy HIV-1/2 dual infection and HIV-2 mono-infection is less pathogenic, compared to HIV-1 mono-infection.

SUMMARY

The purpose of this study was to shed light on HIV-2, its replication dynamics, infectivity, and the role it plays in dual infection. Compared to HIV-1, studies on this virus are indeed lacking.

In summary, we presented a cell culture model to study and analyze HIV-1 and HIV-2 dual infection. In the presence of HIV-2, HIV-1 transducing capability was significantly decreased. After carrying out loss-of-function mutations in HIV-2 accessory and regulatory genes, we were able to identify viral protein X as the protein implicated in the diminishment of HIV-1`s infectivity. HIV-1 transduction of Vpx transfected cells resulted in decreased quantity of 2-LTR circle junctions, impaired capsid (p24) production, and hindered reverse transcriptase activity of HIV-1. Having optimized the transfection and transduction protocols of activated and differentiated THP-1 monocytes, a similar result was obtained, when we controlled the level of SAMHD1. We can conclude from our cell culture and other *in vitro* experiments that HIV-2 Vpx is indeed involved in the reduction of HIV-1's infectivity in dual infection, at least on the cellular level.

Also, we were able to show that even though HIV-2 Tat protein shares similarities in its structure and function with its HIV-1 counterpart, the N-terminal region; which differs the most between the two proteins, plays a crucial role in viral replication, unlike the acidic domain of HIV-1's Tat. We studied the effects of Y44A mutation in Tat protein using *in silico* and *in vitro* methods, as well. Our results suggest that Tat Y44A mutation has a negative effect on the infectivity, expression and stability of HIV-2 RT. Our findings highlight the importance of the N-terminal, Pro-rich domain in the regulation and activity of HIV-2 RT, unlike in Tat protein of HIV-1.

To understand the mechanism of disease progression of HIV-2, we analysed HIV-2 envelope sequences to determine the connection between disease progression and viral evolutionary rate, with our collaboration partners. Our analysis shows that CD4 % level, or the combined CD4 % level and decline rate stratifications are associated with evolutionary rate of HIV-2. Furthermore, we were able to classify the study participants into groups of slower and faster progressors, based

on their longitudinal T helper cell datas. Our results show that the evolutionary rate of faster progressors is twice as high, compared to that of slower progressors, and this would appear to indicate that high evolutionary rate implies faster disease progression. Additionally, we could determine that more residues in the C2 region of envelope went under positive selection for slower progressors, compared to faster progressors; and these residues are surface exposed.

Last but not least, we developed a sensitive HIV-2 DNA quantification protocol, which could be applied when viral plasma RNA level is undetectable. It is important to have a sensitive and specialized protocol for the detection and monitoring of HIV-2 viral load. We are confident that our proviral DNA assay provides a sensitive approach to HIV-2 DNA viral quantification from whole blood, and will aid in the monitoring and diagnosis of HIV-2 infection in the future.

Altogether, we believe that our findings may help to understand the mechanism of dual-infection and disease progression of HIV-2; highlight the importance of the acidic domain of HIV-2 Tat, and help to monitor HIV-2 infection and the success of therapy, when viral RNA is under quantification level or undetectable.

ÖSZEFOGLALÁS-MAGYAR NYELVEN

Vizsgálataink célja az volt, hogy jobban megértsük a HIV-2 vírus replikációjának dinamikáját, a vírus fertőzőképességét és a dupla fertőzésben betöltött szerepét.

A HIV-1 és HIV-2 dupla fertőzés modellezésére és tanulmányozására sejtkultúrás modellrendszert alkalmaztunk. A HIV-2 jelenlétében a HIV-1 infektivitása szignifikánsan lecsökkent. Miután kisérleteinket „funkció-vesztett" HIV-2 regulatorikus és / tartozék géneket hordozó plaszmidokkal elvégeztük, megállapítottuk, hogy a virális protein X képes a HIV-1 transzdukció gátlására. Ez a gátló hatás megmutatkozott a 2-LTR junkciók számának csökkenésében, a kapszid fehérje (p24) termelésben és a HIV-1 reverse transzkriptáz aktivitás csökkenésében egyaránt. A HEK293T sejtekhez hasonlóan, az aktivált és differencált THP1 monocyta sejteken is a Vpx HIV-1 „infektivitással" szembeni gátló hatását észleltük. Fontos kiemelni, hogy ezen gátlás csak abban az esetben volt tapasztalható, amikor a PMA-val történt aktiválás révén feltehetőleg le tudtuk csökkenteni a sejten belül SAMHD1 szintet. A sejtkultúrás és *in vitro* kísérleteink alapján feltételezhető, hogy celluláris szinten a HIV-2 Vpx felelős a HIV-1 transzdukciós képességének gátlásáért.

Továbbá, eredményeink azt mutatják, hogy habár a HIV-2 Tat hasonló szerkezettel és funkcióval rendelkezik mint a HIV-1 Tat; az N-terminális régió – mely a leginkább eltérő szerkezettel rendelkezik a két HIV vírus Tat fehérjéje esetén - jelentős szerepet tölt be a vírus replikációban, ellentétben a HIV-1 Tat proteinjének azonos doménjével. *In silico* és *in vitro* kísérleteink révén a Y44A mutáció hatását tanulmányoztuk. Eredményeink arra engednek következtetni, hogy az Y44A mutáció negatív hatással van a fertőzőképességre, a HIV-2 RT expressziójára és stabilitására. Eredményeink arra engednek következtetni, hogy az N-terminális, Prolin-gazdag domén szerepet játszik a HIV-2 RT regulációjában és aktivitásában, ellentétben a HIV-1 Tat Pro-gazdag doménjével.

Annak megértése céljából, hogy milyen mechanizmus állhat a HIV-2 progressziójának hátterében, HIV-2 burokfehérje (Enc) kódoló szekvenciákat analizáltunk kollaborációs

partnereinkkel és ezek betegség progresszióhoz és vírus evolúcióhoz való kapcsolódását vizsgáltuk. Analíziseink azt mutatják, hogy a CD4 % szint vagy a kombinált CD4 % szint / csökkenés a HIV-2 vírus evolúcióhoz kapcsolódik. Továbbá a longitudinális CD4 sejtes adatok alapján a kohort résztvevőit lassú és gyors progressziós csoportokra osztottuk. Eredményeink azt mutatják, hogy a gyors progressziójú csoportba tarozó betegek vírus evolúciós rátája kétszer olyan magas, mint a lassú progressziós csoportba tartozó betegeké. Az Env szekvenciák azonosítása során azt is megfigyeltük, hogy a fertőzés során a burok fehérje C2 régiójában lévő bizonyos amino savak pozitívan szelektálódnak a lassú progressziós csoport esetén, a gyors progressziós coportokéhoz képest. Illetve analízisenk azt mutatják, hogy e pozitívan szelektálódott aminosavak a burok fehérje felszínén expozálódnak.

Nem utolsó sorban, szintén kollaborációs partnerünk segítségével egy szenzitív HIV-2 DNS mennyiségét meghatározó protokollt is beállítottunk. Az általunk beállított protokoll kiemelendő jelentőséggel bír abban az esetben, amikor a vírus plazma RNS szintje nem detektálható. A HIV-2 plazma RNS szintje a fertőzöttek jelentős hányadánál nem detektálható, ezért szükséges egy olyan megfelelő szenzitivitási és specifitási protokoll, mely lehetővé teszi a HIV-2 detektálását és a fertőzés monitorozását. Az általunk beállított módszer lehetőséget biztosít a HIV-2 fertőzések jövőbeni monitorozására, illetve e diagnosis felállításának megerősítéséhez is.

Eredményeink hozzájárulnak a HIV-1/2 dupla fertőzés és a HIV-2 mono-infekció progressziójának és mechanizmusának megértéséhez. Továbbá analíziseink rávilágítanak a HIV-2 Tat savas doménjének a vírus replikációban betöltött szerepére, ezzel is kiemelve, hogy habár mind a két HIV vírus Tat proteinje hasonló szerkezettel rendelkezik, azoban jelentős eltérések figyelhetőek meg azok funkciójában. És nem utolsó sorban sikeresen beállítottunk egy olyan protokollt, mely lehetővé teszi a HIV-2 infekció és a terápia monitorozását abban az esetben is amior a vírus RNS szinte a kvantifikálási szint alatti vagy egyáltalán nem detektálható.

REFERENCES

1. (2019). "who.int/hiv/pub/arv/arv-update-2019-policy/en."
2. Adjorlolo-Johnson, G., K. M. De Cock, E. Ekpini, K. M. Vetter, T. Sibailly, K. Brattegaard, D. Yavo, R. Doorly, J. P. Whitaker, L. Kestens and et al. (1994). "Prospective comparison of mother-to-child transmission of HIV-1 and HIV-2 in Abidjan, Ivory Coast." JAMA 272(6): 462-466.
3. Aiken, C., J. Konner, N. R. Landau, M. E. Lenburg and D. Trono (1994). "Nef induces CD4 endocytosis: requirement for a critical dileucine motif in the membrane-proximal CD4 cytoplasmic domain." Cell 76(5): 853-864.
4. Akimoto, H., H. Kaneko, I. Sekigawa, H. Hashimoto, Y. Kaneko and N. Yamamoto (1998). "Binding of HIV-2 envelope glycoprotein to CD8 molecules and related chemokine production." Immunology 95(2): 214-218.
5. Al-Harthi, L., M. Owais and S. K. Arya (1998). "Molecular inhibition of HIV type 1 by HIV type 2: effectiveness in peripheral blood mononuclear cells." AIDS Res Hum Retroviruses 14(1): 59-64.
6. Alvarez, M., M. Nevot, J. Mendieta, M. A. Martinez and L. Menendez-Arias (2018). "Amino acid residues in HIV-2 reverse transcriptase that restrict the development of nucleoside analogue resistance through the excision pathway." J Biol Chem 293(7): 2247-2259.
7. Andersson, S., H. Norrgren, Z. da Silva, A. Biague, S. Bamba, S. Kwok, C. Christopherson, G. Biberfeld and J. Albert (2000). "Plasma viral load in HIV-1 and HIV-2 singly and dually infected individuals in Guinea-Bissau, West Africa: significantly lower plasma virus set point in HIV-2 infection than in HIV-1 infection." Arch Intern Med 160(21): 3286-3293.
8. Andrews, S. M. and S. Rowland-Jones (2017). "Recent advances in understanding HIV evolution." F1000Res 6: 597.
9. Anisimova, M., M. Gil, J. F. Dufayard, C. Dessimoz and O. Gascuel (2011). "Survey of branch support methods demonstrates accuracy, power, and robustness of fast likelihood-based approximation schemes." Syst Biol 60(5): 685-699.
10. Anonymus (1999). "Guidelines for national human immunodeficiency virus case surveillance, including monitoring for human immunodeficiency virus infection and acquired immunodeficiency syndrome." MMWR Recomm Rep 48: 1-27, 29-31.
11. Apetrei, C., A. Kaur, N. W. Lerche, M. Metzger, I. Pandrea, J. Hardcastle, S. Falkenstein, R. Bohm, J. Koehler, V. Traina-Dorge, T. Williams, S. Staprans, G. Plauche, R. S. Veazey, H. McClure, A. A. Lackner, B. Gormus, D. L. Robertson and P. A. Marx (2005). "Molecular epidemiology of simian immunodeficiency virus SIVsm in U.S. primate centers unravels the origin of SIVmac and SIVstm." J Virol 79(14): 8991-9005.
12. Apolloni, A., L. W. Meredith, A. Suhrbier, R. Kiernan and D. Harrich (2007). "The HIV-1 Tat protein stimulates reverse transcription in vitro." Curr HIV Res 5(5): 473-483.
13. Arien, K. K., A. Abraha, M. E. Quinones-Mateu, L. Kestens, G. Vanham and E. J. Arts (2005). "The replicative fitness of primary human immunodeficiency virus type 1 (HIV-1) group M, HIV-1 group O, and HIV-2 isolates." J Virol 79(14): 8979-8990.
14. Ariyoshi, K., M. Schim van der Loeff, P. Cook, D. Whitby, T. Corrah, S. Jaffar, F. Cham, S. Sabally, D. O'Donovan, R. A. Weiss, T. F. Schulz and H. Whittle (1998). "Kaposi's sarcoma in the Gambia, West Africa is less frequent in human immunodeficiency virus type 2 than in human immunodeficiency virus type 1 infection despite a high prevalence of human herpesvirus 8." J Hum Virol 1(3): 193-199.
15. Arya, S. K. (1993). "Human immunodeficiency virus type 2 (HIV-2) trans-activator (Tat): functional domains and the search for trans-dominant negative mutants." AIDS Res Hum Retroviruses 9(9): 839-848.
16. Arya, S. K. and R. C. Gallo (1996). "Human immunodeficiency virus (HIV) type 2-mediated inhibition of HIV type 1: a new approach to gene therapy of HIV-infection." Proc Natl Acad Sci U S A 93(9): 4486-4491.
17. Audige, A., P. Taffe, M. Rickenbach, M. Battegay, P. Vernazza, D. Nadal, R. F. Speck and H. I. V. C. S. Swiss (2010). "Low postseroconversion CD4 count and rapid decrease of CD4 density identify HIV+ fast progressors." AIDS Res Hum Retroviruses 26(9): 997-1005.
18. Avettand-Fenoel, V., F. Damond, M. Gueudin, S. Matheron, A. Melard, G. Collin, D. Descamps, M. L. Chaix, C. Rouzioux, J. C. Plantier, H. I. V. Anrs-Co and A.-A. C. Q. W. G. the (2014). "New sensitive one-step real-time duplex PCR method for group A and B HIV-2 RNA load." J Clin Microbiol 52(8): 3017-3022.
19. Ayouba, A., C. Akoua-Koffi, S. Calvignac-Spencer, A. Esteban, S. Locatelli, H. Li, Y. Li, B. H. Hahn, E. Delaporte, F. H. Leendertz and M. Peeters (2013). "Evidence for continuing cross-species transmission of SIVsmm to humans: characterization of a new HIV-2 lineage in rural Cote d'Ivoire." AIDS 27(15): 2488-2491.
20. Azevedo-Pereira, J. M. and Q. Santos-Costa (2016). "HIV Interaction With Human Host: HIV-2 As a Model of a Less Virulent Infection." AIDS Rev 18(1): 44-53.
21. Ba, S., D. N. Raugi, R. A. Smith, F. Sall, K. Faye, S. E. Hawes, P. S. Sow, M. Seydi, G. S. Gottlieb and H. I. V. S. G. University of Washington-Dakar (2018). "A Trial of a Single-tablet Regimen of Elvitegravir, Cobicistat, Emtricitabine, and Tenofovir Disoproxil Fumarate for the Initial Treatment of Human Immunodeficiency Virus

Type 2 Infection in a Resource-limited Setting: 48-Week Results From Senegal, West Africa." Clin Infect Dis 67(10): 1588-1594.
22. Babu, P. G., N. K. Saraswathi, F. Devapriya and T. J. John (1993). "The detection of HIV-2 infection in southern India." Indian J Med Res 97: 49-52.
23. Baldauf, H. M., L. Stegmann, S. M. Schwarz, I. Ambiel, M. Trotard, M. Martin, M. Burggraf, G. M. Lenzi, H. Lejk, X. Y. Pan, O. I. Fregoso, E. S. Lim, L. Abraham, L. A. Nguyen, F. Rutsch, R. Konig, B. Kim, M. Emerman, O. T. Fackler and O. T. Keppler (2017). "Vpx overcomes a SAMHD1-independent block to HIV reverse transcription that is specific to resting CD4 T cells." Proceedings of the National Academy of Sciences of the United States of America 114(10): 2729-2734.
24. Barillari, G., C. Sgadari, V. Fiorelli, F. Samaniego, S. Colombini, V. Manzari, A. Modesti, B. C. Nair, A. Cafaro, M. Sturzl and B. Ensoli (1999). "The Tat protein of human immunodeficiency virus type-1 promotes vascular cell growth and locomotion by engaging the alpha5beta1 and alphavbeta3 integrins and by mobilizing sequestered basic fibroblast growth factor." Blood 94(2): 663-672.
25. Barin, F., F. Cazein, F. Lot, J. Pillonel, S. Brunet, D. Thierry, F. Damond, F. Brun-Vezinet, J. C. Desenclos and C. Semaille (2007). "Prevalence of HIV-2 and HIV-1 group O infections among new HIV diagnoses in France: 2003-2006." AIDS 21(17): 2351-2353.
26. Barraud, P., J. C. Paillart, R. Marquet and C. Tisne (2008). "Advances in the structural understanding of Vif proteins." Curr HIV Res 6(2): 91-99.
27. Barre-Sinoussi, F., J. C. Chermann, F. Rey, M. T. Nugeyre, S. Chamaret, J. Gruest, C. Dauguet, C. Axler-Blin, F. Vezinet-Brun, C. Rouzioux, W. Rozenbaum and L. Montagnier (1983). "Isolation of a T-lymphotropic retrovirus from a patient at risk for acquired immune deficiency syndrome (AIDS)." Science 220(4599): 868-871.
28. Barroso, H., P. Borrego, I. Bartolo, J. M. Marcelino, C. Familia, A. Quintas and N. Taveira (2011). "Evolutionary and structural features of the C2, V3 and C3 envelope regions underlying the differences in HIV-1 and HIV-2 biology and infection." PLoS One 6(1): e14548.
29. Barroso, H. and N. Taveira (2005). "Evidence for negative selective pressure in HIV-2 evolution in vivo." Infect Genet Evol 5(3): 239-246.
30. Bayer, P., M. Kraft, A. Ejchart, M. Westendorp, R. Frank and P. Rosch (1995). "Structural studies of HIV-1 Tat protein." J Mol Biol 247(4): 529-535.
31. Belshan, M., L. A. Mahnke and L. Ratner (2006). "Conserved amino acids of the human immunodeficiency virus type 2 Vpx nuclear localization signal are critical for nuclear targeting of the viral preintegration complex in non-dividing cells." Virology 346(1): 118-126.
32. Belshan, M. and L. Ratner (2003). "Identification of the nuclear localization signal of human immunodeficiency virus type 2 Vpx." Virology 311(1): 7-15.
33. Belshan, M. and L. Ratner (2003). "Identification of the nuclear localization signal of human immunodeficiency virus type 2 Vpx." Virology 311(1): 7-15.
34. Bercoff, D. P., P. Triqueneaux, C. Lambert, A. A. Oumar, A. M. Ternes, S. Dao, P. Goubau, J. C. Schmit and J. Ruelle (2010). "Polymorphisms of HIV-2 integrase and selection of resistance to raltegravir." Retrovirology 7: 98.
35. Bienert, S., A. Waterhouse, T. A. de Beer, G. Tauriello, G. Studer, L. Bordoli and T. Schwede (2017). "The SWISS-MODEL Repository-new features and functionality." Nucleic Acids Res 45(D1): D313-D319.
36. Bieniasz, P. D. (2009). "The cell biology of HIV-1 virion genesis." Cell Host Microbe 5(6): 550-558.
37. Blaak, H., P. H. Boers, R. A. Gruters, H. Schuitemaker, M. E. van der Ende and A. D. Osterhaus (2005). "CCR5, GPR15, and CXCR6 are major coreceptors of human immunodeficiency virus type 2 variants isolated from individuals with and without plasma viremia." J Virol 79(3): 1686-1700.
38. Blissenbach, M., B. Grewe, B. Hoffmann, S. Brandt and K. Uberla (2010). "Nuclear RNA export and packaging functions of HIV-1 Rev revisited." J Virol 84(13): 6598-6604.
39. Borrego, P., J. M. Marcelino, C. Rocha, M. Doroana, F. Antunes, F. Maltez, P. Gomes, C. Novo, H. Barroso and N. Taveira (2008). "The role of the humoral immune response in the molecular evolution of the envelope C2, V3 and C3 regions in chronically HIV-2 infected patients." Retrovirology 5: 78.
40. Bose, D., J. Gagnon and Y. Chebloune (2015). "Comparative Analysis of Tat-Dependent and Tat-Deficient Natural Lentiviruses." Vet Sci 2(4): 293-348.
41. Boyer, P. L., P. K. Clark and S. H. Hughes (2012). "HIV-1 and HIV-2 reverse transcriptases: different mechanisms of resistance to nucleoside reverse transcriptase inhibitors." J Virol 86(10): 5885-5894.
42. Boyer, P. L., S. G. Sarafianos, P. K. Clark, E. Arnold and S. H. Hughes (2006). "Why do HIV-1 and HIV-2 use different pathways to develop AZT resistance?" PLoS Pathog 2(2): e10.
43. Brennan, C. A., J. Yamaguchi, A. S. Vallari, R. K. Hickman and S. G. Devare (1997). "Genetic variation in human immunodeficiency virus type 2: identification of a unique variant from human plasma." AIDS Res Hum Retroviruses 13(5): 401-404.
44. Bruen, T. C., H. Philippe and D. Bryant (2006). "A simple and robust statistical test for detecting the presence of recombination." Genetics 172(4): 2665-2681.

45. Budhiraja, S., H. Liu, J. Couturier, A. Malovannaya, J. Qin, D. E. Lewis and A. P. Rice (2015). "Mining the human complexome database identifies RBM14 as an XPO1-associated protein involved in HIV-1 Rev function." J Virol 89(7): 3557-3567.
46. Burgard, M., C. Jasseron, S. Matheron, F. Damond, K. Hamrene, S. Blanche, A. Faye, C. Rouzioux, J. Warszawski, L. Mandelbro and A. F. P. C. EPF-CO (2010). "Mother-to-child transmission of HIV-2 infection from 1986 to 2007 in the ANRS French Perinatal Cohort EPF-CO1." Clin Infect Dis 51(7): 833-843.
47. Campbell, E. M. and T. J. Hope (2015). "HIV-1 capsid: the multifaceted key player in HIV-1 infection." Nat Rev Microbiol 13(8): 471-483.
48. Campbell-Yesufu, O. T. and R. T. Gandhi (2011). "Update on human immunodeficiency virus (HIV)-2 infection." Clin Infect Dis 52(6): 780-787.
49. Capriotti, E., P. Fariselli and R. Casadio (2005). "I-Mutant2.0: predicting stability changes upon mutation from the protein sequence or structure." Nucleic Acids Res 33(Web Server issue): W306-310.
50. Cavaco-Silva, P., N. C. Taveira, L. Rosado, M. H. Lourenco, J. Moniz-Pereira, N. W. Douglas, R. S. Daniels and M. O. Santos-Ferreira (1998). "Virological and molecular demonstration of human immunodeficiency virus type 2 vertical transmission." J Virol 72(4): 3418-3422.
51. Cavaleiro, R., A. E. Sousa, A. Loureiro and R. M. Victorino (2000). "Marked immunosuppressive effects of the HIV-2 envelope protein in spite of the lower HIV-2 pathogenicity." AIDS 14(17): 2679-2686.
52. CB, H. (2006). WHO Staging System for HIV Infection and Disease in Adolescents and Adults,Table 3; Clinical Overview of HIV Disease, HIV InSite Knowledge Base.
53. Chang, L. J., V. Urlacher, T. Iwakuma, Y. Cui and J. Zucali (1999). "Efficacy and safety analyses of a recombinant human immunodeficiency virus type 1 derived vector system." Gene Ther 6(5): 715-728.
54. Chang, Y. N. and K. T. Jeang (1992). "The basic RNA-binding domain of HIV-2 Tat contributes to preferential trans-activation of a TAR2-containing LTR." Nucleic Acids Res 20(20): 5465-5472.
55. Charpentier, C., S. Eholie, X. Anglaret, M. Bertine, C. Rouzioux, V. Avettand-Fenoel, E. Messou, A. Minga, F. Damond, J. C. Plantier, F. Dabis, G. Peytavin, F. Brun-Vezinet, D. K. Ekouevi and D. E. A. W. A. C. Ie (2014). "Genotypic resistance profiles of HIV-2-treated patients in West Africa." AIDS 28(8): 1161-1169.
56. Charpentier, C., B. Visseaux, A. Benard, G. Peytavin, F. Damond, C. Roy, A. Taieb, G. Chene, S. Matheron, F. Brun-Vezinet, D. Descamps and A. C. H.-. Cohort (2013). "Transmitted drug resistance in French HIV-2-infected patients." AIDS 27(10): 1671-1674.
57. Chen, Z., A. Luckay, D. L. Sodora, P. Telfer, P. Reed, A. Gettie, J. M. Kanu, R. F. Sadek, J. Yee, D. D. Ho, L. Zhang and P. A. Marx (1997). "Human immunodeficiency virus type 2 (HIV-2) seroprevalence and characterization of a distinct HIV-2 genetic subtype from the natural range of simian immunodeficiency virus-infected sooty mangabeys." J Virol 71(5): 3953-3960.
58. Chesebro, B., K. Wehrly, J. Nishio and S. Perryman (1992). "Macrophage-tropic human immunodeficiency virus isolates from different patients exhibit unusual V3 envelope sequence homogeneity in comparison with T-cell-tropic isolates: definition of critical amino acids involved in cell tropism." J Virol 66(11): 6547-6554.
59. Chougui, G. and F. Margottin-Goguet (2019). "HUSH, a Link Between Intrinsic Immunity and HIV Latency." Front Microbiol 10: 224.
60. Ciftci, H. I., H. Fujino, R. Koga, M. Yamamoto, S. Kawamura, H. Tateishi, Y. Iwatani, M. Otsuka and M. Fujita (2015). "Mutational analysis of HIV-2 Vpx shows that proline residue 109 in the poly-proline motif regulates degradation of SAMHD1." FEBS Lett 589(13): 1505-1514.
61. Clark, E., B. Nava and M. Caputi (2017). "Tat is a multifunctional viral protein that modulates cellular gene expression and functions." Oncotarget 8(16): 27569-27581.
62. Clavel, F., D. Guetard, F. Brun-Vezinet, S. Chamaret, M. A. Rey, M. O. Santos-Ferreira, A. G. Laurent, C. Dauguet, C. Katlama, C. Rouzioux and et al. (1986). "Isolation of a new human retrovirus from West African patients with AIDS." Science 233(4761): 343-346.
63. Coffin, J. M., S. H. Hughes and H. E. Varmus (1997). The Interactions of Retroviruses and their Hosts. Retroviruses. J. M. Coffin, S. H. Hughes and H. E. Varmus. Cold Spring Harbor (NY).
64. Cuevas, J. M., R. Geller, R. Garijo, J. Lopez-Aldeguer and R. Sanjuan (2015). "Extremely High Mutation Rate of HIV-1 In Vivo." PLoS Biol 13(9): e1002251.
65. da Silva, Z. J., I. Oliveira, A. Andersen, F. Dias, A. Rodrigues, B. Holmgren, S. Andersson and P. Aaby (2008). "Changes in prevalence and incidence of HIV-1, HIV-2 and dual infections in urban areas of Bissau, Guinea-Bissau: is HIV-2 disappearing?" AIDS 22(10): 1195-1202.
66. Damond, F., C. Apetrei, D. L. Robertson, S. Souquiere, A. Lepretre, S. Matheron, J. C. Plantier, F. Brun-Vezinet and F. Simon (2001). "Variability of human immunodeficiency virus type 2 (hiv-2) infecting patients living in france." Virology 280(1): 19-30.
67. Damond, F., M. Gueudin, S. Pueyo, I. Farfara, D. L. Robertson, D. Descamps, G. Chene, S. Matheron, P. Campa, F. Brun-Vezinet and F. Simon (2002). "Plasma RNA viral load in human immunodeficiency virus type 2 subtype A and subtype B infections." J Clin Microbiol 40(10): 3654-3659.

68. Damond, F., M. Worobey, P. Campa, I. Farfara, G. Colin, S. Matheron, F. Brun-Vezinet, D. L. Robertson and F. Simon (2004). "Identification of a highly divergent HIV type 2 and proposal for a change in HIV type 2 classification." AIDS Res Hum Retroviruses 20(6): 666-672.
69. Dar, M. J., B. Monel, L. Krishnan, M. C. Shun, F. Di Nunzio, D. E. Helland and A. Engelman (2009). "Biochemical and virological analysis of the 18-residue C-terminal tail of HIV-1 integrase." Retrovirology 6: 94.
70. Das, A. T., B. Klaver, A. Harwig, M. Vink, M. Ooms, M. Centlivre and B. Berkhout (2007). "Construction of a doxycycline-dependent simian immunodeficiency virus reveals a nontranscriptional function of tat in viral replication." J Virol 81(20): 11159-11169.
71. Das, S. R. and S. Jameel (2005). "Biology of the HIV Nef protein." Indian J Med Res 121(4): 315-332.
72. Davenport, Y. W., A. P. West and P. J. Bjorkman (2016). "Structure of an HIV-2 gp120 in Complex with CD4." Journal of Virology 90(4): 2112-2118.
73. De Cock, K. M. and F. Brun-Vezinet (1989). "Epidemiology of HIV-2 infection." AIDS 3 Suppl 1: S89-95.
74. De Cock, K. M., F. Brun-Vezinet and B. Soro (1991). "HIV-1 and HIV-2 infections and AIDS in West Africa." AIDS 5 Suppl 1: S21-28.
75. de Mendoza, C., E. Caballero, A. Aguilera, M. Piron, R. Ortiz de Lejarazu, C. Rodriguez, T. Cabezas, R. Gonzalez, A. Trevino, V. Soriano and H. I. V. H. G. Spanish (2014). "HIV-2 and HTLV-1 infections in Spain, a non-endemic region." AIDS Rev 16(3): 152-159.
76. de Mendoza, C., T. Cabezas, E. Caballero, S. Requena, M. J. Amengual, M. Penaranda, A. Saez, R. Tellez, A. B. Lozano, A. Trevino, J. M. Ramos, J. L. Perez, P. Barreiro, V. Soriano and H. I. V. N. Spanish (2017). "HIV type 2 epidemic in Spain: challenges and missing opportunities." AIDS 31(10): 1353-1364.
77. de, P.-A., II, M. L. Guimaraes, G. Bello, A. C. Vicente and M. G. Morgado (2014). "Profile of the HIV epidemic in Cape Verde: molecular epidemiology and drug resistance mutations among HIV-1 and HIV-2 infected patients from distinct islands of the archipelago." PLoS One 9(4): e96201.
78. D'Ettorre, G., A. Lo Presti, C. Gori, E. Cella, A. Bertoli, V. Vullo, C. F. Perno, M. Ciotti, B. T. Foley, M. Ciccozzi and H. I. V. S. Group (2013). "An HIV type 2 case series in Italy: a phylogenetic analysis." AIDS Res Hum Retroviruses 29(9): 1254-1259.
79. Dillon, P. J., P. Nelbock, A. Perkins and C. A. Rosen (1990). "Function of the Human-Immunodeficiency-Virus Type-1 and Type-2 Rev Proteins Is Dependent on Their Ability to Interact with a Structured Region Present in Env Gene Messenger-Rna." Journal of Virology 64(9): 4428-4437.
80. DJ, Z. (2006). Genetic algorithm approaches for the phylogenetic analysis of large biological sequence datasets under the maximum likelihood criterion.
81. Doring, M., P. Borrego, J. Buch, A. Martins, G. Friedrich, R. J. Camacho, J. Eberle, R. Kaiser, T. Lengauer, N. Taveira and N. Pfeifer (2016). "A genotypic method for determining HIV-2 coreceptor usage enables epidemiological studies and clinical decision support." Retrovirology 13(1): 85.
82. Dosztanyi, Z., V. Csizmok, P. Tompa and I. Simon (2005). "IUPred: web server for the prediction of intrinsically unstructured regions of proteins based on estimated energy content." Bioinformatics 21(16): 3433-3434.
83. Dougan, S., B. Patel, J. H. Tosswill and K. Sinka (2005). "Diagnoses of HIV-1 and HIV-2 in England, Wales, and Northern Ireland associated with west Africa." Sex Transm Infect 81(4): 338-341.
84. Drozdetskiy, A., C. Cole, J. Procter and G. J. Barton (2015). "JPred4: a protein secondary structure prediction server." Nucleic Acids Res 43(W1): W389-394.
85. Drummond, A. J. and A. Rambaut (2007). "BEAST: Bayesian evolutionary analysis by sampling trees." BMC Evol Biol 7: 214.
86. Echetebu, C. O. and A. P. Rice (1993). "Mutational analysis of the amino and carboxy termini of the HIV-2 Tat protein." J Acquir Immune Defic Syndr (1988) 6(6): 550-557.
87. Edo-Matas, D., P. Lemey, J. A. Tom, C. Serna-Bolea, A. E. van den Blink, A. B. van 't Wout, H. Schuitemaker and M. A. Suchard (2011). "Impact of CCR5delta32 host genetic background and disease progression on HIV-1 intrahost evolutionary processes: efficient hypothesis testing through hierarchical phylogenetic models." Mol Biol Evol 28(5): 1605-1616.
88. Edwards, C. T., E. C. Holmes, O. G. Pybus, D. J. Wilson, R. P. Viscidi, E. J. Abrams, R. E. Phillips and A. J. Drummond (2006). "Evolution of the human immunodeficiency virus envelope gene is dominated by purifying selection." Genetics 174(3): 1441-1453.
89. Engelman, A. and P. Cherepanov (2012). "The structural biology of HIV-1: mechanistic and therapeutic insights." Nat Rev Microbiol 10(4): 279-290.
90. Esbjornsson, J., F. Mansson, A. Kvist, Z. J. da Silva, S. Andersson, E. M. Fenyo, P. E. Isberg, A. J. Biague, J. Lindman, A. A. Palm, S. L. Rowland-Jones, M. Jansson, P. Medstrand, H. Norrgren, Sweden and G. Guinea-Bissau Cohort Research (2018). "Long-term follow-up of HIV-2-related AIDS and mortality in Guinea-Bissau: a prospective open cohort study." Lancet HIV.
91. Esbjornsson, J., F. Mansson, A. Kvist, P. E. Isberg, S. Nowroozalizadeh, A. J. Biague, Z. J. da Silva, M. Jansson, E. M. Fenyo, H. Norrgren and P. Medstrand (2012). "Inhibition of HIV-1 disease progression by contemporaneous HIV-2 infection." N Engl J Med 367(3): 224-232.

92. Esbjornsson, J., F. Mansson, A. Kvist, P. E. Isberg, S. Nowroozalizadeh, A. J. Biague, Z. J. da Silva, M. Jansson, E. M. Fenyo, H. Norrgren and P. Medstrand (2014). "Effect of HIV-2 infection on HIV-1 disease progression and mortality." AIDS 28(4): 614-615.
93. Esposito, D. and R. Craigie (1999). "HIV integrase structure and function." Adv Virus Res 52: 319-333.
94. Faria, N. R., I. Hodges-Mameletzis, J. C. Silva, B. Rodes, S. Erasmus, S. Paolucci, J. Ruelle, D. Pieniazek, N. Taveira, A. Trevino, M. F. Goncalves, S. Jallow, L. Xu, R. J. Camacho, V. Soriano, P. Goubau, J. D. de Sousa, A. M. Vandamme, M. A. Suchard and P. Lemey (2012). "Phylogeographical footprint of colonial history in the global dispersal of human immunodeficiency virus type 2 group A." J Gen Virol 93(Pt 4): 889-899.
95. Fletcher, T. M., 3rd, B. Brichacek, N. Sharova, M. A. Newman, G. Stivahtis, P. M. Sharp, M. Emerman, B. H. Hahn and M. Stevenson (1996). "Nuclear import and cell cycle arrest functions of the HIV-1 Vpr protein are encoded by two separate genes in HIV-2/SIV(SM)." EMBO J 15(22): 6155-6165.
96. Folks, T. M., J. Justement, A. Kinter, C. A. Dinarello and A. S. Fauci (1987). "Cytokine-induced expression of HIV-1 in a chronically infected promonocyte cell line." Science 238(4828): 800-802.
97. Gallo, S. A., J. D. Reeves, H. Garg, B. Foley, R. W. Doms and R. Blumenthal (2006). "Kinetic studies of HIV-1 and HIV-2 envelope glycoprotein-mediated fusion." Retrovirology 3: 90.
98. Gallo, S. A., K. Sackett, S. S. Rawat, Y. Shai and R. Blumenthal (2004). "The stability of the intact envelope glycoproteins is a major determinant of sensitivity of HIV/SIV to peptidic fusion inhibitors." J Mol Biol 340(1): 9-14.
99. Gao, F., E. Bailes, D. L. Robertson, Y. Chen, C. M. Rodenburg, S. F. Michael, L. B. Cummins, L. O. Arthur, M. Peeters, G. M. Shaw, P. M. Sharp and B. H. Hahn (1999). "Origin of HIV-1 in the chimpanzee Pan troglodytes troglodytes." Nature 397(6718): 436-441.
100. Gao, F., L. Yue, D. L. Robertson, S. C. Hill, H. Hui, R. J. Biggar, A. E. Neequaye, T. M. Whelan, D. D. Ho, G. M. Shaw and et al. (1994). "Genetic diversity of human immunodeficiency virus type 2: evidence for distinct sequence subtypes with differences in virus biology." J Virol 68(11): 7433-7447.
101. German Advisory Committee Blood (Arbeitskreis Blut), S. (2016). "Assessment of Pathogens Transmissible by Blood'. Human Immunodeficiency Virus (HIV).."). Transfus Med Hemother 43(3): 203-222.
102. Gilbert, P. B., I. W. McKeague, G. Eisen, C. Mullins, N. A. Gueye, S. Mboup and P. J. Kanki (2003). "Comparison of HIV-1 and HIV-2 infectivity from a prospective cohort study in Senegal." Stat Med 22(4): 573-593.
103. Goldman, N. and Z. Yang (1994). "A codon-based model of nucleotide substitution for protein-coding DNA sequences." Mol Biol Evol 11(5): 725-736.
104. Goldstone, D. C., V. Ennis-Adeniran, J. J. Hedden, H. C. Groom, G. I. Rice, E. Christodoulou, P. A. Walker, G. Kelly, L. F. Haire, M. W. Yap, L. P. de Carvalho, J. P. Stoye, Y. J. Crow, I. A. Taylor and M. Webb (2011). "HIV-1 restriction factor SAMHD1 is a deoxynucleoside triphosphate triphosphohydrolase." Nature 480(7377): 379-382.
105. Gomes, P., A. Abecasis, M. Almeida, R. Camacho and K. Mansinho (2003). "Transmission of HIV-2." Lancet Infect Dis 3(11): 683-684.
106. Gottlieb, G. S., S. P. Eholie, J. N. Nkengasong, S. Jallow, S. Rowland-Jones, H. C. Whittle and P. S. Sow (2008). "A call for randomized controlled trials of antiretroviral therapy for HIV-2 infection in West Africa." AIDS 22(16): 2069-2072; discussion 2073-2064.
107. Gottlieb, G. S., S. E. Hawes, H. D. Agne, J. E. Stern, C. W. Critchlow, N. B. Kiviat and P. S. Sow (2006). "Lower levels of HIV RNA in semen in HIV-2 compared with HIV-1 infection: implications for differences in transmission." AIDS 20(6): 895-900.
108. Gottlieb, G. S., D. N. Raugi and R. A. Smith (2018). "90-90-90 for HIV-2? Ending the HIV-2 epidemic by enhancing care and clinical management of patients infected with HIV-2." Lancet HIV 5(7): e390-e399.
109. Gottlieb, G. S., P. S. Sow, S. E. Hawes, I. Ndoye, A. M. Coll-Seck, M. E. Curlin, C. W. Critchlow, N. B. Kiviat and J. I. Mullins (2003). "Molecular epidemiology of dual HIV-1/HIV-2 seropositive adults from Senegal, West Africa." AIDS Res Hum Retroviruses 19(7): 575-584.
110. Greenberg, A. E. (2001). "Possible protective effect of HIV-2 against incident HIV-1 infection: review of available epidemiological and in vitro data." AIDS 15(17): 2319-2321.
111. Grez, M., U. Dietrich, P. Balfe, H. von Briesen, J. K. Maniar, G. Mahambre, E. L. Delwart, J. I. Mullins and H. Rubsamen-Waigmann (1994). "Genetic analysis of human immunodeficiency virus type 1 and 2 (HIV-1 and HIV-2) mixed infections in India reveals a recent spread of HIV-1 and HIV-2 from a single ancestor for each of these viruses." J Virol 68(4): 2161-2168.
112. Guerois, R., J. E. Nielsen and L. Serrano (2002). "Predicting changes in the stability of proteins and protein complexes: a study of more than 1000 mutations." J Mol Biol 320(2): 369-387.
113. Guindon, S., J. F. Dufayard, V. Lefort, M. Anisimova, W. Hordijk and O. Gascuel (2010). "New algorithms and methods to estimate maximum-likelihood phylogenies: assessing the performance of PhyML 3.0." Syst Biol 59(3): 307-321.

114. Hamel, D. J., J. L. Sankale, G. Eisen, S. T. Meloni, C. Mullins, A. Gueye-Ndiaye, S. Mboup and P. J. Kanki (2007). "Twenty years of prospective molecular epidemiology in Senegal: changes in HIV diversity." AIDS Res Hum Retroviruses 23(10): 1189-1196.
115. Hanel, K., L. Mockel, M. Brummel, K. Peiris, R. Hartmann, A. J. Dingley, D. Willbold and A. Loidl-Stahlhofen (2014). "Expression and purification of soluble HIV-2 viral protein R (Vpr) using a sandwich-fusion protein strategy." Protein Expr Purif 95: 156-161.
116. Heitzinger, K., P. S. Sow, N. M. Dia Badiane, G. S. Gottlieb, I. N'Doye, M. Toure, N. B. Kiviat, S. E. Hawes, H. I. V. University of Washington-Dakar and G. Cervical Cancer Study (2012). "Trends of HIV-1, HIV-2 and dual infection in women attending outpatient clinics in Senegal, 1990-2009." Int J STD AIDS 23(10): 710-716.
117. Heitzinger, K., P. S. Sow, N. M. Dia Badiane, G. S. Gottlieb, I. N'Doye, M. Toure, N. B. Kiviat, S. E. Hawes, H. I. V. University of Washington-Dakar and G. Cervical Cancer Study (2012). "Trends of HIV-1, HIV-2 and dual infection in women attending outpatient clinics in Senegal, 1990-2009." Int J STD AIDS 23(10): 710-716.
118. Heredia, A., A. Vallejo, V. Soriano, M. Gutierrez, S. Puente, J. S. Epstein and I. K. Hewlett (1997). "Evidence of HIV-2 infection in Equatorial Guinea (central Africa): partial genetic analysis of a B subtype virus." AIDS Res Hum Retroviruses 13(5): 439-440.
119. Hollenbaugh, J. A., S. Tao, G. M. Lenzi, S. Ryu, D. H. Kim, F. Diaz-Griffero, R. F. Schinazi and B. Kim (2014). "dNTP pool modulation dynamics by SAMHD1 protein in monocyte-derived macrophages." Retrovirology 11: 63.
120. Horsburgh, C. R., Jr. and S. D. Holmberg (1988). "The global distribution of human immunodeficiency virus type 2 (HIV-2) infection." Transfusion 28(2): 192-195.
121. Hu, Q., J. O. Trent, G. D. Tomaras, Z. Wang, J. L. Murray, S. M. Conolly, J. M. Navenot, A. P. Barry, M. L. Greenberg and S. C. Peiper (2000). "Identification of ENV determinants in V3 that influence the molecular anatomy of CCR5 utilization." J Mol Biol 302(2): 359-375.
122. Huet, T., R. Cheynier, A. Meyerhans, G. Roelants and S. Wain-Hobson (1990). "Genetic organization of a chimpanzee lentivirus related to HIV-1." Nature 345(6273): 356-359.
123. Izzedine, H., F. Damond, I. Brocheriou, J. Ghosn, H. Lassal and G. Deray (2006). "HIV-2 infection and HIV-associated nephropathy." AIDS 20(6): 949-950.
124. Jaffar, S., A. Wilkins, P. T. Ngom, S. Sabally, T. Corrah, J. E. Bangali, M. Rolfe and H. C. Whittle (1997). "Rate of decline of percentage CD4+ cells is faster in HIV-1 than in HIV-2 infection." J Acquir Immune Defic Syndr Hum Retrovirol 16(5): 327-332.
125. Jeang, K. T., H. Xiao and E. A. Rich (1999). "Multifaceted activities of the HIV-1 transactivator of transcription, Tat." J Biol Chem 274(41): 28837-28840.
126. Jones, K. A. and B. M. Peterlin (1994). "Control of Rna Initiation and Elongation at the Hiv-1 Promoter." Annual Review of Biochemistry 63: 717-743.
127. Kalantari, P., V. Narayan, S. K. Natarajan, K. Muralidhar, U. H. Gandhi, H. Vunta, A. J. Henderson and K. S. Prabhu (2008). "Thioredoxin reductase-1 negatively regulates HIV-1 transactivating protein Tat-dependent transcription in human macrophages." J Biol Chem 283(48): 33183-33190.
128. Kanki P, DeCock K. Epidemiology and natural history of HIV-2. *AIDS.* 1994;8:S1–9.
129. Kanki, P. J., G. Eisen, K. U. Travers, R. G. Marlink, M. E. Essex, C. C. Hsieh and S. Mboup (1996). "Response: HIV-2 and Natural Protection Against HIV-1 Infection." Science 272(5270): 1959b-1960b.
130. Kannangai, R., S. C. Nair, G. Sridharan, S. Prasannakumar and D. Daniel (2010). "Frequency of HIV type 2 infections among blood donor population from India: a 10-year experience." Indian J Med Microbiol 28(2): 111-113.
131. Kappes, J. C., J. S. Parkin, J. A. Conway, J. Kim, C. G. Brouillette, G. M. Shaw and B. H. Hahn (1993). "Intracellular transport and virion incorporation of vpx requires interaction with other virus type-specific components." Virology 193(1): 222-233.
132. Karn, J. and C. M. Stoltzfus (2012). "Transcriptional and posttranscriptional regulation of HIV-1 gene expression." Cold Spring Harb Perspect Med 2(2): a006916.
133. Kass, R. E. and A. E. Raftery (1995). "Bayes Factors." Journal of the American Statistical Association 90(430): 773-795.
134. Khamsri, B., F. Murao, A. Yoshida, A. Sakurai, T. Uchiyama, H. Shirai, Y. Matsuo, M. Fujita and A. Adachi (2006). "Comparative study on the structure and cytopathogenic activity of HIV Vpr/Vpx proteins." Microbes Infect 8(1): 10-15.
135. Kirchhoff, F., T. C. Greenough, D. B. Brettler, J. L. Sullivan and R. C. Desrosiers (1995). "Brief report: absence of intact nef sequences in a long-term survivor with nonprogressive HIV-1 infection." N Engl J Med 332(4): 228-232.
136. Klutch, M., A. M. Woerner, C. J. Marcus-Sekura and J. G. Levin (1998). "Generation of HIV-1/HIV-2 cross-reactive peptide antisera by small sequence changes in HIV-1 reverse transcriptase and integrase immunizing peptides." Journal of Biomedical Science 5(3): 192-202.

137. Koblavi-Deme, S., L. Kestens, D. Hanson, R. A. Otten, M. Y. Borget, C. Bile, S. Z. Wiktor, T. H. Roels, T. Chorba and J. N. Nkengasong (2004). "Differences in HIV-2 plasma viral load and immune activation in HIV-1 and HIV-2 dually infected persons and those infected with HIV-2 only in Abidjan, Cote D'Ivoire." AIDS 18(3): 413-419.
138. Kokkotou, E. G., J. L. Sankale, I. Mani, A. Gueye-Ndiaye, D. Schwartz, M. E. Essex, S. Mboup and P. J. Kanki (2000). "In vitro correlates of HIV-2-mediated HIV-1 protection." Proc Natl Acad Sci U S A 97(12): 6797-6802.
139. Krakoff, E., R. B. Gagne, S. VandeWoude and S. Carver (2019). "Variation in Intra-individual Lentiviral Evolution Rates: a Systematic Review of Human, Nonhuman Primate, and Felid Species." J Virol 93(16).
140. Kurnaeva, M. A., E. V. Sheval, Y. R. Musinova and Y. S. Vassetzky (2019). "Tat basic domain: A "Swiss army knife" of HIV-1 Tat?" Rev Med Virol 29(2): e2031.
141. Kwong, P. D., R. Wyatt, J. Robinson, R. W. Sweet, J. Sodroski and W. A. Hendrickson (1998). "Structure of an HIV gp120 envelope glycoprotein in complex with the CD4 receptor and a neutralizing human antibody." Nature 393(6686): 648-659.
142. Laguette, N., B. Sobhian, N. Casartelli, M. Ringeard, C. Chable-Bessia, E. Segeral, A. Yatim, S. Emiliani, O. Schwartz and M. Benkirane (2011). "SAMHD1 is the dendritic- and myeloid-cell-specific HIV-1 restriction factor counteracted by Vpx." Nature 474(7353): 654-657.
143. Landman, R., F. Damond, J. Gerbe, F. Brun-Vezinet, P. Yeni and S. Matheron (2009). "Immunovirological and therapeutic follow-up of HIV-1/HIV-2-dually seropositive patients." AIDS 23(3): 426-428.
144. Lata, S., R. Mishra and A. C. Banerjea (2018). "Proteasomal Degradation Machinery: Favorite Target of HIV-1 Proteins." Frontiers in Microbiology 9.
145. Lemey, P., I. Derdelinckx, A. Rambaut, K. Van Laethem, S. Dumont, S. Vermeulen, E. Van Wijngaerden and A. M. Vandamme (2005). "Molecular footprint of drug-selective pressure in a human immunodeficiency virus transmission chain." J Virol 79(18): 11981-11989.
146. Lemey, P., S. L. Kosakovsky Pond, A. J. Drummond, O. G. Pybus, B. Shapiro, H. Barroso, N. Taveira and A. Rambaut (2007). "Synonymous substitution rates predict HIV disease progression as a result of underlying replication dynamics." PLoS Comput Biol 3(2): e29.
147. Lemey, P., V. N. Minin, F. Bielejec, S. L. Kosakovsky Pond and M. A. Suchard (2012). "A counting renaissance: combining stochastic mapping and empirical Bayes to quickly detect amino acid sites under positive selection." Bioinformatics 28(24): 3248-3256.
148. Lemey, P., O. G. Pybus, B. Wang, N. K. Saksena, M. Salemi and A. M. Vandamme (2003). "Tracing the origin and history of the HIV-2 epidemic." Proc Natl Acad Sci U S A 100(11): 6588-6592.
149. Li, G., S. Piampongsant, N. R. Faria, A. Voet, A. C. Pineda-Pena, R. Khouri, P. Lemey, A. M. Vandamme and K. Theys (2015). "An integrated map of HIV genome-wide variation from a population perspective." Retrovirology 12: 18.
150. Li, L., S. Dahiya, S. Kortagere, B. Aiamkitsumrit, D. Cunningham, V. Pirrone, M. R. Nonnemacher and B. Wigdahl (2012). "Impact of Tat Genetic Variation on HIV-1 Disease." Adv Virol 2012: 123605.
151. Lin, M. H., H. Sivakumaran, A. Apolloni, T. Wei, D. A. Jans and D. Harrich (2012). "Nullbasic, a potent anti-HIV tat mutant, induces CRM1-dependent disruption of HIV rev trafficking." PLoS One 7(12): e51466.
152. Lusso, P., F. Cocchi, C. Balotta, P. D. Markham, A. Louie, P. Farci, R. Pal, R. C. Gallo and M. S. Reitz, Jr. (1995). "Growth of macrophage-tropic and primary human immunodeficiency virus type 1 (HIV-1) isolates in a unique CD4+ T-cell clone (PM1): failure to downregulate CD4 and to interfere with cell-line-tropic HIV-1." J Virol 69(6): 3712-3720.
153. Machuca, A., M. Gutierrez, A. Holguin, M. Camba, J. Belda and V. Soriano (1998). "[7 new cases of HIV-2 infection recognized in Madrid in 1996 and 1997]." Rev Clin Esp 198(10): 660-664.
154. MacNeil, A., J. L. Sankale, S. T. Meloni, A. D. Sarr, S. Mboup and P. Kanki (2007). "Long-term intrapatient viral evolution during HIV-2 infection." J Infect Dis 195(5): 726-733.
155. MacNeil, A., A. D. Sarr, J. L. Sankale, S. T. Meloni, S. Mboup and P. Kanki (2007). "Direct evidence of lower viral replication rates in vivo in human immunodeficiency virus type 2 (HIV-2) infection than in HIV-1 infection." J Virol 81(10): 5325-5330.
156. Macreadie, I. G., L. A. Castelli, D. R. Hewish, A. Kirkpatrick, A. C. Ward and A. A. Azad (1995). "A domain of human immunodeficiency virus type 1 Vpr containing repeated H(S/F)RIG amino acid motifs causes cell growth arrest and structural defects." Proc Natl Acad Sci U S A 92(7): 2770-2774.
157. Mahdi, M., K. Matuz, F. Toth and J. Tozser (2014). "A modular system to evaluate the efficacy of protease inhibitors against HIV-2." PLoS One 9(11): e113221.
158. Mahdi, M., Z. Szojka, J. A. Motyan and J. Tozser (2018). "Inhibitory Effects of HIV-2 Vpx on Replication of HIV-1." J Virol 92(14).
159. Makroo, R. N., M. Chowdhry, A. Bhatia, B. Arora and N. L. Rosamma (2011). "Prevalence of HIV among blood donors in a tertiary care centre of north India." Indian J Med Res 134(6): 950-953.

160. Mansson, F., A. Biague, Z. J. da Silva, F. Dias, L. A. Nilsson, S. Andersson, E. M. Fenyo and H. Norrgren (2009). "Prevalence and incidence of HIV-1 and HIV-2 before, during and after a civil war in an occupational cohort in Guinea-Bissau, West Africa." AIDS 23(12): 1575-1582.
161. Matheron, S., D. Descamps, S. Gallien, A. Besseghir, P. Sellier, L. Blum, E. Mortier, C. Charpentier, R. Tubiana, F. Damond, G. Peytavin, D. Ponscarme, F. Collin, F. Brun-Vezinet, G. Chene, R. N. France and H. I. V. T. S. G. Sud Sida-Hiv Hepatites (2018). "First-line Raltegravir/Emtricitabine/Tenofovir Combination in Human Immunodeficiency Virus Type 2 (HIV-2) Infection: A Phase 2, Noncomparative Trial (ANRS 159 HIV-2)." Clin Infect Dis 67(8): 1161-1167.
162. Mattei, S., A. Tan, B. Glass, B. Muller, H. G. Krausslich and J. A. G. Briggs (2018). "High-resolution structures of HIV-1 Gag cleavage mutants determine structural switch for virus maturation." Proc Natl Acad Sci U S A 115(40): E9401-E9410.
163. McCulley, A. and L. Ratner (2012). "HIV-2 viral protein X (Vpx) ubiquitination is dispensable for ubiquitin ligase interaction and effects on macrophage infection." Virology 427(1): 67-75.
164. Mikhail, M., B. Wang, P. Lemey, B. Beckthold, A. M. Vandamme, M. J. Gill and N. K. Saksena (2005). "Role of viral evolutionary rate in HIV-1 disease progression in a linked cohort." Retrovirology 2: 41.
165. Miklossy, G., J. Tozser, J. Kadas, R. Ishima, J. M. Louis and P. Bagossi (2008). "Novel macromolecular inhibitors of human immunodeficiency virus-1 protease." Protein Eng Des Sel 21(7): 453-461.
166. Miller, C., Z. Abdo, A. Ericsson, J. Elder and S. VandeWoude (2018). "Applications of the FIV Model to Study HIV Pathogenesis." Viruses 10(4).
167. Miller, S., J. Janin, A. M. Lesk and C. Chothia (1987). "Interior and Surface of Monomeric Proteins." Journal of Molecular Biology 196(3): 641-656.
168. Moore, J. P. (1990). "Simple methods for monitoring HIV-1 and HIV-2 gp120 binding to soluble CD4 by enzyme-linked immunosorbent assay: HIV-2 has a 25-fold lower affinity than HIV-1 for soluble CD4." AIDS 4(4): 297-305.
169. Morner, A., A. Bjorndal, J. Albert, V. N. Kewalramani, D. R. Littman, R. Inoue, R. Thorstensson, E. M. Fenyo and E. Bjorling (1999). "Primary human immunodeficiency virus type 2 (HIV-2) isolates, like HIV-1 isolates, frequently use CCR5 but show promiscuity in coreceptor usage." J Virol 73(3): 2343-2349.
170. Motomura, K., J. Chen and W. S. Hu (2008). "Genetic recombination between human immunodeficiency virus type 1 (HIV-1) and HIV-2, two distinct human lentiviruses." J Virol 82(4): 1923-1933.
171. Mukherjee, S., H. L. Lee, A. L. Pacchia, Y. Ron and J. P. Dougherty (2007). "A HIV-2-based self-inactivating vector for enhanced gene transduction." J Biotechnol 127(4): 745-757.
172. N, G. and Y. Z (1994). "A codon-based model of nucleotide substitution for protein-coding DNA sequences." Mol Biol Evol 11: 725-736.
173. Nabatov, A. A., G. Pollakis, T. Linnemann, A. Kliphius, M. I. Chalaby and W. A. Paxton (2004). "Intrapatient alterations in the human immunodeficiency virus type 1 gp120 V1V2 and V3 regions differentially modulate coreceptor usage, virus inhibition by CC/CXC chemokines, soluble CD4, and the b12 and 2G12 monoclonal antibodies." J Virol 78(1): 524-530.
174. Newell, M. L., D. T. Dunn, C. S. Peckham, A. E. Semprini and G. Pardi (1996). "Vertical transmission of HIV-1: maternal immune status and obstetric factors. The European Collaborative Study." AIDS 10(14): 1675-1681.
175. Nicolas, D., J. Ambrosioni, R. Paredes, M. A. Marcos, C. Manzardo, A. Moreno and J. M. Miro (2015). "Infection with human retroviruses other than HIV-1: HIV-2, HTLV-1, HTLV-2, HTLV-3 and HTLV-4." Expert Rev Anti Infect Ther 13(8): 947-963.
176. Norrgren, H., S. Andersson, A. J. Biague, Z. J. da Silva, F. Dias, A. Naucler and G. Biberfeld (1999). "Trends and interaction of HIV-1 and HIV-2 in Guinea-Bissau, west Africa: no protection of HIV-2 against HIV-1 infection." AIDS 13(6): 701-707.
177. Norrgren, H., S. Andersson, A. Naucler, F. Dias, I. Johansson and G. Biberfeld (1995). "HIV-1, HIV-2, HTLV-I/II and Treponema pallidum infections: incidence, prevalence, and HIV-2-associated mortality in an occupational cohort in Guinea-Bissau." J Acquir Immune Defic Syndr Hum Retrovirol 9(4): 422-428.
178. Norrgren, H., S. Marquina, T. Leitner, P. Aaby, M. Melbye, A. G. Poulsen, O. Larsen, F. Dias, D. Escanilla, S. Andersson, J. Albert and A. Naucler (1997). "HIV-2 genetic variation and DNA load in asymptomatic carriers and AIDS cases in Guinea-Bissau." J Acquir Immune Defic Syndr Hum Retrovirol 16(1): 31-38.
179. Oberste, M. S. and M. A. Gonda (1992). "Conservation of amino-acid sequence motifs in lentivirus Vif proteins." Virus Genes 6(1): 95-102.
180. O'Donovan, D., K. Ariyoshi, P. Milligan, M. Ota, L. Yamuah, R. Sarge-Njie and H. Whittle (2000). "Maternal plasma viral RNA levels determine marked differences in mother-to-child transmission rates of HIV-1 and HIV-2 in The Gambia. MRC/Gambia Government/University College London Medical School working group on mother-child transmission of HIV." AIDS 14(4): 441-448.
181. Pagtakhan, A. S. and S. E. Tong-Starksen (1997). "Interactions between Tat of HIV-2 and transcription factor Sp1." Virology 238(2): 221-230.

182. Pandurangan, A. P., B. Ochoa-Montano, D. B. Ascher and T. L. Blundell (2017). "SDM: a server for predicting effects of mutations on protein stability." Nucleic Acids Res 45(W1): W229-W235.
183. Peeters, M., M. D'Arc and E. Delaporte (2014). "Origin and diversity of human retroviruses." AIDS Rev 16(1): 23-34.
184. Perelson, A. S. (2002). "Modelling viral and immune system dynamics." Nat Rev Immunol 2(1): 28-36.
185. Phillips, R. E., S. Rowland-Jones, D. F. Nixon, F. M. Gotch, J. P. Edwards, A. O. Ogunlesi, J. G. Elvin, J. A. Rothbard, C. R. Bangham, C. R. Rizza and et al. (1991). "Human immunodeficiency virus genetic variation that can escape cytotoxic T cell recognition." Nature 354(6353): 453-459.
186. Plantier, J. C., M. Leoz, J. E. Dickerson, F. De Oliveira, F. Cordonnier, V. Lemee, F. Damond, D. L. Robertson and F. Simon (2009). "A new human immunodeficiency virus derived from gorillas." Nat Med 15(8): 871-872.
187. Pond, S. L. K., S. D. W. Frost and S. V. Muse (2005). "HyPhy: hypothesis testing using phylogenies." Bioinformatics 21(5): 676-679.
188. Popper, S. J., A. D. Sarr, A. Gueye-Ndiaye, S. Mboup, M. E. Essex and P. J. Kanki (2000). "Low plasma human immunodeficiency virus type 2 viral load is independent of proviral load: low virus production in vivo." J Virol 74(3): 1554-1557.
189. Popper, S. J., A. D. Sarr, K. U. Travers, A. Gueye-Ndiaye, S. Mboup, M. E. Essex and P. J. Kanki (1999). "Lower human immunodeficiency virus (HIV) type 2 viral load reflects the difference in pathogenicity of HIV-1 and HIV-2." J Infect Dis 180(4): 1116-1121.
190. Post, K., J. Guo, K. J. Howard, M. D. Powell, J. T. Miller, A. Hizi, S. F. Le Grice and J. G. Levin (2003). "Human immunodeficiency virus type 2 reverse transcriptase activity in model systems that mimic steps in reverse transcription." J Virol 77(13): 7623-7634.
191. Poulsen, A. G., B. Kvinesdal, P. Aaby, K. Molbak, K. Frederiksen, F. Dias and E. Lauritzen (1989). "Prevalence of and mortality from human immunodeficiency virus type 2 in Bissau, West Africa." Lancet 1(8642): 827-831.
192. Poveda, E., B. Rodes, C. Toro and V. Soriano (2004). "Are fusion inhibitors active against all HIV variants?" AIDS Res Hum Retroviruses 20(3): 347-348.
193. Prince, P. D., A. Matser, C. van Tienen, H. C. Whittle and M. F. Schim van der Loeff (2014). "Mortality rates in people dually infected with HIV-1/2 and those infected with either HIV-1 or HIV-2: a systematic review and meta-analysis." AIDS 28(4): 549-558.
194. Rambaut, A., D. Posada, K. A. Crandall and E. C. Holmes (2004). "The causes and consequences of HIV evolution." Nat Rev Genet 5(1): 52-61.
195. Reeves, J. D. and R. W. Doms (2002). "Human immunodeficiency virus type 2." J Gen Virol 83(Pt 6): 1253-1265.
196. Ren, J., L. E. Bird, P. P. Chamberlain, G. B. Stewart-Jones, D. I. Stuart and D. K. Stammers (2002). "Structure of HIV-2 reverse transcriptase at 2.35-A resolution and the mechanism of resistance to non-nucleoside inhibitors." Proc Natl Acad Sci U S A 99(22): 14410-14415.
197. Rice, A. P. (2017). "The HIV-1 Tat Protein: Mechanism of Action and Target for HIV-1 Cure Strategies." Curr Pharm Des 23(28): 4098-4102.
198. Rodes, B., C. Toro, V. Jimenez and V. Soriano (2005). "Viral response to antiretroviral therapy in a patient coinfected with HIV type 1 and type 2." Clin Infect Dis 41(2): e19-21.
199. Ross, H. A. and A. G. Rodrigo (2002). "Immune-mediated positive selection drives human immunodeficiency virus type 1 molecular variation and predicts disease duration." J Virol 76(22): 11715-11720.
200. Rossenkhan, R., V. Novitsky, T. K. Sebunya, R. Musonda, B. A. Gashe and M. Essex (2012). "Viral diversity and diversification of major non-structural genes vif, vpr, vpu, tat exon 1 and rev exon 1 during primary HIV-1 subtype C infection." PLoS One 7(5): e35491.
201. Ruben, S., A. Perkins, R. Purcell, K. Joung, R. Sia, R. Burghoff, W. A. Haseltine and C. A. Rosen (1989). "Structural and functional characterization of human immunodeficiency virus tat protein." J Virol 63(1): 1-8.
202. Ruelle, J., F. Roman, A. T. Vandenbroucke, C. Lambert, K. Fransen, F. Echahidi, D. Pierard, C. Verhofstede, K. Van Laethem, M. L. Delforge, D. Vaira, J. C. Schmit and P. Goubau (2008). "Transmitted drug resistance, selection of resistance mutations and moderate antiretroviral efficacy in HIV-2: analysis of the HIV-2 Belgium and Luxembourg database." BMC Infect Dis 8: 21.
203. Salemi, M. (2013). "The intra-host evolutionary and population dynamics of human immunodeficiency virus type 1: a phylogenetic perspective." Infect Dis Rep 5(Suppl 1): e3.
204. Santiago, M. L., F. Range, B. F. Keele, Y. Li, E. Bailes, F. Bibollet-Ruche, C. Fruteau, R. Noe, M. Peeters, J. F. Brookfield, G. M. Shaw, P. M. Sharp and B. H. Hahn (2005). "Simian immunodeficiency virus infection in free-ranging sooty mangabeys (Cercocebus atys atys) from the Tai Forest, Cote d'Ivoire: implications for the origin of epidemic human immunodeficiency virus type 2." J Virol 79(19): 12515-12527.
205. Santos-Costa, Q., M. M. Lopes, M. Calado and J. M. Azevedo-Pereira (2014). "HIV-2 interaction with cell coreceptors: amino acids within the V1/V2 region of viral envelope are determinant for CCR8, CCR5 and CXCR4 usage." Retrovirology 11: 99.

206. Sawaya, B. E., K. Khalili, J. Gordon, A. Srinivasan, M. Richardson, J. Rappaport and S. Amini (2000). "Transdominant activity of human immunodeficiency virus type 1 Vpr with a mutation at residue R73." J Virol 74(10): 4877-4881.
207. Schaller, T., H. Bauby, S. Hue, M. H. Malim and C. Goujon (2014). "New insights into an X-traordinary viral protein." Front Microbiol 5: 126.
208. Schim van der Loeff, M. F., S. Jaffar, A. A. Aveika, S. Sabally, T. Corrah, E. Harding, A. Alabi, A. Bayang, K. Ariyoshi and H. C. Whittle (2002). "Mortality of HIV-1, HIV-2 and HIV-1/HIV-2 dually infected patients in a clinic-based cohort in The Gambia." AIDS 16(13): 1775-1783.
209. Schindler, M., J. Munch, O. Kutsch, H. Li, M. L. Santiago, F. Bibollet-Ruche, M. C. Muller-Trutwin, F. J. Novembre, M. Peeters, V. Courgnaud, E. Bailes, P. Roques, D. L. Sodora, G. Silvestri, P. M. Sharp, B. H. Hahn and F. Kirchhoff (2006). "Nef-mediated suppression of T cell activation was lost in a lentiviral lineage that gave rise to HIV-1." Cell 125(6): 1055-1067.
210. Schulze-Gahmen, U. and J. H. Hurley (2018). "Structural mechanism for HIV-1 TAR loop recognition by Tat and the super elongation complex." Proc Natl Acad Sci U S A 115(51): 12973-12978.
211. Schwarz, G., S. Baumler, A. Block, F. G. Felsenstein and G. Wenzel (2004). "Determination of detection and quantification limits for SNP allele frequency estimation in DNA pools using real time PCR." Nucleic Acids Res 32(3): e24.
212. Schwefel, D., H. C. Groom, V. C. Boucherit, E. Christodoulou, P. A. Walker, J. P. Stoye, K. N. Bishop and I. A. Taylor (2014). "Structural basis of lentiviral subversion of a cellular protein degradation pathway." Nature 505(7482): 234-238.
213. Seo, T. K., H. Kishino and J. L. Thorne (2004). "Estimating absolute rates of synonymous and nonsynonymous nucleotide substitution in order to characterize natural selection and date species divergences." Molecular Biology and Evolution 21(7): 1201-1213.
214. Shah, S., A. Alexaki, V. Pirrone, S. Dahiya, M. R. Nonnemacher and B. Wigdahl (2014). "Functional properties of the HIV-1 long terminal repeat containing single-nucleotide polymorphisms in Sp site III and CCAAT/enhancer binding protein site I." Virol J 11: 92.
215. Sharp, P. M., E. Bailes, F. Gao, B. E. Beer, V. M. Hirsch and B. H. Hahn (2000). "Origins and evolution of AIDS viruses: estimating the time-scale." Biochem Soc Trans 28(2): 275-282.
216. Sharp, P. M. and B. H. Hahn (2011). "Origins of HIV and the AIDS pandemic." Cold Spring Harb Perspect Med 1(1): a006841.
217. Simon, F., P. Mauclere, P. Roques, I. Loussert-Ajaka, M. C. Muller-Trutwin, S. Saragosti, M. C. Georges-Courbot, F. Barre-Sinoussi and F. Brun-Vezinet (1998). "Identification of a new human immunodeficiency virus type 1 distinct from group M and group O." Nat Med 4(9): 1032-1037.
218. Skar, H., P. Borrego, T. C. Wallstrom, M. Mild, J. M. Marcelino, H. Barroso, N. Taveira, T. Leitner and J. Albert (2010). "HIV-2 genetic evolution in patients with advanced disease is faster than that in matched HIV-1 patients." J Virol 84(14): 7412-7415.
219. Smallman-Raynor, M. and A. Cliff (1991). "The spread of human immunodeficiency virus type 2 into Europe: a geographical analysis." Int J Epidemiol 20(2): 480-489.
220. Smith, K. M., Z. Himiari, S. Tsimbalyuk and J. K. Forwood (2017). "Structural Basis for Importin-alpha Binding of the Human Immunodeficiency Virus Tat." Sci Rep 7(1): 1650.
221. Smith, R. A., D. N. Raugi, V. H. Wu, C. G. Zavala, J. Song, K. M. Diallo, M. Seydi, G. S. Gottlieb and H. I. V. S. G. University of Washington-Dakar (2019). "Comparison of the Antiviral Activity of Bictegravir against HIV-1 and HIV-2 Isolates and Integrase Inhibitor-Resistant HIV-2 Mutants." Antimicrob Agents Chemother 63(5).
222. Smith, S. M., S. Pentlicky, Z. Klase, M. Singh, C. Neuveut, C. Y. Lu, M. S. Reitz, Jr., R. Yarchoan, P. A. Marx and K. T. Jeang (2003). "An in vivo replication-important function in the second coding exon of Tat is constrained against mutation despite cytotoxic T lymphocyte selection." J Biol Chem 278(45): 44816-44825.
223. Soriano, V., P. Gomes, W. Heneine, A. Holguin, M. Doruana, R. Antunes, K. Mansinho, W. M. Switzer, C. Araujo, V. Shanmugam, H. Lourenco, J. Gonzalez-Lahoz and F. Antunes (2000). "Human immunodeficiency virus type 2 (HIV-2) in Portugal: clinical spectrum, circulating subtypes, virus isolation, and plasma viral load." J Med Virol 61(1): 111-116.
224. Soriano, V., M. Gutierrez, E. Caballero, G. Cilla, J. L. Fernandez, A. Aguilera, C. Tuset, F. Dronda, A. M. Martin, E. Carballo, I. Lopez and J. Gonzalez-Lahoz (1996). "Epidemiology of HIV-2 infection in Spain. The HIV-2 Spanish Study Group." Eur J Clin Microbiol Infect Dis 15(5): 383-388.
225. Sousa, J. D., M. P. Temudo, B. S. Hewlett, R. J. Camacho, V. Muller and A. M. Vandamme (2016). "Male Circumcision and the Epidemic Emergence of HIV-2 in West Africa." PLoS One 11(12): e0166805.
226. Switzer, W. M., S. Wiktor, V. Soriano, A. Silva-Graca, K. Mansinho, I. M. Coulibaly, E. Ekpini, A. E. Greenberg, T. M. Folks and W. Heneine (1998). "Evidence of Nef truncation in human immunodeficiency virus type 2 infection." J Infect Dis 177(1): 65-71.

227. Szilvay, A. M., K. A. Brokstad, R. Kopperud, G. Haukenes and K. H. Kalland (1995). "Nuclear export of the human immunodeficiency virus type 1 nucleocytoplasmic shuttle protein Rev is mediated by its activation domain and is blocked by transdominant negative mutants." J Virol 69(6): 3315-3323.
228. Tahirov, T. H., N. D. Babayeva, K. Varzavand, J. J. Cooper, S. C. Sedore and D. H. Price (2010). "Crystal structure of HIV-1 Tat complexed with human P-TEFb." Nature 465(7299): 747-751.
229. Tamura, K., D. Peterson, N. Peterson, G. Stecher, M. Nei and S. Kumar (2011). "MEGA5: molecular evolutionary genetics analysis using maximum likelihood, evolutionary distance, and maximum parsimony methods." Mol Biol Evol 28(10): 2731-2739.
230. Tien, M. Z., A. G. Meyer, D. K. Sydykova, S. J. Spielman and C. O. Wilke (2013). "Maximum Allowed Solvent Accessibilites of Residues in Proteins." Plos One 8(11).
231. Torian, L. V., J. J. Eavey, A. P. Punsalang, R. E. Pirillo, L. A. Forgione, S. A. Kent and W. R. Oleszko (2010). "HIV type 2 in New York City, 2000-2008." Clin Infect Dis 51(11): 1334-1342.
232. Touw, W. G., C. Baakman, J. Black, T. A. H. te Beek, E. Krieger, R. P. Joosten and G. Vriend (2015). "A series of PDB-related databanks for everyday needs." Nucleic Acids Research 43(D1): D364-D368.
233. Travers, K., S. Mboup, R. Marlink, A. Gueye-Nidaye, T. Siby, I. Thior, I. Traore, A. Dieng-Sarr, J. L. Sankale, C. Mullins and et al. (1995). "Natural protection against HIV-1 infection provided by HIV-2." Science 268(5217): 1612-1615.
234. Triki, D., M. E. Cano Contreras, D. Flatters, B. Visseaux, D. Descamps, A. C. Camproux and L. Regad (2018). "Analysis of the HIV-2 protease's adaptation to various ligands: characterization of backbone asymmetry using a structural alphabet." Sci Rep 8(1): 710.
235. Uhlen, M., L. Fagerberg, B. M. Hallstrom, C. Lindskog, P. Oksvold, A. Mardinoglu, A. Sivertsson, C. Kampf, E. Sjostedt, A. Asplund, I. Olsson, K. Edlund, E. Lundberg, S. Navani, C. A. Szigyarto, J. Odeberg, D. Djureinovic, J. O. Takanen, S. Hober, T. Alm, P. H. Edqvist, H. Berling, H. Tegel, J. Mulder, J. Rockberg, P. Nilsson, J. M. Schwenk, M. Hamsten, K. von Feilitzen, M. Forsberg, L. Persson, F. Johansson, M. Zwahlen, G. von Heijne, J. Nielsen and F. Ponten (2015). "Proteomics. Tissue-based map of the human proteome." Science 347(6220): 1260419.
236. Ulich, C., A. Dunne, E. Parry, C. W. Hooker, R. B. Gaynor and D. Harrich (1999). "Functional domains of tat required for efficient human immunodeficiency virus type 1 reverse transcription." Journal of Virology 73(3): 2499-2508.
237. Usami, Y., S. Popov, E. Popova, M. Inoue, W. Weissenhorn and G. G. H (2009). "The ESCRT pathway and HIV-1 budding." Biochem Soc Trans 37(Pt 1): 181-184.
238. Vallari, A., V. Holzmayer, B. Harris, J. Yamaguchi, C. Ngansop, F. Makamche, D. Mbanya, L. Kaptue, N. Ndembi, L. Gurtler, S. Devare and C. A. Brennan (2011). "Confirmation of putative HIV-1 group P in Cameroon." J Virol 85(3): 1403-1407.
239. van der Loeff, M. F. S., N. Larke, S. Kaye, N. Berry, K. Ariyoshi, A. Alabi, C. van Tienen, A. Leligdowicz, R. Sarge-Njie, Z. da Silva, A. Jaye, D. Ricard, T. Vincent, S. R. Jones, P. Aaby, S. Jaffar and H. Whittle (2010). "Undetectable plasma viral load predicts normal survival in HIV-2-infected people in a West African village." Retrovirology 7.
240. Vanden Haesevelde, M. M., M. Peeters, G. Jannes, W. Janssens, G. van der Groen, P. M. Sharp and E. Saman (1996). "Sequence analysis of a highly divergent HIV-1-related lentivirus isolated from a wild captured chimpanzee." Virology 221(2): 346-350.
241. Verhoef, K. and B. Berkhout (1999). "A second-site mutation that restores replication of a Tat-defective human immunodeficiency virus." J Virol 73(4): 2781-2789.
242. Verhoef, K., M. Koper and B. Berkhout (1997). "Determination of the minimal amount of Tat activity required for human immunodeficiency virus type 1 replication." Virology 237(2): 228-236.
243. Visseaux, B., C. Charpentier, G. Collin, M. Bertine, G. Peytavin, F. Damond, S. Matheron, E. Lefebvre, F. Brun-Vezinet, D. Descamps and A. C. H.-. Cohort (2015). "Cenicriviroc, a Novel CCR5 (R5) and CCR2 Antagonist, Shows In Vitro Activity against R5 Tropic HIV-2 Clinical Isolates." PLoS One 10(8): e0134904.
244. Visseaux, B., C. Charpentier, A. Ozanne, A. Nizard, S. Drumard, C. Fagard, D. Glohi, F. Damond, F. Brun-Vezinet, S. Matheron, D. Descamps and A. C. H.-. Cohort (2015). "Tropism distribution among antiretroviral-naive HIV-2-infected patients." AIDS 29(16): 2209-2212.
245. Visseaux, B., F. Damond, S. Matheron, D. Descamps and C. Charpentier (2016). "Hiv-2 molecular epidemiology." Infect Genet Evol 46: 233-240.
246. Visseaux, B., M. Hurtado-Nedelec, C. Charpentier, G. Collin, A. Storto, S. Matheron, L. Larrouy, F. Damond, F. Brun-Vezinet, D. Descamps and A. C. H.-. Cohort (2012). "Molecular determinants of HIV-2 R5-X4 tropism in the V3 loop: development of a new genotypic tool." J Infect Dis 205(1): 111-120.
247. Vodros, D. and E. M. Fenyo (2005). "Quantitative evaluation of HIV and SIV co-receptor use with GHOST(3) cell assay." Methods Mol Biol 304: 333-342.
248. VR, P. and K. GV, Eds. (2008). HIV protocols.

249. Weissman, J. D., J. A. Brown, T. K. Howcroft, J. Hwang, A. Chawla, P. A. Roche, L. Schiltz, Y. Nakatani and D. S. Singer (1998). "HIV-1 tat binds TAFII250 and represses TAFII250-dependent transcription of major histocompatibility class I genes." Proc Natl Acad Sci U S A 95(20): 11601-11606.
250. Wertheim, J. O. and M. Worobey (2009). "Dating the age of the SIV lineages that gave rise to HIV-1 and HIV-2." PLoS Comput Biol 5(5): e1000377.
251. Whittle, H., J. Morris, J. Todd, T. Corrah, S. Sabally, J. Bangali, P. T. Ngom, M. Rolfe and A. Wilkins (1994). "HIV-2-infected patients survive longer than HIV-1-infected patients." AIDS 8(11): 1617-1620.
252. Witvrouw, M., C. Pannecouque, W. M. Switzer, T. M. Folks, E. De Clercq and W. Heneine (2004). "Susceptibility of HIV-2, SIV and SHIV to various anti-HIV-1 compounds: implications for treatment and postexposure prophylaxis." Antivir Ther 9(1): 57-65.
253. Wolfe, L. S., B. J. Stanley, C. Liu, W. K. Eliason and Y. Xiong (2010). "Dissection of the HIV Vif Interaction with Human E3 Ubiquitin Ligase." Journal of Virology 84(14): 7135-7139.
254. Yamaguchi, J., S. G. Devare and C. A. Brennan (2000). "Identification of a new HIV-2 subtype based on phylogenetic analysis of full-length genomic sequence." AIDS Res Hum Retroviruses 16(9): 925-930.
255. Yang, X. and D. Gabuzda (1998). "Mitogen-activated protein kinase phosphorylates and regulates the HIV-1 Vif protein." J Biol Chem 273(45): 29879-29887.
256. Yu, Y., Z. Xiao, E. S. Ehrlich, X. Yu and X. F. Yu (2004). "Selective assembly of HIV-1 Vif-Cul5-ElonginB-ElonginC E3 ubiquitin ligase complex through a novel SOCS box and upstream cysteines." Genes Dev 18(23): 2867-2872.
257. Zbinden, A., R. Durig, C. Shah, J. Boni and J. Schupbach (2016). "Importance of an Early HIV Antibody Differentiation Immunoassay for Detection of Dual Infection with HIV-1 and HIV-2." PLoS One 11(6): e0157690.
258. Zhu, Y., T. Pe'ery, J. Peng, Y. Ramanathan, N. Marshall, T. Marshall, B. Amendt, M. B. Mathews and D. H. Price (1997). "Transcription elongation factor P-TEFb is required for HIV-1 tat transactivation in vitro." Genes Dev 11(20): 2622-2632.

LIST OF PUBLICATIONS PREPARED BY THE KENÉZY LIFE SCIENCE LIBRARY

UNIVERSITY of DEBRECEN

UNIVERSITY AND NATIONAL LIBRARY
UNIVERSITY OF DEBRECEN
H-4002 Egyetem tér 1, Debrecen
Phone: +3652/410-443, email: publikaciok@lib.unideb.hu

Registry number: DEENK/263/2020.PL
Subject: PhD Publication List

Candidate: Zsófia Szojka
Doctoral School: Doctoral School of Molecular Cellular and Immune Biology
MTMT ID: 10056719

List of publications related to the dissertation

1. **Szojka, Z.**, Mótyán, J. A., Miczi, M., Mahdi, M., Tőzsér, J.: Y44A Mutation in the Acidic Domain of HIV-2 Tat Impairs Viral Reverse Transcription and LTR-Transactivation.
   Int. J. Mol. Sci. 21 (16), 1-17, 2020.
   DOI: http://dx.doi.org/10.3390/ijms21165907
   IF: 4.556 (2019)
2. Palm, A. A., Lemey, P., Jansson, M., Månsson, F., Kvist, A., **Szojka, Z.**, Biague, A., da Silva, Z., Rowland-Jones, S. L., Norrgren, H., Esbjörnsson, J., Medstrand, P., SWEGUB CORE Group: Low Postseroconversion CD4+ T-cell Level Is Associated with Faster Disease Progression and Higher Viral Evolutionary Rate in HIV-2 Infection.
   mBio. 10 (1), e01245-18, 2019.
   DOI: http://dx.doi.org/10.1128/mBio.01245-18
   IF: 6.784
3. **Szojka, Z.**, Karlson, S., Jansson, M., Medstrand, P.: Quantification of HIV-2 DNA in Whole Blood.
   BIO-PROTOCOL. 9 (20), 1-20, 2019.
   DOI: http://dx.doi.org/10.21769/BioProtoc.3404
4. Mahdi, M., **Szojka, Z.**, Mótyán, J. A., Tőzsér, J.: Inhibitory effects of HIV-2 Vpx on replication of HIV-1.
   J. Virol. 92 (14), 1-46, 2018.
   IF: 4.324

UNIVERSITY AND NATIONAL LIBRARY
UNIVERSITY OF DEBRECEN
H-4002 Egyetem tér 1, Debrecen
Phone: +3652/410-443, email: publikaciok@lib.unideb.hu

List of other publications

5. Karlsson, I., Tingstedt, J. L., Şahin, G. Ö., Hansen, M., **Szojka, Z.**, Buggert, M., Biague, A., da Silva, Z., Månsson, F., Esbjörnsson, J., Norrgren, H., Medstrand, P., Fomsgaard, A., Jansson, M., Sweden-Guinea-Bissau Cohort Research Group: Cross-Reactive Antibodies With the Capacity to Mediate HIV-1 Envelope Glycoprotein-Targeted Antibody-Dependent Cellular Cytotoxicity Identified in HIV-2-Infected Individuals.
J. Infect. Dis. 219 (11), 1749-1754, 2019.
DOI: http://dx.doi.org/10.1093/infdis/jiz001
IF: 5.022

6. Mahdi, M., **Szojka, Z.**, Mótyán, J. A., Tőzsér, J.: Inhibition Profiling of Retroviral Protease Inhibitors Using an HIV-2 Modular System.
Viruses. 7 (12), 6152-6162, 2015.
DOI: http://dx.doi.org/10.3390/v7122931
IF: 3.042

Total IF of journals (all publications): 23,728
Total IF of journals (publications related to the dissertation): 15,664

The Candidate's publication data submitted to the iDEa Tudóstér have been validated by DEENK on the basis of the Journal Citation Report (Impact Factor) database.

10 September, 2020

DEBRECENI EGYETEM
Egyetemi és Nemzeti Könyvtár

KEYWORDS

HIV-2, HIV-1 and HIV-2 dual infection, Model system for dual infection, Inhibitory effect of HIV-2, Viral protein X, Tat, Stability analysis, RT activity, DNA load, Quantification, qPCR, Whole Blood, Disease progression and viral evolutionary rate

KULCSSZAVAK

HIV-2, HIV-1 és HIV-2 dupla fertőzés, Modell rendszer dupla fertőzéshez, HIV-2 gátló hatása, Virális protein X, Tat, Stabilitási analízis, RT aktivitás, DNS szint, Kvantifikáció, qPCR, Teljes vér, Betegség progresszió és vírus evolúciós ráta

ACKNOWLEDGEMENTS

I would like to express my sincere gratitude to my supervisor Professor Dr. József Tőzsér for providing me the opportunity to work in HIV research and for the support and advices regarding my PhD study and research since I was a bachelor student.

Besides my supervisor, I am greatly indebted to my Bachelor's / Master's supervisor, and my mentor during my PhD, Dr. Mohamed Mahdi for the continuous support, for his immerse knowledge, for his patience, motivation, ethusiasim. I could not have imagined having a better mentor, you created a researcher out of me!

My sincere thanks also goes to my Swedish mentors, Prof. Dr. Marianne Jansson and Prof. Dr. Patrik Medstrand for providing me the opportunuty to work in their groups in Lund, and leading me working on several exciting projects, for their insightful comments, guidence and last but not least for their endless patience.

I thank the two most amazing lab assistants Janics-Pető Szilvia and Sara Karlson for their help and assistance during my research work. I would like to thank my fellow labmates and friends: Jamirah Nazziwa Dr, Joakim Esbjörnsson, Tiger (Yunji Zheng) for their help in Lund; Márió Miczi, Vanda

Toldi, Nataly Morales Granda for all the coffee time and fun what we had in the lab; Mária Golda, Tamás Richárd Linkner, Dr Krisztina Matúz and Balázs Kunkli, Norbert Kassay and Dr. András Szabó for their feedback and help, Dr, János András Mótyán for all the analysis and predications. I greatly appreciate the encouragement and support of my academic advisors; Prof. Mónika Fuxreither and Dr. Beáta Scholtz. My PhD work was financed by the Hungarian Scientific Research Fund (OTKA-NFKI-6), grant number: 125238, in part by the GINOP-2.3.2-15-2016-00044 "PHARMPROT teaming" project, GINOP-2.3.3-15-2016-00020 and also financed by the Higher Education Institutional Excellence Programme (NKFIH-1150-6/2019) and by EFOP-3.6.3-VEKOP-16-2017-00009.

And last but not least, my appreciation goes to my fantastic family and friends (Süti, Rita, Éva, Olga Brigi and Betti), and to my other half without your patients, undertanding, support and love I coudn't make it through.

I would like to dedicate my PhD thesis to my beloved Mom and Dad; who supported me from the heaven, and teached me to never give up.

POSTERS

2020: V. Varga, *Zs. Szojka,*T. R. Linkner, M. Mahdi and J. Tőzsér. The role of HIV-2 Vpx in dual HIV infectionand analysis of its function in the virallife cycle, 13th Molecular Cell and Immune Biology Winter Symposium, Debrecen, Hungary

2020: *Zs. Szojka,*T. R. Linkner, V. Varga*,* M. Mahdi and J. Tőzsér. Elucidating the role of HIV-2 viral protein X. Viruses conference. Barcelona, Spain

2019: M. Mahdi, *Zs. Szojka,* J. A. Mótyán and J. Tőzsér. HIV-2 Vpx mediates inhibition of HIV-1 through interaction with the reverse transcriptase. GINOP, Debrecen, Hungary

2015: M. Mahdi, *Zs. Szojka,* and J. Tőzsér. Evaluating the efficacy of protease inhibitors against HIV-2, and the effect of the I54M-L90M double mutation. 27th International Workshop on Retroviral Pathogenesis. Mülheim an der Ruhr, Germany.

2015: M. Mahdi, *Zs. Szojka,* and J. Tőzsér. Inhibition profiling of currently used protease inhibitors using an HIV-2 modular system, and the effect of the I54M-L90M double mutation. 40th annual meeting on Retroviruses. Cold Spring Harbor, NY, USA.

2014: M. Mahdi, *Zs. Szojka,* K. Matuz, F. Tóth and J. Tőzsér. A modular system to study the effect of protease inhibitors on the action of Human Immunodeficiency Virus type 2 (HIV-2). Hungarian Molecular Life Sciences. Debrecen, Hungary.

2013: M. Mahdi, *Zs. Szojka,* K. Matuz and J. Tőzsér. HIV-2 protease as a chemotherapeutic target. Hungarian Molecular Life Sciences. Siofok, Hungary

2013. *Zs. Szojka*, M. Mahdi, J. Tőzsér. Biochemical and Kinetic characterization of HIV-2 Protease. 6th Molecular Cell and Immune Biology Winter Symposium, Galyatető, Hungary